Department of
BIOLOGY

UNIVERSITY OF
OXFORD

Reducing Respiratory Losses of Carbon to Improve Carbon Use Efficiency and Growth in Plants

Corinna Hartinger

University College

University of Oxford

A thesis presented for the degree of

Doctor of Philosophy

Hilary Term 2024/25

Acknowledgements

I would like to sincerely thank my supervisor Lee for his endless patience and guidance throughout this journey. Your support has been invaluable from start to finish.

An immense thanks also to all members of the Sweetlove group, especially those whose work I built on and the colleagues who listened to my frequent venting about coding problems and were always ready to help out.

I'm grateful also to the Department of Biology (formerly Plant Sciences) and all its occupants, with whom I spent so many delightful lunch breaks. Thank you also to the Interdisciplinary Biosciences DTP. The first-year courses introduced me to computational work and allowed me to pursue this new research direction and to escape the lab.

Thank you to all the wonderful people I got to meet along the way in Oxford and beyond. Huge thanks also to the music and dance, and all the people involved in it. You certainly helped to keep me sane during these years.

And lastly, to Oscar - wish we could have worn those silly hats together.

Declaration

I declare that all the work presented for this thesis is my own.

In Chapter 4, for the identification and quantification of metabolites using gas chromatography-mass spectrometry, I used calibration curves for pure metabolites generated by Pedro Bota (Department of Biology, University of Oxford, UK).

This thesis has not been submitted, either partially or in full, for any degree at this university or another institution.

Corinna Hartinger

Abstract

Enhancing agricultural productivity remains critical for global food security. While many strategies target improved photosynthetic carbon fixation, reducing respiratory carbon losses has recently emerged as a complementary approach, as suggested by comprehensive mapping of plant metabolic networks.

This thesis investigates a novel strategy to reduce respiratory carbon losses by refixing CO_2 produced by nocturnal respiration and making it available again for reassimilation into metabolism before it escapes to the atmosphere.

Using constraint-based metabolic modelling of central metabolism, I examined whether plant metabolic networks possess inherent capacity for nocturnal CO_2 refixation under carbon-limited conditions. Multiple approaches to induce carbon limitation in a diel leaf model revealed that CAM cycling emerged as the only plant-native pathway allowing substantial recovery of nocturnal respiratory CO_2. Despite additional metabolic costs, CAM cycling enhanced growth under carbon-limited conditions in the absence of water stress.

To explore alternative nocturnal CO_2 refixation strategies, I developed a baseline model, which experienced carbon limitation, but was indirectly prevented from using CAM cycling. This model was then used to evaluate the potential of a heterologous CO_2-fixing pathway to enhance carbon conversion efficiency and plant growth. Integration of the synthetic crotonyl-CoA/ethylmalonyl-CoA/hydroxybutyryl-CoA (CETCH) cycle into the model revealed that its NADPH costs and the limited capacity of the plant metabolic network to regenerate NADPH at night substantially restricted the cycle's effectiveness for nocturnal CO_2 refixation in plants.

Finally, a reinvestigation of a Marchantia-specific model with experimentally determined parameters indicated that, contrary to previous modelling results, noc-

turnal CO_2 refixation through CAM cycling is likely unnecessary for this plant to achieve observed growth rates.

This research provides insights into the feasibility of nocturnal respiratory CO_2 refixation strategies and offers important design considerations for future metabolic engineering approaches.

Table of Contents

List of Figures

List of Tables

List of Abbreviations

2OG 2-Oxoglutarate

2PG 2-Phosphoglycolate

3PGA 3-Phosphoglycerate

ATP . . . . . Adenosine tri-phosphate

CAM . . . . . Crassulacean acid metabolism

CBB cycle . . . . . Calvin-Benson-Bassham cycle

CETCH cycle . . Crotonyl-CoA/ethylmalonyl-CoA/hydroxybutyryl-CoA cycle

FACE . . . . . Free-Air CO_2 Enrichment

FBA . . . . . Flux Balance Analysis

FDH . . . . . formate dehydrogenase

GAPDH . . . . . glyceraldehyde 3-phosphate dehydrogenase

GC-MS . . . . . Gas chromatography-mass spectrometry

ICDH . . . . . Isocitrate dehydrogenase

MDH . . . . . Malate dehydrogenase

OAA . . . . . Oxalate

OPPP . . . . . Oxidative pentose phosphate pathway

PEP 2-Phosphoenolpyruvate

PEPC . . . . . PEP carboxylase

pFBA . . . . . parsimonious Flux Balance Analysis

pMDH . . . . . plastidic NADP-malate dehydrogenase

PPFD . . . . . photosynthetic photon flux density

RUBP . . . . . Ribulose 1,5-bisphosphate

Rubisco . . . . . Ribulose-1,5-bisphosphate carboxylase/oxygenase

1 | Introduction

Summary

In plants, a substantial amount of the carbon that is gained during the day by carbon fixation, is lost again to respiration, especially at night (Amthor, 2000; Cannell and Thornley, 2000). In agricultural settings, where carbon can be a limiting resource to plant growth (Amthor et al., 2019), it would be beneficial to explore strategies for alleviating carbon limitation. While increasing photosynthetic CO_2 fixation already receives considerable attention in research, reducing carbon losses to respiration remains an underexplored avenue (Amthor et al., 2019; Joshi et al., 2023). This thesis aims to investigate carbon limitation in plants using metabolic models and explore strategies to reduce nocturnal, respiratory CO_2 losses by implementing plant-native or artificial, nocturnal CO_2 refixation pathways. Additionally, the carbon metabolism of the liverwort *Marchantia polymorpha* will be examined using modelling and experimental approaches, to investigate claims from previous metabolic modelling, which suggested CAM cycling (a naturally occurring form of nocturnal, respiratory CO_2 refixation) was required in this species to increase carbon conversion efficiency and meet expected growth rates (Cannell, 2021).

1.1 Carbon limitation in plants

In agricultural settings, the growth of C3 crop plants can become limited by the availability of carbon (Amthor et al., 2019). Irrigation provides water and the application of liquid or solid fertilisers supplies crops with essential nutrients, such as nitrate and phosphate, leaving carbon gain as one of the main remaining

limitations to growth, especially in closed canopy cropping systems (Wang et al., 2017).

Evidence that, carbon can be a growth-limiting resource comes from free-air CO_2 enrichment (FACE) experiments. In FACE experiments, CO_2 gas is released at ground level within crop fields to elevate local CO_2 concentrations. Current global mean atmospheric CO_2 concentrations are approximately 420 ppm (Lan et al., 2023), while in FACE experiments these concentrations are increased to 475-600 ppm (Ainsworth and Long, 2005). When grown in CO_2-enriched environments, staple crops, including wheat, rice, and soybean, typically achieve 10-20% higher yields (Long et al., 2006; Kimball, 2016; Leakey et al., 2009).

While boosting crop productivity via CO_2 enrichment is widely applicable to diverse crop species, it does not lend itself well to scaling up. A lot of infrastructure would need to be built and maintained to purify and deliver gas collected from high CO_2-emitting industries across whole agricultural fields. FACE experiments are mainly used to understand the impact of elevated CO_2 concentrations on crops to refine predictions about agricultural productivity due to human-made increased CO_2 emissions (Long et al., 2006). It would therefore be beneficial to find ways to modify crops to intrinsically improve their capabilities to cope with current atmospheric CO_2 concentrations, eliminating the need for additional CO_2 provision.

Two distinct but complementary strategies could be followed to address the challenge of enhancing the innate capacities of plants for growth at current atmospheric CO_2 levels (Fig. 1.1A). The first approach, which has already received considerable research attention, focuses on improving the rate of CO_2 fixation. The second, less explored strategy, aims to reduce carbon losses that occur downstream of the CO_2 assimilation process, across central metabolism. These approaches could be combined to act together, yielding improved crops that not only

capture more carbon from the atmosphere but also retain a greater proportion of it, ultimately channelling this additional carbon into increased biomass production (Amthor et al., 2019).

1.2 Carbon fixation in plants

In plants, the enzyme that catalyses CO_2 assimilation is ribulose-1,5-bisphosphate carboxylase/oxygenase (Rubisco), which operates as part of the Calvin-Benson-Bassham (CBB) cycle. The carboxylation of ribulose 1,5-bisphosphate (RuBP) by Rubisco produces two molecules of 3-phosphoglycerate (3PGA). For every three CO_2 molecules fixed, five out of the six 3PGA molecules produced are required to regenerate the three RuBP molecules consumed, while one 3PGA molecule can be withdrawn from the cycle for synthesis of sugars and other carbon compounds.

1.2.1 Limitations of CO_2 assimilation in plants

Especially in C3 plants, which include many staple crops, such as wheat, rice, soybean and cassava, CO_2 assimilation is subject to efficiency and energetic limitations.

The Rubisco enzyme is often referred to as a major limiting factor in plant CO_2 assimilation, being both unspecific and slow (Tcherkez et al., 2006; Erb and Zarzycki, 2018). Rubisco catalyses not just the carboxylation of RuBP but can also use O_2 to oxygenate its substrate, generating 2-phosphoglycolate (2PG), which is processed in the photorespiratory pathway to recycle it back to 3PGA, which re-enters the CBB cycle. Photorespiration incurs losses of CO_2, nitrogen and energy. Photorespiration is therefore considered highly wasteful, albeit essential not only for recovery of 2PG but also due to its integration with amino acid and C1 metabolism (Rosa-Téllez et al., 2024). In C3 crops grown at atmospheric CO_2 concentrations,

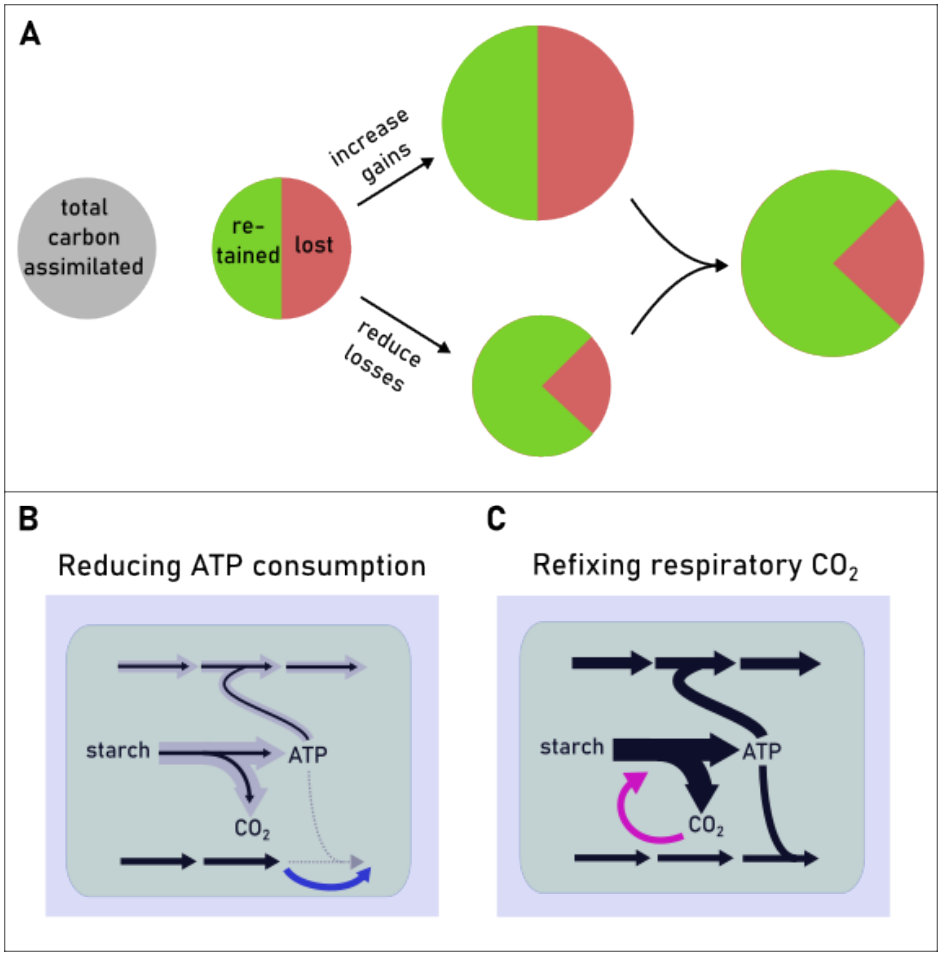

Figure 1.1: **Strategies to reduce respiratory carbon losses in plants.** (A) Schematic representation of plant carbon balance, reproduced with modifications from Amthor et al. (2019). The total carbon assimilated is represented by circles, with green areas indicating carbon retained in harvestable and non-harvestable biomass, and red areas indicating carbon lost through respiration and released as CO_2. Increasing net carbon gain can be achieved either by increasing assimilation or by reducing respiratory losses. (B) Conceptual basis of strategies proposed by Amthor et al., which aim to reduce CO_2 losses by decreasing ATP consumption. (C) Conceptual illustration of the approach developed in this thesis, in which respiratory CO_2 released at night is refixed before escaping to the atmosphere.

oxygenation accounts for 20-50% of all Rubisco catalytic events, thereby diverting a lot of cellular resources away from carbon assimilation (Walker et al., 2016).

Another property of Rubisco that is often cited as a problem is its slow catalytic rate (Ellis, 2010). An analysis of the catalytic rates of the Rubisco enzyme from different organisms showed that it varies from 1-13 reactions per s per mole. The activity of Rubisco in C3 plants typically falls around 3 reactions per s (Sage, 2002; Tcherkez et al., 2006).

Why would an enzyme as important as Rubisco evolve to be so inefficient? The prevailing theory is that from when Rubisco first evolved, it has been unable to adapt to the huge shift in atmospheric compositions, which photosynthesis itself caused (Whitney et al., 2011). During the initial evolution of Rubisco, the composition of Earth's atmosphere was very high in CO_2 and low in O_2 and therefore, there was no selective pressure to achieve high specificity for CO_2 over O_2. But over millions of years, oxygenic photosynthesis transformed the atmosphere, increasing O_2 from negligible amounts to about 30% of atmospheric gases at its peak, thereby limiting the efficiency of Rubisco-dependent CO_2 assimilation (Erb and Zarzycki, 2018).

However, a large-scale survey of enzyme properties (Bar-Even et al., 2011) put Rubisco's properties in a different perspective. Bathellier et al. (2018) point out that, despite being called unspecific throughout literature, Rubisco's affinity for CO_2 is actually very high, with a K_m value of less than 10 µM. In comparison, the median K_m value for all surveyed enzymes in this study was 130 µM. Furthermore, the catalytic rate of Rubisco is not unusually low when compared to these other enzymes, the median turnover number being 10 per s.

Nevertheless, Rubisco's properties are not sufficient for optimal growth in agricultural settings. The main problem is that it catalyses a side reaction with oxygen,

which other carboxylating enzymes do not (Bierbaumer et al., 2023). While plants have evolved to use the photorespiratory pathway to compensate (Busch et al., 2013), it is evident from FACE experiments and natural adaptations described below, that photorespiration could be reduced without detrimental consequences.

Furthermore, Rubisco's inability to distinguish between CO_2 and O_2 is predicted to become a more severe problem as global average temperatures rise (Long, 1991). At temperatures around 25 °C the average ratio of carboxylation to oxygenation reactions catalysed by Rubisco is 3:1 (Jordan and Ogren, 1984). As temperatures increase beyond, this ratio shifts towards more oxygenation reactions because the solubility of O_2 decreases less than that of CO_2, making O_2 comparatively more available to Rubisco than CO_2 (Jordan and Ogren, 1984). This leads to more photorespiration, and therefore increased losses of carbon, nitrogen and energy.

1.2.2 Natural adaptations to increase CO_2 assimilation

Adaptations to increase CO_2 assimilation rates can be found in diverse species of photosynthetic organisms, not just in plants but also cyanobacteria and microalgae.

1.2.3 Increasing Rubisco abundance

One relatively simple strategy C3 plants employ to enhance carbon fixation is to increase the expression of Rubisco (Evans, 1989). Because of Rubisco's low catalytic rate, only a few molecules of CO_2 will be bound every second. Increasing the amount of Rubisco per cell also increases the number of enzyme active sites available and more carboxylation events can happen over the same time period. Nevertheless, the number of oxygenation events will also increase proportionally.

Rubisco is a large protein, composed of eight small subunits and eight large subunits, with a total molecular weight of approximately 550 kDa (Andersson and Backlund, 2008). Increasing the abundance of this enzyme therefore represents a huge investment of cellular resources. In photosynthetic tissues, Rubisco typically accounts for 30-50% of the total soluble protein and can represent up to 25% of leaf nitrogen content (Carmo-Silva et al., 2015). Plant engineering strategies would therefore benefit from allowing cells to produce less Rubisco, while maintaining equal carbon fixation, making these resources available for other biosynthetic processes instead (Bar-Even, 2018).

1.2.3.1 C4 photosynthesis

One naturally occurring mechanism to reduce photorespiration rates is termed C4 metabolism. C4 metabolism combines both biochemical and anatomical changes to substantially reduce the rate of Rubisco oxygenase activity (Sage et al., 2012). C4 has evolved many times independently, especially in plants in hotter climates, which indicates C4 evolved under the selective pressure to circumvent the otherwise temperature-induced increase of photorespiration (Ehleringer et al., 1997).

In C4 plants, the first carbon-fixing enzyme is phosphoenolpyruvate carboxylase (PEPC), which binds bicarbonate (HCO_3^-) to phosphoenolpyruvate (PEP), producing the four-carbon compound oxaloacetate (OAA). OAA is further processed to malate or aspartate, depending on the subtype of C4 metabolism (Furbank, 2011). CO_2-fixation by PEPC occurs throughout the mesophyll. C4 plants possess specialised bundle sheath cells, which form a tight ring around the leaf vasculature, termed Kranz anatomy, and are highly enriched in Rubisco (Muhaidat et al., 2007). Malate or aspartate are transported to the bundle sheath cells where they are decarboxylated for assimilation of the released CO_2 by Rubisco.

Unlike Rubisco, PEPC does not catalyse a reaction with O_2 (Bierbaumer et al., 2023) and can therefore selectively fix CO_2 within mesophyll cells during the day, which also produce oxygen via light-dependent photosynthesis. By sequestering Rubisco inside the bundle sheath cells lacking oxygenic photosynthesis, local CO_2 concentrations around Rubisco are greatly increased while O_2 is excluded, leading to lower rates of photorespiration and a higher catalytic rate of Rubisco carboxylation reactions (Von Caemmerer and Furbank, 2003).

Nevertheless, using C4 metabolism comes at an energetic cost as PEP needs to be regenerated to provide a continuous supply of the carboxylation substrate (Yin and Struik, 2018). The exact costs depend on the subtype of C4 photosynthesis. For the fixation of 1 mol CO_2 in maize, which utilises the NADP-malic enzyme C4 subtype, the CBB cycle requires 3 mol ATP and C4 metabolism adds to this a further 2 mol ATP (Hatch, 1987). Because of this energetic cost, C4 metabolism has evolved and spread mainly in hotter climates, where the rate of photorespiration is sufficiently high due to the elevated temperatures, that it becomes beneficial to invest in C4 metabolism (Ehleringer et al., 1991).

1.2.3.2 Biophysical CO_2-concentrating mechanisms

Aquatic photosynthetic organisms inhabit a particularly low CO_2 environment, due to the slow diffusion of CO_2 from the atmosphere into water. In response, microalgae, diatoms and cyanobacteria convergently evolved biophysical mechanisms to concentrate the available CO_2 around Rubisco (Shen et al., 2017; Catherall et al., 2025; Rae et al., 2013). The shared principles of these mechanisms include using conversion of CO_2 to bicarbonate by carbonic anhydrase (CA) at the cell periphery, and its active transport into a non-membrane-bound compartment enriched with Rubisco, where another CA converts it back to CO_2. In cyanobacteria, this compartment is called the carboxysome, and is formed by a protein shell.

In microalgae and diatoms it is called a pyrenoid, and the compartment forms via liquid-liquid phase separation (Barrett et al., 2021). Rubisco is aggregated in these droplets with the help of the linker protein essential pyrenoic component 1 (EPYC1). The droplet is further encased by sheaths made of starch, which represent an additional barrier to prevent CO_2 from escaping from the compartment.

Pyrenoids can also be found in some non-vascular land plants, the hornworts (Smith and Griffiths, 1996). While hornworts are not aquatic like microalgae, they nevertheless face additional challenges to obtaining carbon compared to vascular plants, as they do not have specialised photosynthetic tissues. Thick cells walls are required to avoid desiccation. This, however, presents a barrier to the diffusion of CO_2 into the cell (Villarreal and Renner, 2012).

Pyrenoids seem to have evolved multiple times independently in hornworts (Villarreal and Renner, 2012). As a recent analysis of the model hornwort *Anthoceros agrestis* found (Robison et al., 2025), hornwort CCMs are different from those found in microalgae. This analysis revealed that, unlike the microalgal model for pyrenoids which has one pyrenoid per chloroplast, hornworts chloroplasts contain multiple pyrenoids. Additionally, hornwort pyrenoids lack the surrounding starch sheath but are encased by stacked thylakoids, which are hypothesised to represent a barrier to CO_2 escaping from the pyrenoid. Furthermore, no analogue of the pyrenoid-localised linker protein EPYC1 could be found in this study, suggesting that pyrenoid condensation may occur via a different mechanism in hornworts compared to microalgae.

1.2.4 Engineering efforts to increase carbon fixation in C3 crops

Increasing the fixation of carbon has been a main target in crop improvement research and is being approached from many different angles. Presented below are

four distinct strategies, which represent a selection of those proposed and under development: i) improvements of the Rubisco enzyme, ii) implementation of biochemical or biophysical CCMs, iii) implementation of photorespiratory bypasses and iv) CO_2-fixation by alternatives to Rubisco and the CBB cycle (Fig. 1.2).

1.2.4.1 Improving the Rubisco enzyme

Considerable research efforts have been devoted to improving the catalytic properties of Rubisco, particularly enhancing its specificity for CO_2 over O_2 and increasing its carboxylation rate (Whitney et al., 2011; Carmo-Silva et al., 2015). Despite these extensive efforts, significant improvements have proven elusive, largely due to an apparent evolutionary trade-off between catalytic rate and substrate specificity (Tcherkez et al., 2006; Savir et al., 2010). Forms of Rubisco with higher specificity for CO_2 typically exhibit slower catalytic rates, while those with faster turnover generally show reduced specificity. This inverse relationship appears to reflect fundamental biophysical constraints in the enzyme's catalytic mechanism rather than simply a lack of evolutionary optimisation (Bathellier et al., 2018).

1.2.4.2 Implementing CCMs in C3 crop plants

Introducing C4 photosynthesis

Engineering C4 photosynthesis into C3 crops represents another major approach to enhance photosynthetic efficiency, with the C4 rice consortium being a prominent long-term initiative in this field (Hibberd et al., 2008). Despite significant progress in understanding the genetic basis of C4 photosynthesis, the engineering challenge has proven subtantial due to the complex suite of changes required. These include not only the modification of C4 cycle enzymes but also the development of Kranz anatomy with its specialised bundle sheath cells, altered chloroplast distribution, increased vein density, and modified metabolite transporters (Schuler

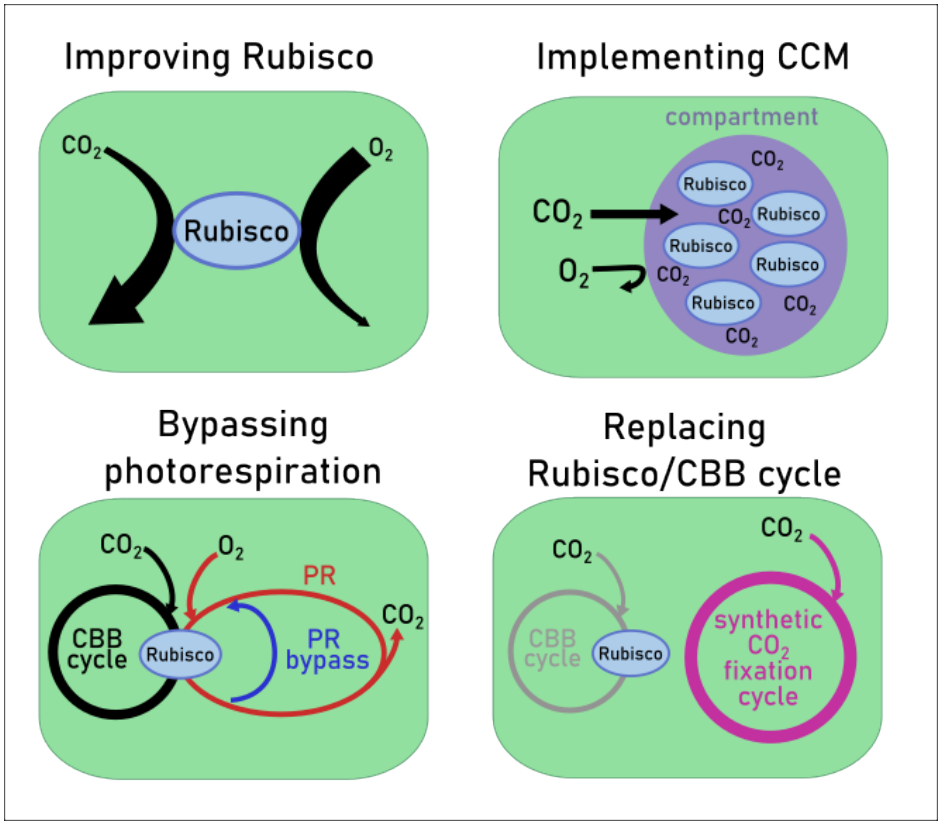

Figure 1.2: **Engineering strategies for increasing CO_2 assimilation.** Schematic illustration of four potential approaches to increase CO_2 fixation in photosynthetic organisms. (i) Engineering Rubisco to improve its specificity for CO_2 over O_2. (ii) Introducing a CO_2-concentrating mechanism (CCM), such as those found in C_4 plants, cyanobacteria, or algae, in which Rubisco is located within a compartment selectively enriched with CO_2. (iii) Minimising or avoiding losses of CO_2 due to photorespiration (PR) by implementing a photorespiratory bypass pathway. (iv) Replacing the Calvin–Benson–Bassham (CBB) cycle with synthetic carbon fixation pathways that are specific for CO_2.

et al., 2016). While individual components of the C4 pathway have been successfully introduced into C3 plants (Lin et al., 2020), achieving the coordinated anatomical and biochemical changes necessary for a fully functional C4 system remains work in progress (Ermakova et al., 2020).

Introducing biophysical CCMs

The first milestones have been achieved by researchers attempting to introduce a carboxysome- and pyrenoid-based CCM in C3 plants. However, several challenges remain to be solved and the introduction of biophysical CCMs has so far not led to increased plant productivity.

Chen et al. (2023) report the correct self-assembly of a carboxysome in *Nicotiana tabacum* chloroplasts. However, these plants were only able to grow under elevated CO_2 levels of 1% CO_2 (v/v), potentially because native CA activity prevented bicarbonate from accumulating, and active transport of bicarbonate into the carboxysome was still missing.

Similarly, Atkinson et al. (2020) succeeded in assembling a proto-pyrenoid, by inducing Rubisco to form a condensate by introducing interactions with the linker protein EPYC1. However, many more features of a full pyrenoid, such as the surrounding starch sheath which acts as a diffusion barrier to retain CO_2, are believed to be necessary to achieve increased CO_2 fixation (Adler et al., 2022; Fei et al., 2022).

Robison et al. (2025) suggest that given the closer evolutionary relationship between hornworts and crop plants, their pyrenoid-based CCM may be easier to implement in higher plants than that from microalgae. Nevertheless, many details of its assembly remain to be elucidated before attempts can be made to implement them in vascular crop plants.

1.2.4.3 Implement photorespiratory bypasses

The photorespiratory pathway, as it has evolved in nature, is not the only possible way to metabolise 2PG and recycle it. Many different designs for alternative photorespiratory pathways, termed photorespiratory bypasses, have been proposed for the purpose of making photorespiration less wasteful.

These artificially create bypasses differ greatly in their mechanisms. They can entail i) full decarboxylation of 2PG (South et al., 2019; Shen et al., 2019), ii) partial decarboxylation of 2PG (Wang et al., 2020a; Kebeish et al., 2007), iii) CO_2-neutral processing of 2PG (Trudeau et al., 2018), or iv) additional CO_2 fixation (Scheffen et al., 2021). However, it is also important to consider several other properties of each pathway, which could impact plant metabolism and overall plant productivity, such as the energetic costs, changes to local CO_2 concentrations which influences Rubisco oxygenation activity, and nitrogen metabolism.

With these considerations in mind, Smith et al. (2025) conducted an analysis of twelve published photorespiratory bypasses, using a multi-modelling approach to consider costs and gains, the wider metabolic implications, and kinetic parameters of each pathway. They concluded that bypasses have different strengths and weaknesses, and their impact will depend on environmental conditions (such as light availability, which affects photosynthetic energy production, or temperatures, which affect Rubisco oxygenation rates), plant physiology and developmental stages.

Overall, the analysis confirmed that a CO_2-fixing pathway such as the tartronyl-CoA (TaCo) pathway should work well in plants under carbon-limited conditions. The TaCo pathway was proposed on a theoretical basis by Trudeau et al. (2018) and the carboxylating enzyme, glycolyl-CoA carboxylase, was engineered by Scheffen et al. (2021). However, this pathway has so far only been tested *in*

vitro, and many of the factors mentioned above could hinder its usefulness in an *in vivo* setting as means of improving photorespiration. Particular concerns were that this carbon-positive photorespiratory bypass is the most energetically costly pathway of the ones included in the study, and that the CO_2-fixation activity of an additional carboxylating enzyme could lower internal CO_2 concentrations, and therefore impede carbon assimilation by Rubisco. Despite these concerns, the analyses conducted by Smith et al. (2025) imply that the TaCo pathway would still be beneficial, because the additional carboxylation activity by the TaCo pathway overall leads to saving ATP and NADPH by requiring fewer turns of the CBB for the same total carbon input.

1.2.4.4 Replacing Rubisco or the CBB cycle

Given the limitations of Rubisco, several strategies have been proposed to either replace the enzyme itself or substitute the CBB cycle entirely with alternatives unable to utilise O_2 as a substrate, thereby reducing or eliminating photorespiration.

As discussed by Bar-Even (2018), one theoretical approach is to replace Rubisco with a set of enzymes that together perform the same catalytic function, so that Rubisco activity could be downregulated or eliminated. In this design, multiple enzymes sequentially catalyse the four consecutive steps normally catalysed by Rubisco (enolization, CO_2/O_2 addition, hydration, and cleavage) but the remaining CBB reactions stay the same. Crucially, the carboxylation step would be carried out by a biotin-dependent enzyme with strict specificity for bicarbonate, thus preventing oxygenation of the substrate.

A more radical strategy is to replace the entire CBB cycle with an alternative CO_2-fixation pathway (Bar-Even, 2018; Erb and Zarzycki, 2016), providing an alternative entry point for inorganic carbon into plant metabolism. Several artifi-

cial CO_2-fixing pathways have been designed (discussed further in chapter 3.1), and some have already been demonstrated *in vitro*. Many of these synthetic pathways possess desirable qualities, including the ability to discriminate effectively between CO_2 and O_2, and the lower energetic costs than the CBB cycle (Bar-Even et al., 2010).

Implementing a strategy of Rubisco/CBB cycle replacement in plants, however, remains highly ambitious. Introducing a novel pathway would require the coordinated expression of multiple heterologous enzymes, as well as optimisation of substrate supply and product utilisation. Moreover, the complete removal of Rubisco and photorespiration should be approached with caution. While photorespiration is often viewed as wasteful, it also provides an important sink for excess reducing equivalents under stress conditions, thereby mitigating the formation of reactive oxygen species (Betti et al., 2016; Smith et al., 2024; Kangasjärvi et al., 2012).

1.3 Respiratory carbon losses in plants

1.3.1 Definition of plant respiration

The term "respiration" has many connotations throughout biology, but even when just applied to plants, sources differ in what it describes and which processes it entails.

Many publications use the term "respiration" to refer only to specific metabolic processes that generate energy and reducing power in the absence of light (Plaxton and Podestá, 2006). During the day, photosynthetic plants can use the energy of sunlight to produce ATP and reducing power in the form of NADPH. In the absence of light, plants have to use a different process to generate ATP and reducing

power. Plants synthesise organic carbon substrates in the light, such as starch or sugars, and store them for use during the dark period. These substrates are broken down via glycolysis, the tricarboxylic acid (TCA) cycle and the electrons transferred to the mitochondrial electron transport chain (mETC), generating ATP in the process. This catabolism breaks the substrates down to CO_2, which, as Rubisco is inactive at night (Portis and Jr., 2003), is released. Some would therefore only consider the CO_2 generated via these pathways - glycolysis, TCA cycle and mETC - as "respiratory CO_2".

However, it is now understood that respiratory pathways serve multiple purposes beyond energy and reducing power generation. These pathways provide essential carbon skeletons for nitrogen assimilation and they also generate precursors for the biosynthesis of amino acids, nucleotides, lipids, and various secondary metabolites (Gauthier et al., 2010; Fernie et al., 2004). In the light, the TCA cycle operates in a non-cyclical manner, with reduced production of NADH (Sweetlove et al., 2010). It would therefore be limiting to define "respiratory CO_2" as only that released by pathways generating energy and reducing power, since these pathways often serve multiple metabolic functions simultaneously.

In contrast to this energisation-centric definition, other publications refer to “respiration” as any CO_2 that is released from processes other than the photorespiratory pathway (Sweetlove et al., 2013; Tcherkez et al., 2017), or the total CO_2 release measured in the dark. This total CO_2 efflux can be readily measured using infrared gas analysers, making it a practical experimental approach. Consequently, the measured CO_2 release rate is often broadly termed "respiration rate" or "dark respiration". However, this measurement approach does not distinguish between CO_2 generated by the abovementioned “respiratory pathways” (glycolysis, TCA cycle, mETC) and the CO_2 produced by other metabolic processes, such as decarboxylation reactions involved in fatty acid synthesis or certain amino acid biosyn-

thetic pathways, which can make substantial contribution to total CO_2 evolution (Sweetlove et al., 2013).

In this thesis, I will use the term "respiratory CO_2" to describe any CO_2 that is generated metabolically, irrespective of the pathway. All analyses of CO_2 release focus on the night-time only, when Rubisco is inactive, and there is consequently no CO_2 release from the photorespiratory pathway.

1.3.2 Engineering efforts to reduce losses of respiratory CO_2 in plants

Carbon is lost in a myriad of processes related to growth and maintenance and can sum up to a substantial amount of the previously fixed CO_2. As much as 30-60% of assimilated carbon can be lost again to respiration (Amthor, 2000, 1989; Cannell and Thornley, 2000). Therefore, reducing CO_2 losses presents an interesting target for increasing crop yield potential (Amthor et al., 2019; Joshi et al., 2023).

Additionally, respiratory losses of CO_2 are further exacerbated by stress. Stressful conditions, such as temperature extremes, drought, flooding or disease increase respiration rates, as proteins must be repaired or replaced more frequently, and additional energy is required for stress response pathways (Flexas et al., 2006; O'Leary et al., 2017). Finding strategies to reduce respiratory losses is therefore poised to become even more valuable in the face of climate change and the associated increase in extreme weather events (Diffenbaugh et al., 2017).

Amthor et al. (2019) presented several potential strategies for reducing respiratory CO_2 losses in plants (Fig. 1.1B). All the proposed approaches describe ways to reduce or circumvent metabolic reactions, pathways, or processes that consume ATP, as respiration rates are linked to ATP production. These strategies include

optimising protein turnover, reducing futile cycling of metabolites, improving ion transport efficiency, and relocating or re-timing processes to occur in the chloroplasts during the day, when there is excess ATP and NADPH from photosynthesis.

However, each of the proposed strategies focus on just one specific metabolic target to reduce or avoid carbon losses associated with a particular pathway or process. While some of these targets presumably make substantial contributions to total carbon loss, when applied on their on their own, only a small increase in biomass gain is to be expected. Amthor et al. (2019) therefore suggest combining multiple targets in a plant, thereby stacking their individual carbon savings.

Nevertheless, it would constitute a substantial engineering effort to implement even just one of these proposed strategies, especially when they require not just the introduction of more carbon-efficient components but also the removal or down-regulation of the inefficient plant-native pathway.

Additionally, some proposed targets for reducing respiratory losses may not be universally applicable across crop species. For instance, Amthor et al. highlighted the replacement of the plant-native THI4 thiazole synthase, which is important for thiamin production, as a very promising strategy. At the time of writing, it was believed that the THI4 enzyme functions as a suicide enzyme in all plants. Suicide enzyme catalyse only a single reaction before being degraded (Chatterjee et al., 2011). Because this necessitates continual *de novo* synthesis of the protein, Amthor et al. suggested that replacing it with the non-suicidal version known in microbes could substantially reduce metabolic costs. However, bioinformatic analyses conducted at a later date (Joshi et al., 2020) indicated that important cereal crops, including wheat and barley, already encode non-suicidal forms of THI4. This means this strategy, once considered highly effective for carbon savings in Amthor et al., would not actually be applicable to some of the world's most

important staple crops.

1.3.3 Refixing respiratory CO_2

Another potential strategy for reducing carbon losses, which has so far not been discussed, is to refix respiratory CO_2 while it is still within the plant cell or tissue, before it is lost to the atmosphere (Fig. 1.1C). In such a system, the captured carbon could either be bound to an intermediary molecule that is decarboxylated during daylight hours when Rubisco is active, or the carboxylated molecule could potentially feed directly into biosynthetic pathways as a precursor.

A key advantage of this nocturnal CO_2 fixation pathway is that it would be entirely agnostic to the original source of CO_2. Such a system should therefore theoretically work in all plants, regardless of which specific metabolic pathways they possess or which ones are active under current environmental conditions. This gives the approach broad potential applicability across different plant species, developmental stages and varying growing conditions.

During daylight hours, Rubisco naturally fixes not just atmospheric CO_2 but also some of the metabolically generated CO_2 released within the leaf. This can be further enhanced by placing chloroplasts at the cell periphery, thereby increasing the chance that internally generated CO_2 will re-enter carbon assimilation (Busch et al., 2013). However, a substantial portion of respiratory carbon loss occurs at night (Tcherkez et al., 2017; O'Leary et al., 2019) when the CBB cycle is inactive and this CO_2 cannot be recaptured by Rubisco (Portis and Jr., 2003).

The central question regarding nocturnal CO_2 refixation is whether the additional expenditure of energy at night to refix respiratory CO_2 would provide a net benefit to plant growth. CO_2 fixation inherently requires energy input (Bar-Even et al., 2012a). The viability of this strategy therefore depends on whether the carbon gain

from refixation exceeds the cost of providing the necessary energy and reducing power at night.

Given the complexity of this problem, it appears prudent to utilise methods to first assess the likely consequences and potential benefits of implementing a nocturnal CO_2 refixation pathway *in silico*, before venturing to test this strategy experimentally in plants.

1.4 Metabolic modelling to investigate respiratory CO_2 refixation strategy

Metabolic modelling provides a theoretical framework for exploring the organisation and behaviour of cellular metabolism. By simulating how metabolites are produced, consumed, and redistributed, modelling can be used both to gain mechanistic insight into metabolic processes and to predict the outcome of perturbations. This has made computational approaches a valuable tool not only in systems biology but also in identifying and evaluating potential metabolic engineering strategies (Nikoloski et al., 2015).

A widely applied approach is *constraint-based metabolic modelling*. This method relies on reaction stoichiometries to represent an organism's metabolic network. Because only the structure of the network and basic physico-chemical constraints (such as mass and charge balance, and reaction directionality) are required, constraint-based models can be built at the genome scale, encompassing essentially all annotated enzymatic reactions of an organism (Sweetlove and Ratcliffe, 2011). Such models allow the simultaneous consideration of interactions between diverse pathways, providing a system-level perspective on metabolic capabilities and limitations.

An alternative computational modelling approach is *kinetic modelling*, which incorporates experimentally determined enzyme kinetic parameters to predict dynamic changes in metabolite concentrations and fluxes. In principle, kinetic models can deliver highly accurate, condition-specific predictions. However, the data requirements are substantial: kinetic parameters must be measured for each enzyme under defined conditions, and these values often vary with environment and cell type (Shameer et al., 2022; Miskovic et al., 2015). As a result, kinetic modelling is usually restricted to individual pathways or small subsystems. For the larger scale questions addressed here concerning the whole of primary carbon metabolism, such data were not readily available, making constraint-based modelling the only practical and appropriate approach.

This systems-level scope offered by constraint-based modelling is particularly relevant to the question of respiratory CO_2 refixation. CO_2 is released by numerous processes across central metabolism, and any attempt to re-assimilate this carbon requires a holistic view of the network. Specifically, one must account for the energetic costs, availability of reducing equivalents, substrate supply, the metabolic fate of refixed carbon, and the handling of potential by-products. Constraint-based modelling provides a framework to address these questions by assessing whether the necessary precursors, energy, and reducing power are available for nocturnal refixation and whether the resulting products can be channelled into useful metabolic routes.

1.4.1 Use of a core metabolic model

In this work, I employed a core model of plant metabolism rather than a genome-scale reconstruction. Core models, such as the one used here, described by Shameer et al. (2018) and related studies, focus on representing the central pathways of primary metabolism. These include photosynthesis, respiration, photorespiration,

carbohydrate metabolism, amino acid biosynthesis, synthesis of cell wall components, and associated energy and redox transformations. By design, such models exclude reactions from specialised or secondary metabolism, which are highly species- and tissue-specific.

The rationale for using a core model is threefold. First, primary metabolic pathways are broadly conserved across photosynthetic plants, meaning the model provides a general representation that is not restricted to a particular species. Second, my research question concerns respiratory CO_2 losses, which predominantly arise from central metabolic processes such as glycolysis, the tricarboxylic acid cycle, the and associated metabolic routes. As such, restricting the network to primary metabolism avoids unnecessary complexity while still capturing the major sources of respiratory CO_2. Third, using a simplified but mechanistically grounded model also facilitates clearer interpretation of predicted flux distributions. Thus, the core model serves as a tractable yet sufficiently representative framework for exploring respiratory CO_2 refixation strategies in photosynthetic plants.

1.4.2 Flux Balance Analysis

Flux Balance Analysis (FBA) is a widely used constraint-based modelling approach that predicts metabolic fluxes through a network at steady state (Orth et al., 2010). The basic assumption is that, over the timescales of interest, intracellular metabolite concentrations remain approximately constant. This allows the system to be described by mass-balance equations, in which the production and consumption of each metabolite must balance out.

In practice, the metabolic network is represented by a stoichiometric matrix S, in which each column corresponds to a reaction and each row to a metabolite. In this matrix, each reaction equation is represented by setting the value for each

metabolite according to its stoichiometric coefficient, or to 0 if it does not participate in the reaction. A flux vector v contains the unknown flux values for all reactions. The steady-state assumption is then expressed as $S \cdot v = 0$, meaning that for every metabolite the total rate of production across all metabolic reactions equals the total rate of consumption. Because metabolic networks usually contain more reactions than metabolites, this system of equations is underdetermined and therefore allows many possible solutions. FBA resolves this by applying linear optimisation to identify one optimal solution that satisfies the constraints while maximising (or minimising) the chosen objective function. Typically assumed objectives for biological systems are the maximisation of biomass output, which represent growth, or the minimisation of energy use.

When optimising for the given objective, multiple constraints are considered simultaneously, including reaction stoichiometry, specified upper and lower bounds for each reaction flux, the overall network structure, and any additional rules such as fixed ratios between related reactions. The resulting flux distribution represents one of the mathematically optimal solutions towards the specified objective, given all these constraints. Because FBA does not require kinetic parameters, but only relies on network topology and constraints, it is particularly well suited for large-scale systems.

To use FBA, one initially only needs to represent the repertoire of enzymes, non-enzymatic reactions and transporters present in the organism of interest by their mass- and charge-balanced chemical equations. Together, these form the metabolic network. Additional equations are added to represent input of substrates, such as atmospheric CO_2 or sugars of the phloem sap, and output of biomass components and compounds that are secreted by the organism. Applying constraints based on experimental data limits the possible solution space and is often sufficient to allow the models to reproduce known metabolic behaviour

(O'Brien et al., 2015).

FBA models have found widespread use in predicting and analysing plant metabolism (Cheung et al., 2014; Shameer et al., 2019; Saadat et al., 2023; Grafahrend-Belau et al., 2009; Tay et al., 2021; Töpfer et al., 2020; Smith et al., 2025). Notably, Cheung et al. (2014) presented a major advance in plant metabolic modelling, allowing the representation of both day and night-time metabolism of plants in a single optimisation problem. The two temporal phases were connected by "linker metabolites", allowing some defined metabolites that are known to be able to accumulate in plants, to transfer between the two time phases. The model could then make predictions as to how daytime metabolism worked to serve night-time metabolism, e.g. by accumulating starch produced during the day for night-time respiration, and vice versa, e.g. by accumulating citrate at night to serve as a carbon skeleton for nitrate assimilation.

To assess the suitability of new engineering strategies, one can add reactions representing the enzymes of heterologous pathways that may be transferred into the organism or remove those for enzymes that should be knocked out. By analysing the impact that these changes have on the rest of the metabolic network, especially the biomass output, we can then select the most promising strategies towards the goal of increasing plant growth.

1.5 Thesis Outline

The remainder of this thesis is organised as follows:

> **Chapter 2** — explores methods to create a carbon-limited plant metabolic model. After establishing carbon limitation in different ways, I investigated the emergence of a plant-native nocturnal CO_2 refixation mechanism,

namely CAM cycling. I then suppressed CAM cycling to create a baseline model that maintains carbon limitation but does not utilise native enzymes for CO_2 recovery pathways as this would be unrealistic for typical C3 crops. This baseline model serves as the foundation for further investigations in Chapter 3.

Chapter 3 — examines the potential of an artificially created CO_2-fixing pathway (the CETCH cycle) when introduced into the carbon-limited plant model developed in Chapter 2. I evaluate its capacity to refix nocturnally generated CO_2 and its potential to improve plant growth rates.

Chapter 4 — presents both computational modelling and experimental investigations of the liverwort *Marchantia polymorpha*, to address claims of enhanced carbon conversion efficiency via CAM cycling.

2 | Implementing carbon limitation in a plant metabolic model

2.1 Introduction

To investigate carbon limitation in the model, and potential nocturnal CO_2 refixation behaviour to alleviate it, my strategy was to set up a model of diel leaf metabolism that is incentivised to be as carbon use efficient as possible while still aiming for maximal growth. This approach necessitates that carbon becomes the most limiting factor in fulfilling the model's given objective. A carbon-limited model should explore all available options to utilise carbon as efficiently as possible, thereby priming it to reduce CO_2 loss due to nocturnal respiration or to refix nocturnal, respiratory CO_2 rather than releasing it to the atmosphere.

There may be multiple ways to induce carbon-limitation in the model. My approach focuses on adjusting carbon inputs and outputs to create a demand for carbon, without directly forcing the model to perform nocturnal CO_2 refixation if it is not the optimal strategy for maximising growth. Forcing certain metabolic behaviours or overconstraining the model could mask cost-benefit trade-offs inherent in metabolic processes. Giving the model the freedom to explore a range of metabolic behaviours yields a more nuanced understanding of the conditions under which nocturnal CO_2 refixation may become advantageous.

This model is set up to represent a photosynthetically active and growing leaf, where CO_2 uptake is the sole carbon input. Other potential sources of carbon, such as uptake of compounds from the phloem, are excluded. Consequently, constraining the flux through the reaction representing atmospheric CO_2 uptake is sufficient to limit the total carbon supply.

Carbon outputs in the model are represented by reactions that remove carbon-containing compounds from the metabolic network. Plant growth is simulated through a "biomass reaction", which converts all expected biomass components (amino acids, proteins, nucleic acids, carboxylic acids, cell wall components, etc.) into a generic "plant biomass" pseudo-metabolite. The stoichiometric coefficients of each biomass component correspond to its contribution to plant dry mass. Apart from minerals, all biomass components contain carbon. In this model setup, the only other potential carbon output is the nocturnal CO_2 exchange reaction which allows CO_2 generated at night to exit the leaf to the atmosphere. The nocturnal copy of the CO_2 exchange reaction is configured to permit CO_2 loss but prevent its uptake from the atmosphere, to avoid net CO_2 uptake at night and instead focus only on losses or refixation of nocturnal respiratory CO_2.

To create carbon demand in the model, carbon outputs must be stimulated to remove carbon from the model while the carbon input is constrained. By setting the primary objective of the model as maximising the flux through the biomass reaction (i.e., maximising growth) and constraining the maximum allowed daytime CO_2 uptake rate, the model should be forced into a state of carbon limitation.

This carbon-limited model is crucial for addressing two key questions regarding the potential to increase carbon use efficiency through nocturnal CO_2 refixation in plants:

1) Does the plant metabolic network possess an inherent capacity to refix respired CO_2 at night using enzymes already present in the plant genome? By imposing carbon limitation on the model, we may discover that plant-native reactions could be repurposed for nocturnal refixation of respired CO_2.

2) Could artificially created CO_2-fixing pathways, when expressed in plants at night, form a nocturnal CO_2 refixation pathway to enhance plant productivity?

To investigate the potential of heterologous pathways, a suitable plant model must first be established. This "baseline" model should ideally still represent C3 metabolism without performing nocturnal CO_2 refixation, despite experiencing carbon stress. This approach ensures that the model is primed to utilise any additional pathways that could alleviate carbon limitation, but only if they can be effectively integrated with the existing metabolic network and result in higher growth rates.

2.2 Methods

2.2.1 General model setup

The initial stoichiometric model, encompassing all core metabolic reactions and transport processes across the subcellular compartments typically found in most plants, was taken from Shameer et al. (2019).

This core model has since undergone updates. Notably, in Shameer et al. the protonation states of metabolites at different subcellular pH levels were represented by creating multiple copies of the same metabolite, one for each protonation state (e.g. “MAL_v” and “aMAL_v”, for malate(2-) and malate(1-) present in the vacuole). Each of these protonation state metabolites was then incorporated into every reaction involving that compound, with stoichiometric coefficients proportional to their abundance at the given pH (i.e. 0.7 MAL_v + 0.3 aMAL_v for malate(2-) and malate(1-) in the vacuole, with a pH of 5.).

This approach has since been changed to represent each compound’s protonation states in a single metabolite entry. This was accomplished by adjusting the chemical formula to include a fractional number of hydrogen atoms that reflects the average of all protonation states. For instance, at the cytosolic pH of 7.0 malate

exists as fully dissociated malate(2-) and was therefore denoted as $C_4H_4O_5$. At the vacuolar of pH 5.0, malate exists as 70% malate(2-) and 30% malate(1-) and therefore the formula is $C_4H_{4.3}O_5$ in the vacuole. This simplifies the model while maintaining accurate representation of protonation states at different pHs of subcellular compartments.

I used the COBRApy package (Ebrahim et al., 2013) for Python 3 to further modify the structure and constraints of the core model as described below and to make predictions of fluxes using FBA. The GNU linear programming kit (GLPK) solver was used for all optimisations.

The core plant metabolic model was adapted to represent distinct day and night phases, following the methodology outlined by Cheung et al. (2014). This involved duplicating all metabolites and reactions and appending "_day" or "_night" suffixes to differentiate between phases. For the day phase, the photon influx reaction was constrained to a maximum of 200 μmol m^{-2} s^{-1} photosynthetic photon flux density (PPFD), simulating typical light conditions in an experimental growth-room or glasshouse setting. The duplicate of this reaction was set to zero for the night phase, to represent complete darkness. Fluxes in these two phases are treated equally, therefore constituting a scenario of equal day and night length, comparable to a 12 h/12 h photoperiod.

To account for metabolite accumulation between phases, linker reactions were introduced for select compounds known to exhibit diel fluctuations. These reactions facilitated the interconversion of "_day" and "_night" metabolites. The metabolites selected for this treatment included starch, sucrose, nitrate, various carboxylic acids (malate, citrate, succinate, fumarate), and all twenty proteinogenic amino acids. Based on data from Scheible et al. (2000), amino acids were only allowed to accumulate from day to night.

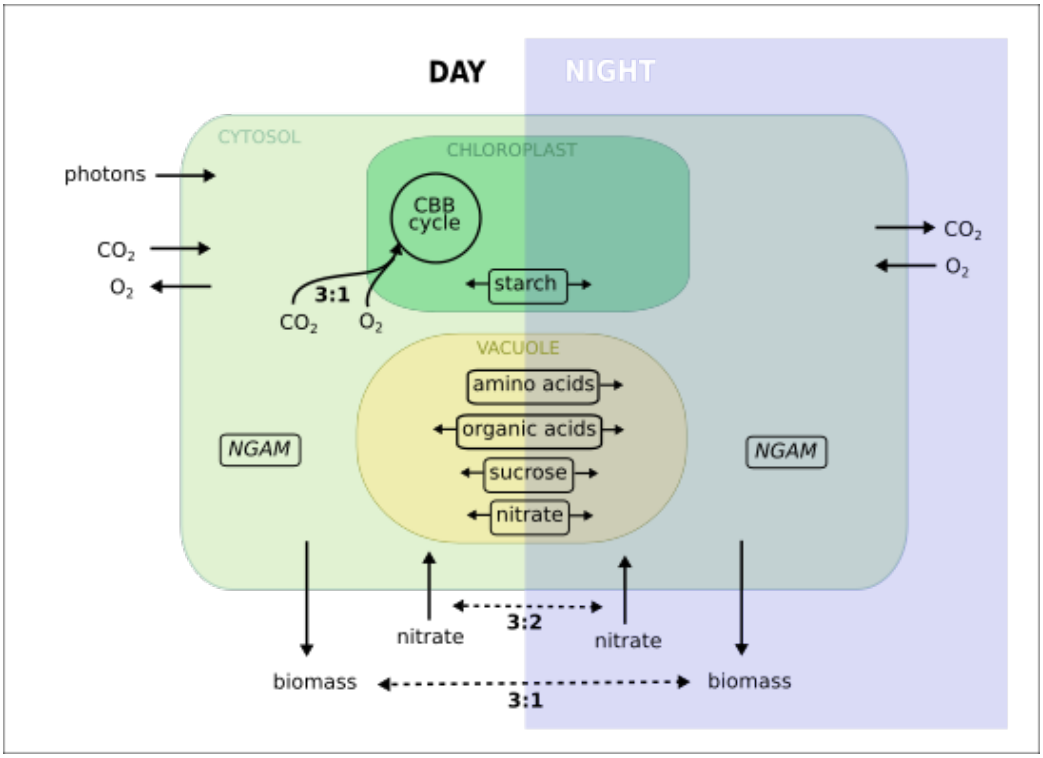

Figure 2.1: **Basic schematic of diel stoichiometric model showing inputs, outputs and constraints applied.**
Abbreviations: NGAM, non-growth-associated maintenance costs; CBB cycle, Calvin-Benson-Bassham cycle

The daytime CO_2 uptake rate ("CO2_tx_day") was initially unrestricted. Then I applied constraints on the upper bound of the reaction as specified in the text.

Additional constraints adapted from Shameer et al. (2019) and the reason behind their implementation are listed in Table 2.1. A simplified schematic, representing diel model architecture and constraints, is given in Figure 2.1 and generic reactions representing non-growth associated maintenance costs (NGAM) are illustrated in Figure 2.2. In this setup, a single optimisation yields a solution for the predicted optimal distribution of flux throughout the network representing diel plant metabolism, more specifically a growing photosynthetic leaf, allowing for interactions between the day and night phase.

Table 2.1: **List of constraints applied for general setup of diel plant metabolic model.**

Constraint	**Reason for constraint**
Primary objective to maximise biomass output reaction flux	To represent growth as the main objective.
Biomass equation set to AraCore Biomass (Arnold and Nikoloski, 2014)	To use biomass composition that includes diverse metabolites, representative of Arabidopsis.
Secondary objective set to minimising sum of all fluxes (pFBA)	To stipulate efficient use of cellular resources (Holzhütter, 2004).
Light input in day phase set to 200 µmol m^{-2} s^{-1}	To limit light energy supply to the model to realistic lab environment levels.
Light input in night phase set to 0 µmol m^{-2} s^{-1}	To represent darkness at night.
Biomass output day to night ratio constrained to 3:1	To force a bit of growth to occur at night.
Rubisco carboxylase : oxygenase activity constrained to 3:1	To represent Rubisco's carboxylation to oxygenation activity ratio typical for C3 plants (Jordan and Ogren, 1984).
Nitrate uptake day to night constrained to 3:2	To require some nitrate uptake to occur at night.
CO_2 exchange reaction at night set to only allow CO_2 going out	To avoid any nocturnal uptake and fixation of atmospheric CO_2.
Specific value for maintenance derived from photon intensity	Flux through ATPase set in relation to PPFD (Shameer et al., 2019).
NGAM reactions ATP hydrolase and NADPH oxidases set to a ratio of 3:2	Requiring NGAM to occur by consuming ATP and NADPH in a set ratio.
NGAM day to night ratio set to be equal day and night	Representing equal maintenance costs during the day and night.
Turn off Rubisco at night	To ensure inactivity of Rubisco at night.

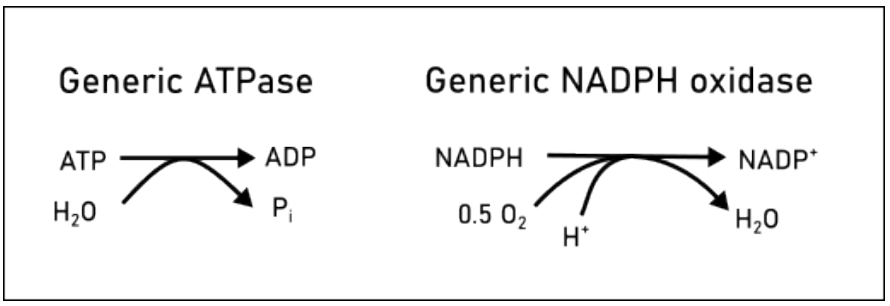

Figure 2.2: **Generic reactions representing non-growth associated maintenance costs.**
Generic ATPase and NADPH oxidase reactions are included in the model, and forced to carry flux, to represent the consumption of ATP and NADPH in processes related to cellular maintenance.

2.2.2 Calculating % nocturnal CO_2 refixation

The focus of this work required me to define a novel metric, % nocturnal CO_2 refixation (%nCO2R), that would specifically capture nocturnal CO_2 refixation behaviour. I developed a function to calculate the percentage of nocturnally produced CO_2 which is refixed. The function identifies all nocturnal reactions in the model involving CO_2. For each reaction producing CO_2, it sums up the product of the reaction flux and the stoichiometric coefficient for CO_2. Similarly, it calculates the total amount of CO_2 consumed, excluding the CO_2 exchange reaction, which represents CO_2 loss to the atmosphere.

The sum of nocturnal CO_2 consumed is then divided by the sum of nocturnal CO_2 produced, and the result is converted to a percentage (Equation 2.1). This percentage reflects the extent of nocturnal CO_2 refixation. A value of 0% would indicate that none of the CO_2 generated at night was refixed by metabolic reactions, and that all respiratory CO_2 was lost as CO_2 exchange to the atmosphere. A value of 100% means that all of the CO_2 generated at night was refixed and none was lost to the atmosphere.

$$nCO_2R\ (\%) = \frac{Total\ CO_2\ _{(nocturnal)\ consumed}}{Total\ CO_2\ _{(nocturnal)\ produced}} \times 100\% \tag{2.1}$$

2.2.3 Extracting % nocturnal CO_2 refixation from previous literature

Predicted fluxes from the model reported in Shameer et al. (2018) were extracted from the publication's supplementary data. All nocturnal CO_2-consuming and CO_2-producing reactions were identified based on the provided reaction equation, and % nocturnal CO_2 refixation was calculated as described above.

2.3 Results

2.3.1 General plant diel model setup

Following the methods described earlier, I set up a model to represent the diel metabolism of a growing leaf. Where available, constraints were chosen to represent a growing Arabidopsis leaf. Arabidopsis has been studied extensively, providing the most comprehensive data to formulate relevant constraints for accurate modelling. Arabidopsis is a C3 plant and so the results obtained may be applicable in broad terms to other C3 plants including important crops. However, crop-specific models would be necessary to make quantitative statements about the impact of nocturnal carbon recovery due to differences in core metabolism, for example different overnight stores of carbon and variations in biomass composition of the leaves.

All optimisations were designed to maximise the flux through a biomass output reaction, thereby representing a model with growth maximisation as its primary

objective. The biomass reaction equation was derived from the AraCore model developed by Arnold and Nikoloski (2014). This reaction reflects the biomass composition of Arabidopsis rosette leaves, encompassing compounds such as the cell wall components, proteins, carbohydrates, lipids, nucleotides, and soluble metabolites accounting for their relative proportions via the set stoichiometry values in the biomass equation.

As a secondary objective, I implemented minimisation of the sum of all fluxes, a technique known as parsimonious FBA (pFBA). High flux through a reaction typically indicates a high demand for enzymatic activity, necessitating high amounts of the associated enzymes. By minimising the sum of fluxes, pFBA favours solutions that reduce the investment in enzyme amount, reflecting a more realistic scenario where metabolism evolved to cope with finite cellular resources (Holzhütter, 2004).

The constraints applied were those listed in Table 2.1. Figure 2.3 shows the metabolic behaviour in the form of a flux map, which is a diagrammatic representation of select metabolic reaction, with the width of arrows scaled by the predicted flux. Key metrics of metabolic behaviour for this and subsequent model optimisations are presented in Table 2.2.

I assessed whether the model achieved the goal of representing metabolism of a growing leaf, by examining the predicted fluxes for reactions representing pathways important to plant metabolism. Most of the predicted major fluxes were as expected for a leaf and are broadly similar to those previously found in this diel model formulation (Cheung et al., 2014). The main fluxes are summarised in Figure 2.3.

For example, during the day, the light-dependent reactions of photosynthesis used photons to produce ATP, NADPH, and O_2. CO_2 was taken up and processed by

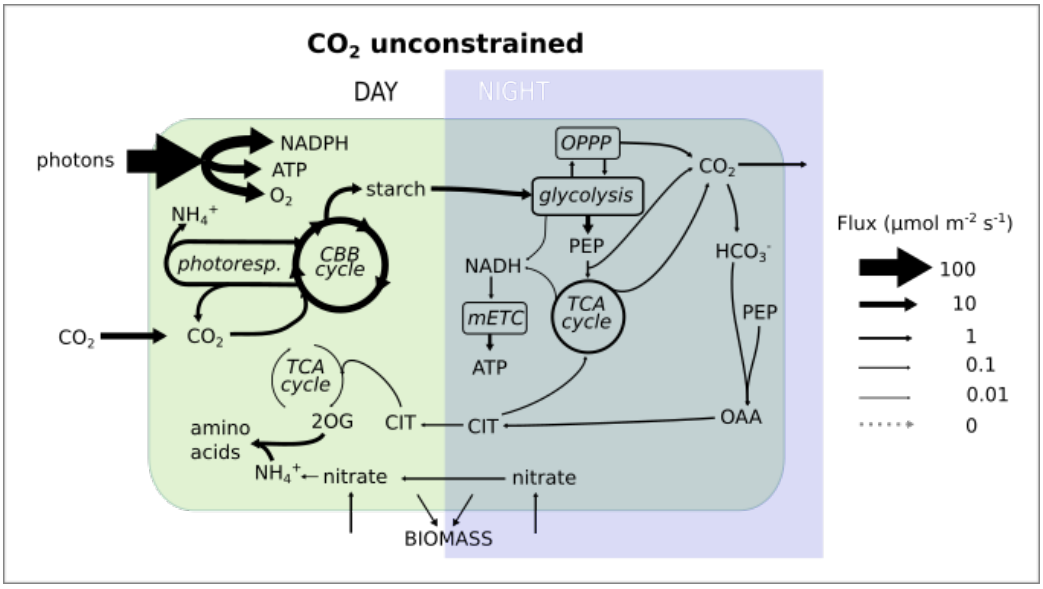

Figure 2.3: **Major flux routes through the "CO_2 unconstrained" diel plant model.**
Subcellular compartments are omitted for clarity. Arrow widths are proportional to the predicted flux. Abbreviations: PEP, phosphoenolpyruvate; OAA, oxaloacetate; MAL, malate; CBB cycle, Calvin-Benson-Bassham cycle; photoresp., photorespiratory pathway; OPPP, oxidative pentose phosphate pathway; TCA cycle, tricarboxylic acid cycle

Table 2.2: **Key metrics for modelling scenarios with specific implementation of CO_2 constraints.**

	CO_2 unconstrained	**CO_2 uptake constrained**	**Objective constrained**	**CO_2 uptake constrained & noct. PEPC limited**
Biomass output rate (µmol m^{-2} s^{-1})	0.1283	0.0767	0.0625	0.0655
Photon use (of 200 µmol m^{-2} s^{-1})	100%	69.56%	55.66%	61.17%
Daytime CO_2 uptake (µmol m^{-2} s^{-1})	12.380	6.643	6.643	6.643
Nocturnal CO_2 loss (µmol m^{-2} s^{-1})	1.278	0.0	1.236	0.970
Rubisco CO_2 assimilation flux (µmol m^{-2} s^{-1})	14.79	9.79	7.94	8.49
% nocturnal CO_2 refixation	35.78%	100%	26.36%	39.50%
Total carbon conversion efficiency	89.81%	100%	81.47%	85.40%
Nighttime carbon conversion efficiency	75.76%	100%	60.84%	87.42%
Total sum of fluxes (µmol m^{-2} s^{-1})	1321.82	972.06	739.90	850.16

Rubisco in the CBB cycle. Some of this carbon was converted to starch in the plastid during the day, to then be transferred to the dark phase of the model. Rubisco oxygenation also occurred as prescribed, with Rubisco catalysing one oxygenation reaction for every three carboxylation reactions. Oxygenation produced 2PG, which was recycled in the classical photorespiratory pathway across the plastid, peroxisome and mitochondrion at the cost of releasing CO_2 and ammonia. All CO_2 generated metabolically during the day was reassimilated by Rubisco, making the rate of CO_2 assimilation by Rubisco higher than the rate of atmospheric CO_2 uptake.

At night, the model predicted that the starch, which had been accumulated during the day, was broken down via glycolysis and the TCA cycle, providing NADH and ATP at night. NADPH was generated via the oxidative pentose phosphate pathway (OPPP). These processes, along with reactions for biomass synthesis, released CO_2.

Citrate was produced at night and accumulated in the vacuole to be transferred to the day phase. During the day, this citrate then entered a non-cyclic TCA cycle, producing 2-oxoglutarate (2OG). 2OG then combines with NH_4^+ to form glutamate and glutamine as part of the nitrogen assimilation pathway. This is consistent with our understanding of the source of carbon skeletons for nitrogen assimilation from ^{13}C-labelling studies (Gauthier et al., 2010).

2.3.2 Carbon metabolism in a C3 leaf model

Given the central role of carbon in this study, the next step was to examine the carbon metabolism in this model more closely, with particular attention to the dark phase. In the following sections I refer to this model as 'CO_2 unconstrained' since there was no limit imposed on the model on the CO_2 uptake reaction. This

contrasts with subsequently explored models in which the CO_2 uptake reaction was constrained to create a carbon-limited model scenario. These constraints were either direct, by applying an upper limit on the CO_2 uptake reaction (referred to as the 'CO_2 uptake constrained' model), indirect via constraining the objective value (referred to as the 'Objective constrained' model) or direct on the CO_2 uptake reaction with an additional constraint on the nocturnal PEPC flux (referred to as 'CO_2 uptake constrained and nocturnal PEPC limited' model).

During the light phase, atmospheric CO_2 uptake in the CO_2 unconstrained model occurred at a rate of 12.380 μmol m^{-2} s^{-1}. The model predicted that all atmospheric CO_2, as well as all metabolically generated CO_2 during the day, was reassimilated by Rubisco, resulting in a CO_2 assimilation rate exceeding the atmospheric CO_2 uptake rate by about 20%. The primary metabolic sources of CO_2 during the light phase were identified as the glycine decarboxylase complex (part of the photorespiratory pathway) (17%), carbonic anhydrase (CA) followed by PEPC (9%), and isocitrate dehydrogenase (ICDH) (4%).

Carbon accumulation from the light to dark phase occurred at a total rate of approximately 5.2 μmol m^{-2} s^{-1}. This accumulated carbon was primarily composed of starch (75.5%), isoleucine (20.5%), and the remaining 4% consisted of the amino acids phenylalanine, lysine, methionine, threonine and arginine.

In the dark phase, the accumulated carbon could follow three potential pathways: 1) incorporation into biomass as carbon-containing components, 2) release to the atmosphere as CO_2, or 3) transfer back to the light phase as carboxylic acids or sugars. It should be noted that in this model configuration, amino acids were specified to accumulate only from the light to dark phase.

CO_2 was generated at night at a rate of 2.067 μmol m^{-2} s^{-1}, predominantly by reactions of glycolysis (pyruvate dehydrogenase), the OPPP (6-phosphogluconate

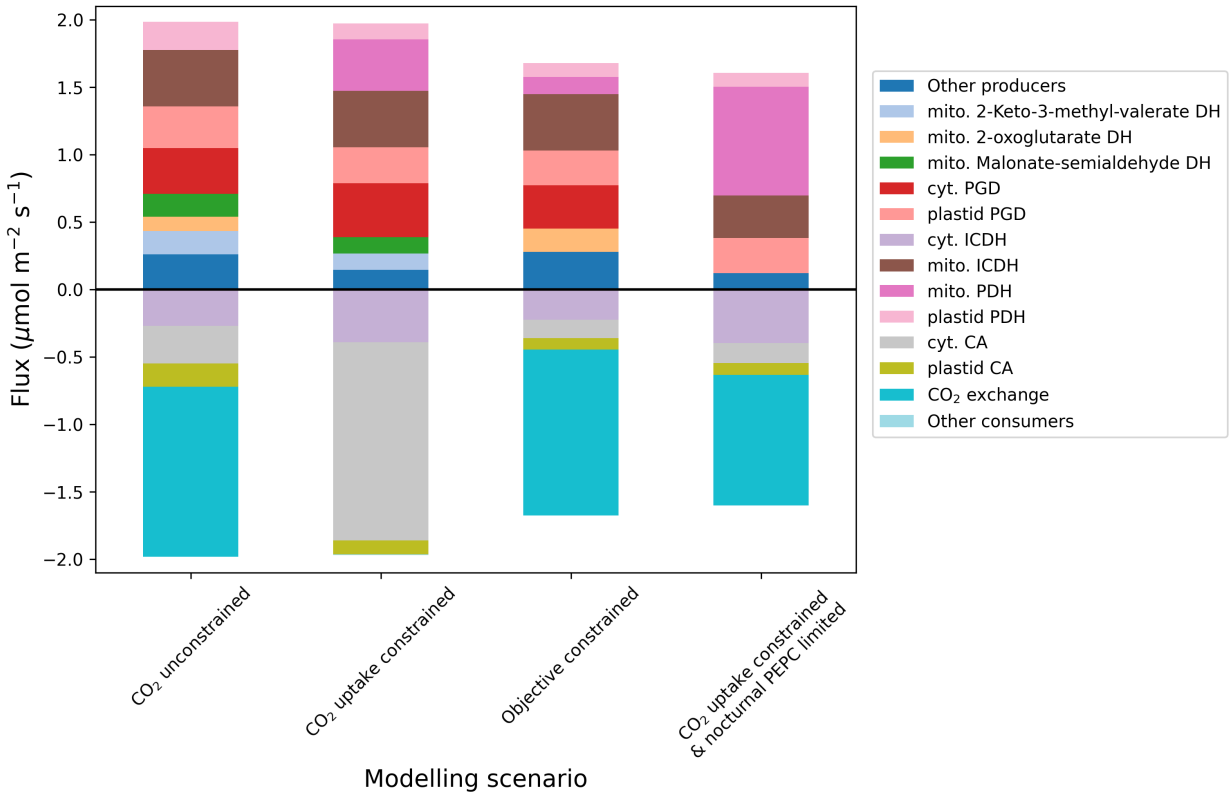

Figure 2.4: **Nocturnal CO_2 budgets across modelling scenarios.**
All reactions contributing to nocturnal CO_2 production or consumption across subcellular compartments were quantified, accounting for flux magnitude, direction, and stoichiometry. Positive values represent CO_2-producing reactions, while negative values indicate CO_2-consuming processes. Abbreviations: cyt., cytosolic; mito., mitochondrial; ICDH, isocitrate dehydrogenase; PDH, pyruvate dehydrogenase; PGD, 6-phosphogluconate dehydrogenase; CA, carbonic anhydrase; DH, dehydrogenase.

dehydrogenase), and the TCA cycle (ICDH and 2OG dehydrogenase) (Fig. 2.4).

The model predicted that 60.5% of nocturnally produced CO_2 was lost to the atmosphere via the CO_2 exchange reaction, while 39.5% was refixed. This refixation process occurred primarily through the action of PEPC (using bicarbonate produced by CA as a substrate) and to a smaller extent by ICDH. Tracing the flux through subsequent reactions suggests that this nocturnal CO_2 refixation primarily resulted in citrate production, with about 55% of this nocturnally produced citrate accumulating from night to day where it served nitrogen assimilation, whereas the rest continued in the TCA cycle.

2.3.3 Nocturnal respiratory CO_2 refixation in a non-carbon-limited model

That this plant diel model should exhibit nocturnal respiratory CO_2 refixation of 39.5% even before any changes to represent carbon-limitation were implemented, was unexpected. % nocturnal CO_2 refixation is a metric that has not been previously reported in modelling studies of plant metabolism. To investigate whether nocturnal CO_2 refixation occurred in previous modelling studies, albeit undetected, I calculated the % nocturnal CO_2 refixation from the data available in Shameer et al. (2018), for their C3 model. This previous modelling study investigated productivity of full CAM by comparing it to a C3 model, which in this case was similarly created by not constraining daytime CO_2 uptake rates. The rest of the model setup was also largely similar, being a diel model with equal day and night periods, and based on the same core plant metabolic model, albeit an earlier version.

In their results, PEPC was inactive during the dark phase, while ICDH functioned solely as a CO_2-producing enzyme. The calculated % nocturnal CO_2 refixation

was 0%, indicating that all CO_2 generated during the dark phase was released to the atmosphere at a rate of 2.28 µmol m^{-2} s^{-1}. This was comparable to the nocturnal rate of total CO_2 production in my model, as was the daytime CO_2 uptake rate which carried a flux of 13.19 µmol m^{-2} s^{-1}.

To elucidate the factors contributing to the marked increase in nocturnal CO_2 refixation in a non-carbon-limited model, from 0% in the Shameer 2018 model to 39.5% in my current model, I closely compared the setup of diel plant model between these two studies. This investigation aimed to identify key differences in model structure, constraints, or assumptions that might account for the emergence of nocturnal CO_2 refixation behaviour in my model.

Notably, in the Shameer 2018 model, the NGAM costs were chosen based on achieving a nocturnal carbon conversion efficiency of 50%. In practise, this meant increasing the flux through the generic ATPase (with the flux through generic NADPH oxidases increasing proportionally) until 50% of the carbon accumulated from the light to the dark phase was lost as CO_2. In my model, based on updates in Shameer et al. (2019), the ATPase flux was chosen according to a linear equation relating its flux to the maximum photon influx.

For the Shameer 2018 model, 50% nocturnal CEE was achieved at an ATPase flux of 8.5 µmol m^{-2} s^{-1}. My model's ATPase flux was less than half of that, at 3.67 µmol m^{-2} s^{-1}, based on the set PPFD of 200 µmol m^{-2} s^{-1}.

To see how different NGAM costs affected nocturnal CO_2 refixation in my model, I performed a scan, systematically increasing the fixed flux through the generic ATPase reaction (Fig. 2.5). While the relationship is non-linear, with a peak forming around an ATPase flux of approximately 2 µmol m^{-2} s^{-1}, it also showed that beyond that, increasing NGAM costs leads to reduced nocturnal CO_2 refixation. However, nocturnal CO_2 refixation was still active (about 22% refixation) at

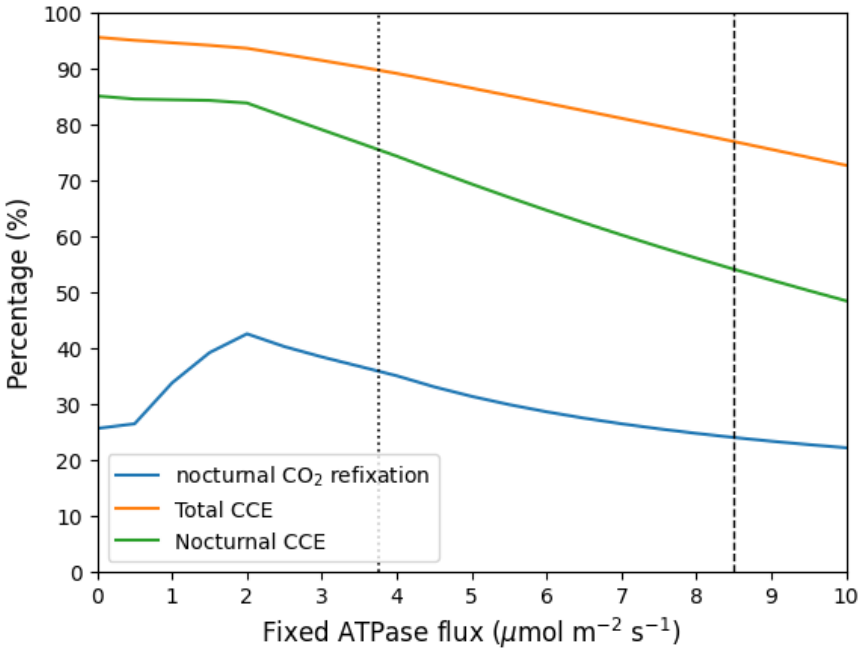

Figure 2.5: **Carbon utilisation efficiencies as a function of increasing non-growth associated maintenance costs.**
The model's nocturnal CO_2 refixation, total CCE and nocturnal CCE are shown in response to increasing non-growth associated maintenance costs, enforced by increasing the fixed ATPase flux in the model. The vertical dotted line indicates ATPase flux value set based on photon intensity, the dashed line indicates ATPase flux value set based on 50% nocturnal CCE efficiency. CCE, carbon conversion efficiency.

the ATPase flux of 8.5 µmol m^{-2} s^{-1} chosen in the Shameer 2018 model.

Another difference between mine and the previous modelling study was the chosen objective. Shameer 2018 used maximisation of phloem output as the primary objective to simulate a mature leaf, whereas my model was set to maximise biomass output to simulate a growing leaf. The specified model output determines which metabolites need to be produced by the model, which can have a big impact on overall carbon metabolism. For example, the biosynthesis of lipid molecules, which are only present in the biomass but not the phloem output, entails multi-

ple decarboxylation steps. The requirement to produce lipid molecules therefore reduces the carbon conversion efficiency.

I used the same phloem output reaction as in the Shameer 2018 model, which is based on tomato phloem output, and set it as the model objective. Compared to when biomass was the objective, with this new objective, nocturnal CO_2 refixation decreased from 39.5% to 18.37%. However, even when combined, the higher NGAM costs and the different objective reaction did not result in eliminating nocturnal CO_2 refixation completely.

There are other factors that could influence the model behaviour which are more difficult to control. For example, Shameer et al. used an earlier version of the core plant metabolic model. Since then, reactions have been modified and added. Because of larger changes made, such as the removal of separate metabolites representing different charge states of the same molecule (see General model setup), it is impractical to use this earlier model version in my current setup for a direct comparison.

PEPC is known to be active in the dark (Gupta et al., 1994), which makes the result from my model plausible. ICDH has also been reported to act in the "reverse" direction to fix CO_2 in plant embryos (Schwender et al., 2006) and predicted as a carbon-fixing reaction in an environment-coupled model of CAM (Töpfer et al., 2020). My model, which performs nocturnal CO_2 fixation, therefore seems reasonable and was used for further analyses.

2.3.4 Survey of experimentally determined net CO_2 uptake rates for Arabidopsis leaves

Next, I explored imposing carbon limitation on the model, by constraining the daytime CO_2 uptake rate, to investigate whether this led to increased fluxes through

native nocturnal CO_2-refixing flux modes. To establish a realistic daytime CO_2 assimilation rate for a C3 plant, I reviewed literature data on CO_2 assimilation rates in *Arabidopsis thaliana*. The CO_2 assimilation rates are dependent on light intensity but increase in a non-linear fashion. More photosynthetically available light allows the plant to produce more ATP and NADPH to power the CBB cycle. However, as light intensity increases further, the rate of CO_2 assimilation eventually plateaus due to limitations in the capacity of the CBB cycle or limits in downstream utilisation of triose phosphates exported from the cycle (Farquhar et al., 1980).

I identified seven studies that reported CO_2 assimilation rates in Arabidopsis (Donahue et al., 1997; Sun et al., 1999; Poulson et al., 2002; Schluter, 2003; Lake, 2004; Tocquin and Périlleux, 2004; Ivanov et al., 2012) at a PPFD of 200 µmol m^{-2} s^{-1}, the same value that was used in the model. At this light intensity, the average CO_2 assimilation rate across these studies was 6.643 µmol m^{-2} s^{-1}, ranging from 5 to 9 µmol m^{-2} s^{-1} (Fig. 2.6).

2.3.5 Restricting daytime CO_2 uptake in the model

Without constraints, the CO_2 uptake reaction reached a flux of 12.380 µmol m^{-2} s^{-1}, which is nearly two times higher than the experimentally determined average value of 6.643 µmol m^{-2} s^{-1} found for Arabidopsis. Consequently, to avoid an unrealistically high carbon influx, it was necessary to implement constraints on the model's daytime CO_2 uptake. Reducing the carbon intake, while still requiring the model to maximise biomass production would also make the model carbon-limited and thus would enable me to explore potential native routes to refixing nocturnally-produced CO_2.

A direct approach to address this issue is to implement an upper bound constraint

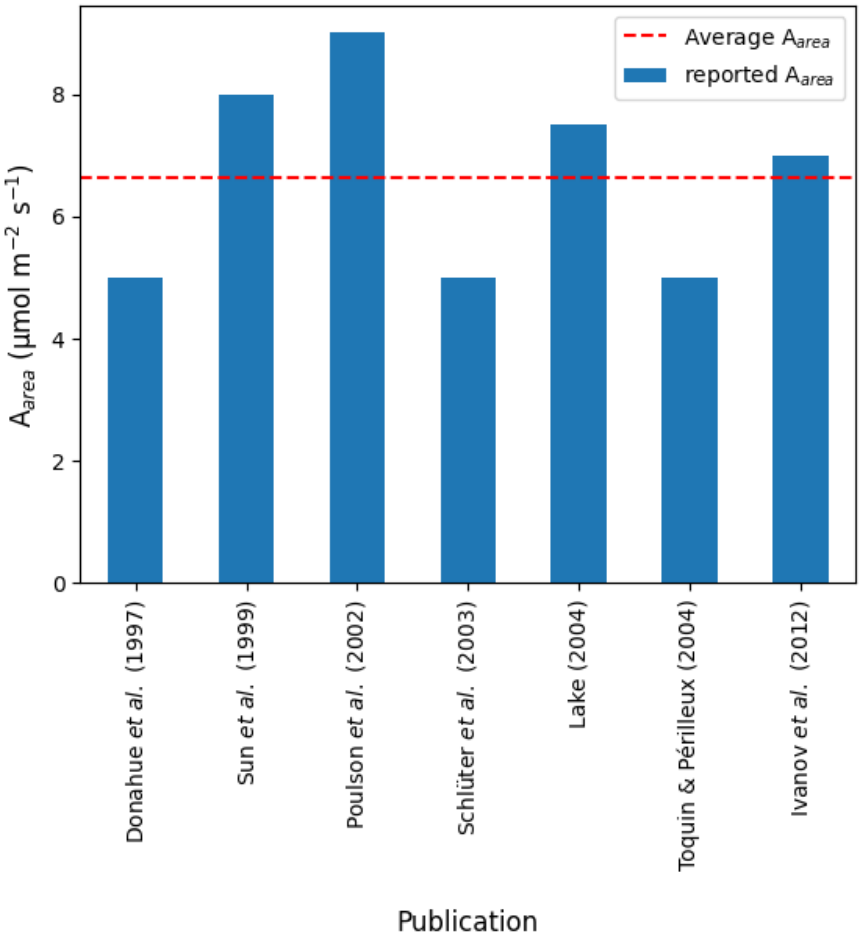

Figure 2.6: **Reported CO_2 assimilation rates in *Arabidopsis thaliana*.** CO_2 assimilation rates normalised by leaf area (A_{area}) were measured experimentally in Arabidopsis at a photosynthetic photon flux density of 200 µmol m^{-2} s^{-1}. The red dashed line represents the average rate across all publications shown.

on the CO_2 uptake reaction during the light phase. To investigate the model's response to reduced carbon availability, I first systematically increased the maximum allowed CO_2 uptake rate by adjusting the upper bound constraint on the light phase CO_2 uptake reaction. At each new maximum CO_2 uptake value, the model was optimised again and the new flux value for each reaction as well as calculated metrics were saved. To assess whether there were shifts in the model's metabolic behaviour in response to changing carbon availability, I focused on key metrics such as % nocturnal CO_2 refixation and fluxes of linker reactions representing metabolite accumulation (Fig. 2.7).

A notable shift in model behaviour occurred even with a slight reduction in the maximum daytime CO_2 uptake rate below its unconstrained maximum value of 12.380 μmol m^{-2} s^{-1}. This shift was characterised by increased starch accumulation from day to night, enhanced accumulation of citrate at night, and the emergence of nocturnal malate accumulation which was consumed during the day phase of the model. Concurrently, % nocturnal CO_2 refixation increased, reaching and maintaining 100% efficiency at daytime CO_2 uptake rates below approximately 11 μmol m^{-2} s^{-1}.

These results suggest that under conditions of limited atmospheric CO_2 uptake, the model adopts a strategy of nocturnal CO_2 refixation to maximise biomass output, which is the optimisation objective of the model. This involved transporting refixed carbon back to the light phase in the form of citrate and malate.

To inspect the metabolic behaviour in detail, I then focused on a single optimisation solution (see Fig. 2.8A). I used the value of 6.643 μmol m^{-2} s^{-1}, identified as the average rate of CO_2 assimilation from experiments in Arabidopsis, as a constraint by applying it directly as the upper limit for the daytime CO_2 uptake reaction in the model. In this solution, 100% nocturnal CO_2 refixation was achieved

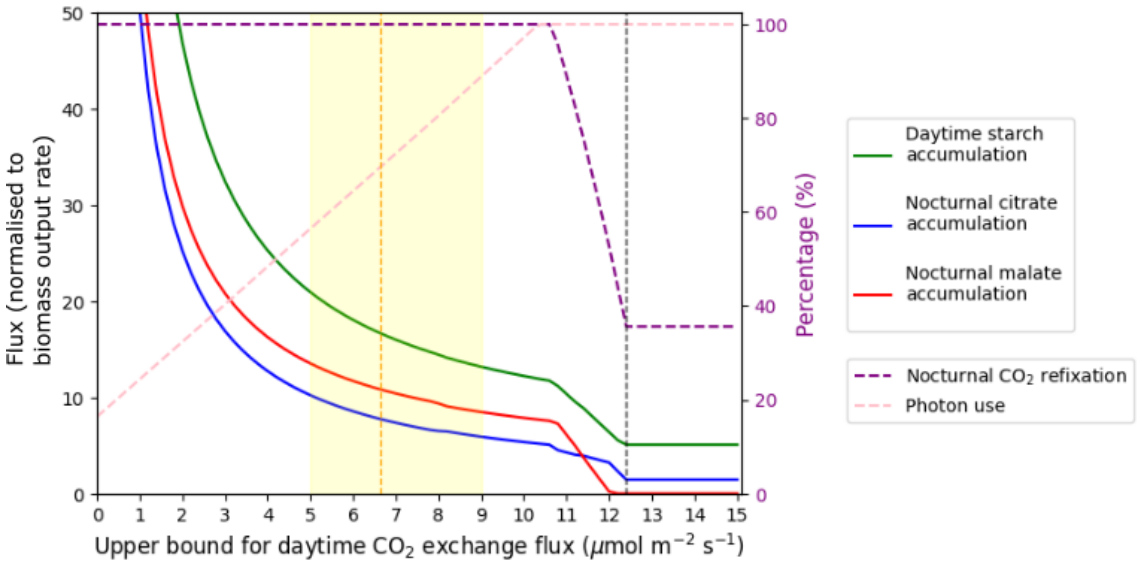

Figure 2.7: **Changes in model behaviour with increasing maximum daytime CO_2 uptake rate.**
The upper bound set for the "CO_2 uptake day" reaction was set to zero and then increased with each iteration and the model was re-optimised. All fluxes were normalised by dividing the reaction flux by the predicted biomass output rate. Normalised fluxes of key metabolic processes are plotted for each iteration (left axis, solid lines) and % nocturnal CO_2 refixation and % photon were calculated (right axis, dashed lines). Yellow highlighted area indicates range of CO_2 assimilation rates reported for Arabidopsis, the orange vertical line indicates the average reported CO_2 assimilation rate. Black vertical line indicates the CO_2 uptake rate reached in CO_2 unconstrained model. For clarity, the left y-axis is truncated at 50 to highlight the change in accumulation processes at higher CO_2 uptake rates.

by a relative increase of the flux through CA, producing bicarbonate from CO_2, followed by PEPC which produced OAA from PEP and bicarbonate. Malate was subsequently produced from the OAA via malate dehydrogenase, and the malate transferred to the vacuole for storage until the day phase. Citrate was also produced via an increase of the flux through ICDH, in the CO_2-fixing direction. During the day phase, nocturnally accumulated malate and citrate were metabolised via malic enzyme, ATP-citrate-lyase and PEP carboxykinase. This released CO_2 in the light phase, for re-assimilation by Rubisco.

Altogether, this is a familiar metabolic behaviour, known as CAM cycling, which is known to occur in some plants, especially under drought conditions (Ting, 1985; Cushman, 2001), and has been investigated, along with other modes of CAM in another FBA modelling study (Tay et al., 2021) (see Discussion). CAM cycling is different from "full CAM", as stomata remain closed at night, and therefore only respiratory CO_2 is refixed at night. As the nocturnal CO_2 exchange reaction is constrained in this model setup to only allow loss of CO_2 and no CO_2 uptake at night, only CAM cycling is available to the model and not full CAM.

It appears that even without considerations of water availability, CAM cycling is beneficial to the model for maximising the biomass output objective, when carbon supply is limited, as CAM cycling circumvents losses of respiratory CO_2 generated at night.

2.3.6 Preventing CAM cycling in a carbon-limited model

CAM cycling emerged as a nocturnal CO_2 refixation pathway in the diel leaf model upon carbon limitation, utilising enzymes typically present in plants as represented by the core metabolic network. This does, however, not mean that it is the only available pathway of this kind within the diel plant metabolic network,

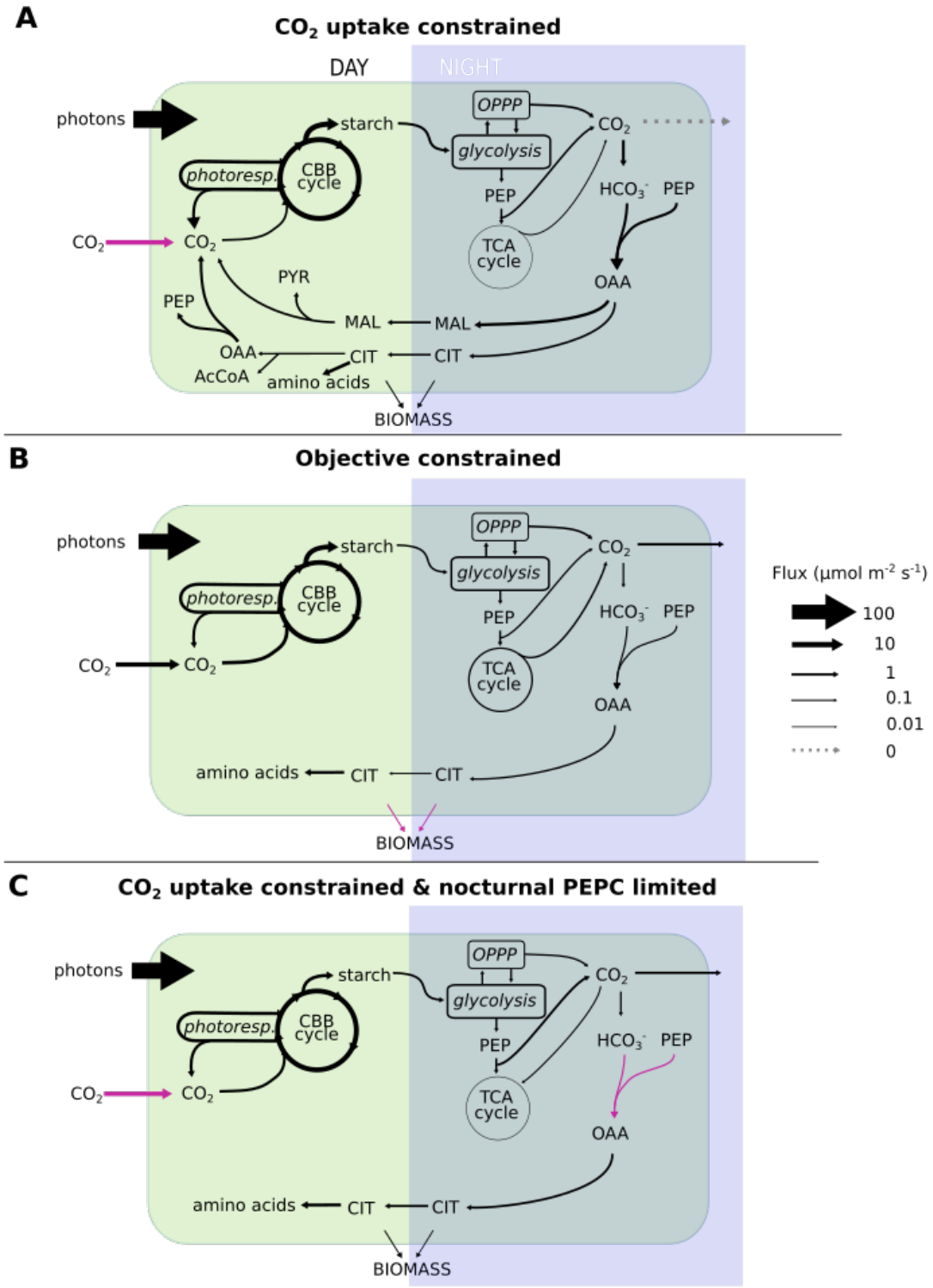
A
CO2 uptake constrained
DAY
NIGHT
photons
starch
OPPP
CO2
glycolysis
photoresp.
CBB cycle
PEP
HCO3- PEP
CO2
CO2
TCA cycle
PYR
OAA
PEP
MAL
MAL
OAA
CIT
CIT
AcCoA
amino acids
BIOMASS
B
Objective constrained
photons
starch
OPPP
CO2
glycolysis
photoresp.
CBB cycle
PEP
HCO3- PEP
CO2
CO2
TCA cycle
OAA
amino acids
CIT
CIT
BIOMASS
Flux (µmol m-2 s-1)
100
10
1
0.1
0.01
0
C
CO2 uptake constrained & nocturnal PEPC limited
photons
starch
OPPP
CO2
glycolysis
photoresp.
CBB cycle
PEP
HCO3- PEP
CO2
CO2
TCA cycle
OAA
amino acids
CIT
CIT
BIOMASS

Figure 2.8: **Major flux routes through three modelling scenarios with specific implementations of carbon constraints.**
Subcellular compartments are omitted for clarity. Reactions constrained to confer the model iteration-specific carbon constraint are marked in magenta. Arrow widths are proportional to the predicted flux. Abbreviations: CIT, citrate; PEP, phosphoenolpyruvate; OAA, oxaloacetate; MAL, malate; PYR, pyruvate; AcCoA, acetyl-CoA; CBB cycle, Calvin-Benson-Bassham cycle; photoresp., photorespiratory pathway; OPPP, oxidative pentose phosphate pathway; TCA cycle, tricarboxylic acid cycle

or that it would be the most feasible one to engineer into C3 plants for the purpose of increasing biomass output. The following section therefore focuses on preventing CAM cycling in the plant model to investigate whether alternative nocturnal CO_2 refixation pathways can emerge, using just the native plant enzymes already represented in the diel plant model.

This approach will furthermore generate a "baseline model" with suboptimal carbon conversion efficiency, which can be used to evaluate the potential impact of heterologous pathways (as explored in Chapter 3). Because of the objective function to maximise biomass production, the baseline model should be primed to utilise any added heterologous pathways, provided they can integrate into the plant metabolic network and offer an efficient means of salvaging nocturnal respiratory CO_2 that would otherwise be lost.

Several different approaches were explored to prevent or limit CAM cycling in the model.

2.3.6.1 Method 1 - Constraining the model objective

The first method used an algorithm to limit daytime CO_2 uptake to realistic values for C3 plants in the diel plant model that was introduced by Shameer et al. (2019). The aim of their study was to examine leaf energy balance in a C3 plant.

Therefore, it was crucial to represent C3 metabolic behaviour. The authors also acknowledged that CO_2 assimilation rates relate to light intensity in a non-linear way, and sought a way to make the model achieve realistic CO_2 uptake rates for the given PPFD. To do this, an additional step was incorporated in their modelling setup. Rather than directly applying the experimentally determined CO_2 assimilation rate (6 μmol m^{-2} s^{-1}) as the upper bound constraint on the daytime CO_2 exchange reaction, Shameer et al. developed a function which iteratively varied the constraint on the objective reaction until the model achieved the desired CO_2 uptake rate. What this effectively does is remove the primary optimisation objective of maximising biomass given a certain light input (because the biomass reaction was constrained to a fixed value) and instead the model is optimised for the secondary objective of minimisation of the total sum of fluxes. Because the model is no longer striving to increase biomass, carbon conversion efficiency becomes less important and so carbon-recovery mechanisms such as CAM cycling may not appear in the optimal flux distribution, particularly as they are likely to increase the total sum of fluxes.

I applied this algorithm in my diel model setup and set a target CO_2 uptake rate of 6.643 μmol m^{-2} s^{-1}. Over many iterations, the algorithm reduced the biomass output reaction flux and when it reached 0.0625 μmol m^{-2} s^{-1} the CO_2 uptake flux reached the target value.

This objective-constrained model appeared to behave more similarly to the CO_2 unconstrained model, with less starch accumulating during the day, less citrate accumulating at night, and no nocturnal accumulation of malate (Table 2.2, Fig. 2.8B). The model also lost CO_2 at night, refixing only 26.36% of nocturnally produced CO_2. Overall, it appeared that while the CO_2 uptake was limited to realistic value, corresponding to experimentally measured CO_2 assimilation rates in Arabidopsis, CAM cycling behaviour was prevented.

Although this method successfully limited the CO_2 uptake rate to realistic values and prevented CAM cycling behaviour, it is not suitable for my research aims. The approach requires directly constraining the objective flux to a fixed value. In the work described in the next chapter, I aimed to add heterologous CO_2 fixation pathways in the plant model, to see whether they could theoretically improve biomass output by allowing an alternative way to refix nocturnally respired CO_2. Therefore, I needed the objective flux to remain unconstrained.

Nevertheless, this approach provides a useful way to compare CAM cycling and C3-like metabolism at identical daytime CO_2 uptake rates. By varying the CO_2 uptake constraint (either directly by limiting CO_2 uptake or indirectly by constraining the biomass output), I can examine how these two metabolic strategies perform across different CO_2 uptake rates.

The comparison reveals that over a large range of CO_2 uptake rates, the biomass output achieved by C3-like metabolism ("Objective constrained model") was only 81.5% of the flux achieved when CAM cycling was active ("CO_2 uptake constrained model") (Fig. 2.9). This was true until CO_2 uptake reached very high levels, beyond the range of CO_2 assimilation rates measured in Arabidopsis. The biomass output of both metabolic strategies converges at approximately 12.3 μmol m^{-2} s^{-1} of CO_2 uptake, which matches what was achieved by the "CO_2 unconstrained" model. Since the unconstrained model used 100% of available photons, this suggests that CAM cycling is advantageous when carbon limits growth, while C3 metabolism becomes more efficient when light availability becomes the primary limiting factor.

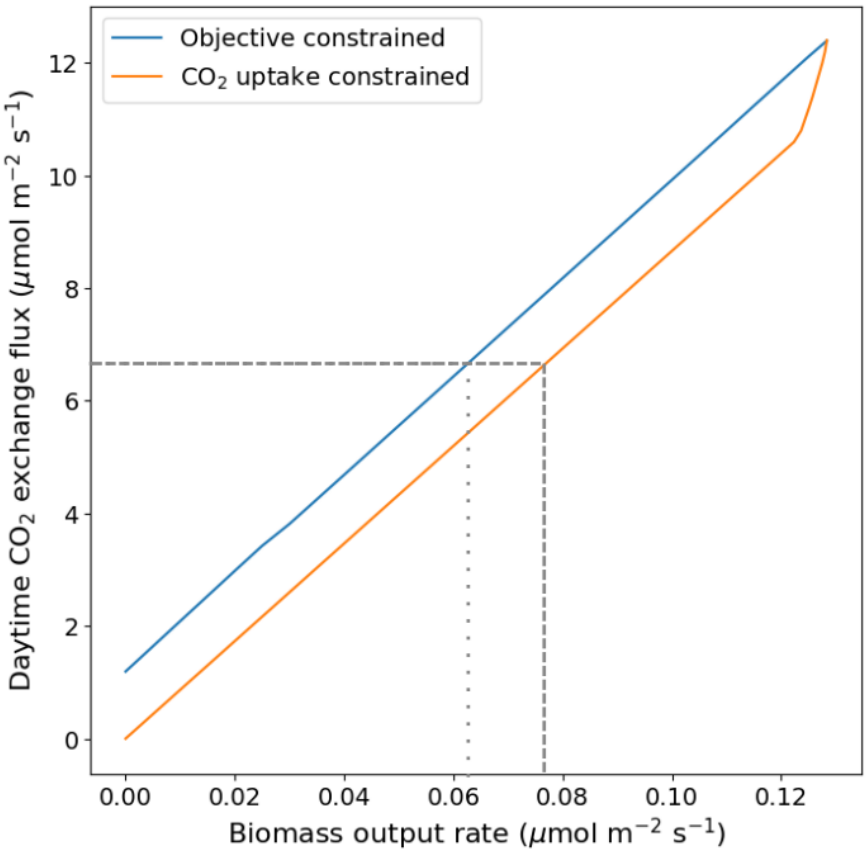

Figure 2.9: **Comparison of predicted CO_2 uptake rate and biomass output rates in models constrained different methods.**
The biomass output rate achieved at the average CO_2 assimilation rate for Arabidopsis (6.643 µmol m^{-2} s^{-1}) is indicated for the "Objective constrained" model (dotted line) and the "CO_2 uptake constrained" model (dashed line).

2.3.6.2 Method 2 – Turning off the dominant nocturnal CO_2-fixing reactions

To investigate alternative methods of limiting CAM cycling behaviour, I explored directly constraining the relevant enzymes to prevent nocturnal CO_2 refixation. After applying the CO_2 uptake constraint, setting the upper bound to 6.643 μmol m^{-2} s^{-1} as before, I identified and systematically disabled the most active nocturnal carbon-fixing enzymes one-by-one by setting their reaction flux to zero in the night phase of the model only. Through several iterations, this approach revealed which enzymes the model could potentially use for nocturnal CO_2 refixation. Table 2.3 shows the dominant carbon-fixing enzyme in each iteration, along with information about the extent of nocturnal CO_2 refixation.

As described above, the direct CO_2 constrained model achieved 100% nocturnal CO_2 refixation by employing CAM cycling. The main enzyme responsible for this nocturnal CO_2 capture was PEPC in the cytosol, which fixed 74.60% of the CO_2 produced at night. The remaining nocturnal CO_2 was fixed by cytosolic ICDH (19.85%), and acetyl-CoA carboxylase (5.25%), after conversion of CO_2 to bicarbonate.

When I then prevented cytosolic PEPC from fixing CO_2 at night, the model still refixed 100% of the CO_2 it produced nocturnally. However, it now used PEPC located in the plastid to do this, which was previously inactive. The switch from cytosolic to plastid PEPC had no impact on biomass production and only a minimal one on photon use (increasing by just 0.00135%). This suggests that the energetic costs of using the plastid PEPC, including substrate and product transport across the chloroplast membrane, were similar to using the cytosolic enzyme. The only notable difference was a small 1.4% increase in the total sum of fluxes. Therefore, the model's initial preference for cytosolic PEPC was likely driven by the secondary objective of minimising the total sum fluxes.

Table 2.3: **Sequence of dominant nocturnal carbon-fixing enzymes in the CO_2 uptake constrained model.**
In successive model iterations, the dominant nocturnal CO_2-fixing reaction of the previous iteration was constrained to carry zero flux in the CO_2-fixing direction. Values in parentheses refer to % of biomass output achieved compared to the initial value. Abbreviations: PEPC, phosphoenolpyruvate carboxylase; ICDH, isocitrate dehydrogenase

Dominant nocturnal carbon-fixing enzyme	**% nocturnal carbon fixed by dominant enzyme**	**Constrained nocturnal carbon-fixing enzymes**	**Biomass synthesis flux (µmol m^{-2} s^{-1})**	**% nocturnal CO_2 refixed total**
cytosolic PEPC	74.60%	none	0.0767	100%
plastid PEPC	74.60%	cytosolic PEPC	0.0767 (100%)	100%
cytosolic ICDH	25.22%	plastid PEPC, cytosolic PEPC	0.0641 (83.57%)	30.95%
peroxisomal ICDH	24.86%	cytosolic ICDH, plastid PEPC, cytosolic PEPC	0.0638 (83.18%)	30.48%
plastid Acetyl-CoA carboxylase & mitochondrial ICDH	6.44% / 6.12%	peroxisomal ICDH, cytosolic ICDH, plastid PEPC, cytosolic PEPC	0.0633 (82.53%)	12.86%
plastid Acetyl-CoA carboxylase & methylcrotonyl-CoA carboxylase	6.39% / 6.08%	mitochdondrial ICDH, peroxisomal ICDH, cytosolic ICDH, plastid PEPC, cytosolic PEPC	0.0632 (82.39%)	12.77%

I then restricted both the cytosolic and plastid forms of PEPC at night. The model's ability to refix CO_2 at night decreased substantially, from previously 100% to 30.95%. Biomass output also decreased by 16.43%. Evidently, without PEPC activity at night, the model had no efficient alternative pathways available to refix the majority of respiratory CO_2. While all model versions showed some CO_2 refixation through ICDH, this enzyme pathway appears to be inefficient for processing large quantities of respiratory CO_2 at night.

Indeed, while the cytosolic ICDH operated in the reverse direction to fix CO_2, the same reaction acted to release CO_2 in other organelles. It could therefore be that the different subcellular activities of ICDH primarily serve the purpose of shuttling NADPH between organelles rather than contributing to net nocturnal CO_2 refixation.

Nevertheless, although not as efficient as the PEPC route, ICDH still allowed about 30% of nocturnal CO_2 to be refixed. To investigate whether there were other routes of similar efficiency to ICDH, the model was analysed with all isoforms of PEPC and ICDH turned off at night. In this situation, 12% of nocturnal CO_2 was still refixed. However, about half of that was due to the activity of acetyl-CoA carboxylase in fatty acid biosynthesis as part of the biomass biosynthesis in the model. The flux of this reaction was proportional to biomass and is therefore not a variable component of CO_2 refixation. It is also worth noting that fatty acid biosynthesis does not lead to net CO_2 refixation due the loss of CO_2 at the pyruvate dehydrogenase and β-ketoacyl-ACP synthase steps.

The other half of nocturnal CO_2 refixation was due to methylcrotonyl-CoA carboxylase, a reaction that was inactive at night before. It was therefore decided that this likely represents an unrealistic measure that emerged in the model as a consequence of the strict constraints on other nocturnal carboxylating enzymes and the

investigation of dominant carbon-fixing enzymes was stopped at this point.

2.3.6.3 Method 3 – Limiting nocturnal PEP carboxylase to activity observed in C3-like model

While the approach described above, successfully prevented CAM cycling when both the cytosolic and the plastid PEPCs were turned off at night, it appears unrealistically restrictive as some PEPC activity can be measured in the dark even in C3 plants and is an important anaplerotic mechanism for topping up the TCA cycle (O'Leary et al., 2011).

Therefore, I tested another approach, which relied on limiting nocturnal PEPC activity to the levels that were observed in the model iteration which behaved more similarly to C3 metabolism (see Method 1), which was achieved by constraining the biomass output flux directly.

To do this, I first performed a constraint scan, varying the fixed flux through the biomass output reaction and at each iteration I extracted the predicted flux through nocturnal PEPC reactions. While the plastid PEPC was inactive throughout the scan, cytosolic PEPC activity increased almost linearly with the biomass output (Fig. 2.10). I could therefore formulate a linear equation based on the slope of nocturnal PEPC activity. I then applied this as a constraint, which stipulated that at the end of the model optimisation, the nocturnal, cytosolic PEPC flux must relate to the biomass output flux according to this linear equation.

Finally, for the model with this new PEPC constraint in place, I released any constraints on the biomass output reaction and reapplied the direct upper bound constraint on the CO_2 uptake reaction of 6.643 µmol m^{-2} s^{-1}. The results are shown in Table 2.2 under "CO_2 uptake constrained & nocturnal PEPC limited" and in Figure 2.8C.

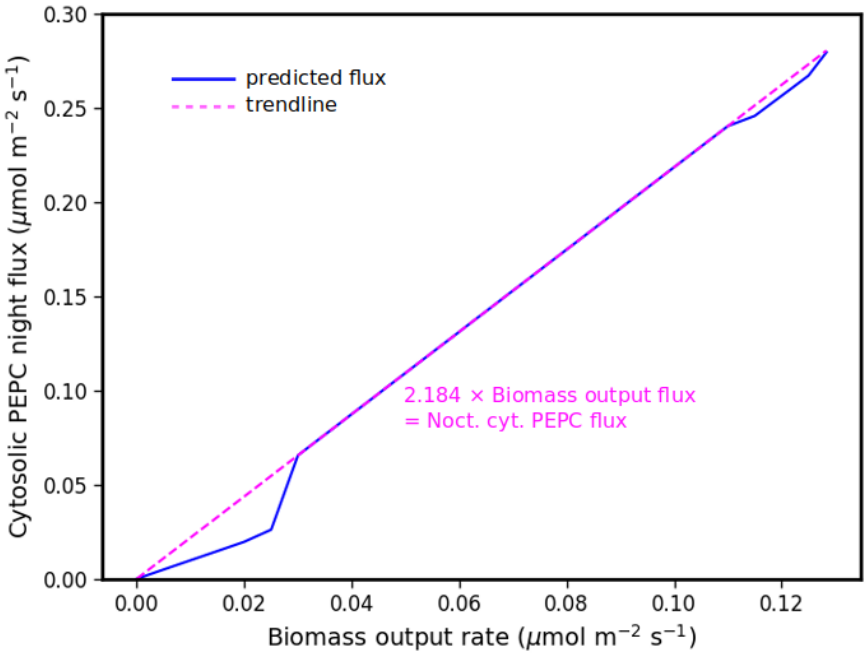

Figure 2.10: **Change in nocturnal cytosolic PEPC activity with increasing fixed constraint on biomass output rate.**
I gradually increased the fixed flux constraint through the biomass output reaction and tracked the flux through the nocturnal, cytosolic PEPC reaction. The slope for nocturnal cytosolic PEPC flux over increasing biomass output rates was calculated (dashed, magenta line), assuming an intercept of (0, 0).

In this new "PEPC-limited" model CAM cycling was prevented. Nocturnal CO_2 refixation reduced from 100% to 39.50% and there was no nocturnal malate accumulation. The CO_2 uptake was limited to experimental values, but the biomass output flux remained unconstrained. Therefore, this version of the model should serve as the baseline model for further investigations of the potential of heterologous, nocturnal CO_2 refixation pathways.

2.4 Discussion

2.4.1 Capacity for nocturnal, respiratory CO_2 refixation in a diel leaf metabolic model

In this chapter, I used metabolic modelling to explore whether plant metabolic networks possess inherent capacity for nocturnal CO_2 refixation - specifically, whether a diel leaf metabolic model could salvage respiratory CO_2 at night to improve carbon conversion efficiency and thereby plant growth under carbon-limited conditions.

Importantly, the goal was to see whether nocturnal CO_2 refixation would emerge under certain conditions without directly forcing it to. For a contrasting example, Tay et al. (2021) explored the different modes of CAM using metabolic modelling. To represent CAM cycling, Tay et al. prevented CO_2 release to the atmosphere at night, which forced their model to refix all nocturnal CO_2. This meant their model had to find ways to fix respiratory CO_2 at night, regardless of whether this was beneficial for the optimisation objective of the model.

My model demonstrated that a diel leaf metabolic model can exhibit nocturnal CO_2 refixation, without being forced to. Surprisingly, this was the case even before specific measures for limiting the carbon supply were implemented. This

metabolic behaviour appeared to be the consequence of modifications made to the core plant model, though the exact reasons for it could not be elucidated here.

To then represent carbon limitation in the model, I chose to limit the maximum flux through the daytime CO_2 uptake reaction. This served as a proxy for the various limitations plants face in real-world CO_2 assimilation, including sub-optimal atmospheric CO_2 concentrations, barriers for gas diffusion into the leaf internal spaces and chloroplasts (Evans et al., 2009; Flexas et al., 2012), limited generation of energy and reducing power at the given light intensity (Zhu et al., 2008) and limitations in CBB cycle enzyme activity when CO_2 is not saturating and/or other substrates are not recycled efficiently (Raines, 2011; Stitt et al., 2010). A combination of these factors likely explains why experimental measurements in Arabidopsis show average CO_2 assimilation rates at approximately half of what the diel leaf model can theoretically achieve when CO_2 uptake remained unconstrained.

Limiting daytime CO_2 uptake to realistic values in the model demonstrated that nocturnal refixation of respiratory CO_2 could theoretically enhance plant growth when carbon is scarce. While this might seem intuitive - since CO_2 lost to the atmosphere cannot contribute to biomass - the process involves complex metabolic trade-offs. Nocturnal CO_2 refixation requires carbon precursors, energy, and reducing power, all of which are derived from starch breakdown at night. FBA models are particularly valuable here, as they can account for these interconnected processes. My model revealed that, under carbon-limited conditions, the metabolic costs of nocturnal CO_2 refixation can be met by the native plant metabolic network while still providing a net benefit to growth.

2.4.2 Natively available pathways for nocturnal CO_2 refixation

Under carbon-limited conditions, the model adopted CAM cycling as its main strategy for nocturnal CO_2 fixation. CAM cycling uses enzymes that are known to be present and active C3 plants (Silvera et al., 2010), albeit at different times of the day (Nimmo, 2000). These enzymes are therefore also present in the core metabolic plant model and without specific constraints the diel setup allows them to carry flux during the night.

Through CAM cycling, the model achieved complete CO_2 refixation and a 22.72% increase in biomass output compared to C3-like metabolism. PEPC proved to be the key enzyme for nocturnal CO_2 refixation capabilities, as it was the only carboxylase that significantly enhanced growth under carbon limitation. While ICDH was also fixing CO_2 at night in the model, it did not provide similar growth benefits when operating alone.

This difference in effectiveness of the two carboxylation routes for nocturnal CO_2 reassimilation likely comes down to substrate availability and the metabolic routes for substrate production. PEPC uses PEP which is readily available from glycolysis, while carboxylation catalysed by ICDH requires 2OG. Typically, the route to 2OG production is via ICDH in the forward direction.

To use reverse ICDH for net CO_2 fixation, the model would therefore require an alternative route for producing 2OG. The model has several reactions available to make 2OG from glutamate, by transferring the amino group of glutamate to another substrate. Since another amino acid is a by-product of this reaction, it is likely that these reactions were not of use to the model as it was set up here, because amino acids were not allowed to accumulate at night and could not be metabolised effectively.

Another plant metabolic model by Töpfer et al. (2020), which represented CAM behaviour by optimising for water use efficiency, allowed amino acid accumulation both during the day and at night. Their model also displayed nocturnal ICDH in the CO_2-fixing direction, which was reported to contribute to water-saving. For this, proline accumulated from the day was degraded to glutamate, then used to make 2OG via aspartate aminotransferase. Aspartate was then converted to asparagine and accumulated at night.

This highlights how the choice of substrate and its metabolic accessibility, as well as that of by-products, strongly influence whether a CO_2-fixing enzyme can operate to benefit the objective reaction in these complex metabolic networks.

2.4.3 CAM (cycling) and carbon saving

2.4.3.1 Previous metabolic modelling of CAM and CAM cycling

Previous metabolic modelling studies typically focused on full CAM, often forcing this behaviour by setting the daytime CO_2 uptake reaction to zero, thereby making it necessary to take up and fix CO_2 at night to gain any carbon (Cheung et al., 2014; Shameer et al., 2018; Tay et al., 2021). Similarly, to also represent the CAM mode of CAM cycling, Tay et al. forced complete nocturnal CO_2 refixation by preventing nocturnal CO_2 exchange. These approaches contrast with my work, where the model was free to adopt nocturnal CO_2 refixation only if it benefited the growth objective. A notable exception was Töpfer et al. (2020), who took a different approach to modelling CAM by incorporating water use efficiency as a model objective. Their model linked daytime CO_2 uptake with water loss, based on daily temperature patterns, which incentivised the model to limit daytime CO_2 exchange when transpiration would be high but without directly forcing it to.

Tay et al. (2021) classified CAM cycling as less efficient than C3 metabolism based on their chosen objective of photon use efficiency. While my results also show that CAM-like behaviours require additional energy for nocturnal CO_2 refixation, this increased the total photon usage by only 15%, reaching just 70% of the maximum allowed PPFD. Moreover, the model's PPFD setting of 200 µmol m^{-2} s^{-1} likely underestimates light availability in typical CAM plant habitats. Given that light is rarely a limiting factor in the arid environments where CAM plants thrive, optimising for photon use efficiency seems an unsuitable choice of objective function, and ranking the efficiency of pathways based on their photon use efficiency appears unreasonable.

Interestingly, Tay et al. included an additional analysis that explored the C3-CAM continuum by gradually reducing daytime CO_2 uptake limits, simulating how increasing temperatures and aridity might force C3 plants to restrict daytime stomatal opening and thereby restrict gas exchange. As daytime CO_2 availability decreased, their model first reduced nocturnal CO_2 loss by employing nocturnal refixation before beginning to even take up additional CO_2 at night. This was true while still optimising for photon use efficiency. However, phloem export rates were set to a fixed value, meaning that a certain level of productivity was the primary objective in this analysis. This finding aligns with my results, providing independent modelling evidence that CAM-like metabolism enhances productivity under carbon-limited conditions.

Indeed, Burgos et al. (2022), in their review of CAM modelling studies, interpreted these results as evidence for the longstanding hypothesis that it is the limited access to CO_2, as stomata remain closed during the day to limit water loss, that drives CAM evolution (Lüttge, 2002). This hypothesis is further supported by the presence of CAM in certain aquatic plants (Keeley, 1998). In aquatic environments, CO_2 availability is naturally limited during the day due to its low solubility

in water and uptake by competing photosynthetic organisms. At night, however, CO_2 concentrations increase as respiratory CO_2 is released by organisms living in the water. Some Isoetes species have evolved CAM metabolism, as seen by large nocturnal carboxylic acid accumulation, allowing them to temporally shift CO_2 acquisition from when it is scarce during the day to when it is more abundant at night (Keeley and Busch, 1984). Given their aquatic habitat, water use efficiency can be excluded as a reason to adopt CAM.

2.4.3.2 Modelling may overstate carbon saving impact of CAM cycling

Given that carbon may be a limiting factor in agricultural settings and my modelling showed that there would be clear benefits of CAM cycling under these conditions, an important question arises: why is CAM cycling not more widespread in the plant kingdom?

This disconnect between model predictions and natural occurrence suggests there may be additional constraints or trade-offs not captured in my current modelling approach, or that carbon-limitation is not a major evolutionary driver in the natural world, contrasting with the situation in closed-canopy, close-cropping monoculture for agriculture.

Various forms of CAM behaviour have been described in the literature, including "C3+CAM", "CAM cycling", "weak CAM", "strong CAM", and "full CAM". Classification criteria for these categories are not standardised and current thinking envisages CAM existing along a continuous spectrum rather than discrete categories (Cushman, 2001; Winter and Holtum, 2014).

CAM cycling is typically described as a form of CAM where only respiratory CO_2 is refixed at night. Therefore, CAM cycling can be particularly challenging to detect. CAM cycling plants exhibit carbon isotope ratios ($\delta^{13}C$) similar to C3

plants, since Rubisco remains the primary CO_2-fixing enzyme, PEPC only refixes respiratory CO_2, which has undergone discrimination by Rubisco previously. The nocturnal acid accumulation is also much smaller than in full CAM, leading to only minor changes in titratable acidity.

One aspect of CAM (cycling) that is not fully captured in the current model setup are changes in pH. Each metabolite in the model is represented to exist in a fractional protonation state according to the fixed pH value specified in the model for each subcellular compartment. Accumulating carboxylic acids in the vacuole would in reality lower the vacuolar pH because protons are pumped into the vacuole to balance the negative charges of the carboxylic acids (Smith, 1987). This proton pumping would require additional expenditure of ATP that is not represented in my model and thus total ATP use will be slightly underestimated. The extent to which this affects the model-predicted benefit of CAM cycling depends on the extent to which the vacuolar pH is acidified. A constitutive CAM plants may have a vacuolar pH as low as 3.3 towards the end of the night (Lüttge et al., 1981). However, because CAM cycling involves accumulation of much smaller amounts of malate than full CAM, the change in titratable acidity is negligible (Ting, 1985) suggesting that vacuolar pH changes are unlikely to have a big impact on the modelled system undergoing CAM cycling.

Furthermore, the model also does not explicitly account for vacuolar storage capacity which could limit the cell's ability to store carboxylic acids produced from nocturnal CO_2 refixation. Many CAM plants in arid environments show succulence (increased cell size and leaf thickness with enlarged vacuoles), which provides extra storage space. While this additional capacity was traditionally thought essential for CAM, recent studies have identified CAM plants without succulent features and the two traits appear to have evolved independently (Nelson and Sage, 2007; Heyduk et al., 2016).

Töpfer et al. (2020) quantified the theoretical storage limits of C3 plant vacuoles. Their calculations, based on typical C3 cell sizes, showed that non-succulent cells could store carboxylic acids equivalent to a combined flux of 7 μmol m^{-2} s^{-1}. The predicted flux for nocturnal carboxylic acid accumulation in my CAM cycling model fell well within this storage limit, suggesting vacuolar capacity would not restrict CAM cycling from happening in plants with cellular anatomy typical for C3.

The benefits of CAM and CAM cycling likely depend on environmental context. In nature, where nutrient availability often limits growth, the additional enzyme requirements of CAM metabolism may be costly. However, in agricultural or experimental settings where nutrients are supplied through fertilisers, carbon assimilation could become the primary limiting factor for growth (Amthor et al., 2019). Under these conditions, CAM-like features might provide unexpected benefits beyond water conservation, as predicted by my model.

2.4.3.3 Experimental evidence for impact of engineered CAM (cycling) in plants

Research is ongoing to engineer CAM into C3 crops as a strategy to enhance drought resistance, which could help maintain food production as water becomes scarcer in agricultural regions (Yuan et al., 2020; Borland et al., 2014; Yang et al., 2015). Research done so far on implementing CAM in C3 plants has primarily been intended to test steps toward engineering drought-resistant crops by introducing individual elements of CAM, one at a time, before combining them all together. However, these results may also reveal whether even partial implementation CAM, potentially giving rise to CAM cycling, could enhance plant growth under typical glasshouse conditions.

Kebeish et al. (2012) expressed potato (*Solanum tuberosum*) PEPC in Arabidopsis using both constitutive and dark-induced promoters. The transgenic lines showed increased stomatal opening and higher respiration rates in the dark. While the authors presented these results as progress toward engineering CAM metabolism, due to the night-time stomatal opening, evidently PEPC overexpression alone did not result in nocturnal CO_2 fixation characteristic of CAM or CAM cycling plants.

Liu et al. (2021) reported the effects of stable transformation of a CAM-specific PEPC from *Agave americana* in tobacco. These transgenic lines showed enhanced growth under well-watered conditions, though especially under drought and salt stress. Gas exchange measurements revealed increased daytime CO_2 uptake while nocturnal CO_2 loss remained similar to wild-type plants. A shift toward less negative $\delta^{13}C$ values was also observed. These data suggest that constitutive PEPC overexpression enhanced daytime CO_2 fixation rather than inducing nocturnal CAM-like behaviour, as PEPC fixed CO_2 alongside Rubisco.

Lim et al. (2019) individually overexpressed 13 CAM-related genes from the common ice plant (*Mesembryanthemum crystallinum*) in Arabidopsis, using a strong constitutive promoter for each gene. Most transgenic lines showed increased leaf size and fresh weight compared to wild-type plants under well-watered conditions. While the authors measured titratable acidity as an indicator of malate content, they did not specify the timing of these measurements, nor did they report gas exchange data. Without this information, it remains unclear whether these plants performed CAM cycling or, similar to plants in the study by Liu et al. discussed above, merely showed enhanced daytime CO_2 uptake through increased stomatal conductance and possibly enhanced PEPC activity during the day.

Recent unpublished work on combined expression of CAM-related enzymes in C3 plants suggests that CAM cycling truly can bring significant growth benefits (John

C. Cushman, personal communication). The study tested three combinations of CAM enzymes from *M. crystallinum*: 1) carboxylation enzymes only, 2) decarboxylation enzymes only, and 3) all 13 CAM enzymes together. Plants expressing only carboxylation enzymes showed characteristics of CAM cycling: reduced night-time CO_2 release, nocturnal malate accumulation, and daytime malate depletion. Unlike plants with decarboxylation enzymes or the full CAM set, these carboxylation-module plants showed little drought resistance. This suggests they maintained daytime stomatal opening, which is typical of CAM cycling rather than full CAM metabolism.

In summary, experimental evidence generally suggests that introducing elements of CAM into C3 plants has a beneficial effect on growth, at least under laboratory growth conditions. Further research will show whether introducing CAM into C3 results in positive growth effects in the absence of water stress under field conditions and whether the simpler engineering target of CAM cycling alone might confer substantial advantages while requiring fewer modifications to plant metabolism.

3 | Modelling artificial CO_2-fixation cycles for nocturnal CO_2 refixation

3.1 Introduction

In Chapter 2, I showed that within the diel plant metabolic model representing the native metabolic capabilities of an Arabidopsis leaf, CAM cycling was the only pathway that could be used to effectively refix CO_2 at night. As efforts to engineer CAM (cycling) in C3 plants are already in progress, I further sought to explore alternative strategies to gain the proposed benefits of nocturnal CO_2 refixation.

For example, we could introduce heterologous pathways for CO_2 fixation in plants at night. These could have additional benefits over CAM cycling. The enzymes and metabolites involved in CAM cycling are central to plant metabolism and may therefore be subject to tight regulation. Furthermore, changing their activity could potentially interfere with central metabolic pathways in unexpected ways. Heterologous enzymes are less likely to be subject to such regulation and may act orthogonally to central metabolic pathways (Erb et al., 2017).

Nevertheless, to alter metabolism for increased productivity, such a heterologous nocturnal CO_2-refixing pathway must be able to integrate effectively into the plant's existing metabolic network (Küken and Nikoloski, 2019). This requires the plant to produce adequate supplies of the substrate needed by the new pathway. Additionally, the pathway's end product must be metabolically useful, meaning it can be used either directly in subsequent biosynthetic pathways, or that it can act as a transient carbon store until it can be decarboxylated during the daytime, followed by CO_2 reassimilation via Rubisco.

There are several other known CO_2 fixation pathways, which could be explored as an option to implement in plants for nocturnal CO_2 refixation. These have either evolved naturally or have been created artificially, by rationally plotting a sequence of feasible metabolic reactions to constitute a pathway with the desired properties.

Alongside the CBB cycle, there are currently five other known, naturally evolved CO_2 fixation pathways (Santos Correa et al., 2023): the natural reductive TCA (rTCA) cycle, the reductive acetyl-CoA pathway (also known as the Wood-Ljungdahl pathway), the 3-hydroxypropionate bicycle, the hydroxypropionate/4-hydroxybutyrate (HP/HB) cycle and the dicarboxylate/4-hydroxybutyrate (DC/HB) cycle. Three of these pathways would be unsuitable for use *in planta*, as they utilise enzymes that are inhibited by oxygen.

Extensive research has been devoted to developing novel CO_2-fixation pathways that do not exist in nature. These synthetic pathways can be constructed through several approaches: combining existing enzymes sourced from diverse organisms, engineering established enzymes to catalyse non-native reactions, or even designing entirely new enzymes from first principles (Erb et al., 2017; Bar-Even et al., 2010). Such designed pathways can potentially overcome limitations that natural evolution has encountered, as evolutionary processes can become trapped in local optima or 'dead ends' where incremental changes no longer yield improvements, preventing the natural emergence of more efficient solutions (Erb et al., 2017).

Some of the artificially created pathways published to date are: the crotonyl-(CoA)/ethylmalonyl-CoA/hydroxybutyryl-CoA (CETCH) cycle (Schwander et al., 2016), the malonyl-CoA–oxaloacetate–glyoxylate (MOG) pathways (Bar-Even et al., 2012b), the synthetic reductive glycine pathway (rGlyP) (Bar-Even et al., 2013), the HydrOxyPropionyl-CoA/Acrylyl-CoA (HOPAC) cycle (McLean et al.,

2023), the reductive tricarboxylic acid branch/4-hydroxybutyryl-CoA/ethylmalonyl-CoA/acetyl-CoA (THETA) cycle (Luo et al., 2023), and the CO_2-reduction (CORE) cycle (Satanowski et al., 2025).

Many of these pathways are typically designed to be used *in vitro*, or in microbes, to enable CO_2-negative microbial fermentation processes. However, Bar-Even (2018) described how some these pathways could be used in plants. The focus was generally to complement or replace the CBB cycle during the day and to the best of my knowledge, there has not yet been a mention of using synthetic CO_2-fixation pathways for the refixation of nocturnal respiratory CO_2.

One of the most prominent examples of artificial CO_2-fixing pathways is the CETCH cycle. It was presented by Schwander et al. (2016), who described its design and successful *in vitro* implementation. The cycle was created by identifying efficient CO_2-fixing reactions and connecting them with known metabolic reactions to form a complete cycle. Through a series of 14 reactions, the CETCH cycle converts CO_2 into malate (Fig. 3.1, Table 3.1). The researchers purified all required enzymes and demonstrated the cycle's function *in vitro* by showing that malate was produced. They further improved the pathway's efficiency through rational enzyme engineering.

The CETCH cycle offers multiple key advantages over the CBB cycle: it requires less ATP to operate, its carboxylating enzymes are catalytically more efficient and they cannot use O_2 as a substrate (Schwander et al., 2016). These features make the CETCH cycle an interesting candidate for *in vivo* implementation, as organisms could potentially fix CO_2, without losses to oxygen-based side reactions.

FBA provides an ideal computational framework to evaluate whether introduced pathways can function within a given organism's metabolism and enhance its metabolic output. Metabolic modelling, by considering the entire metabolic net-

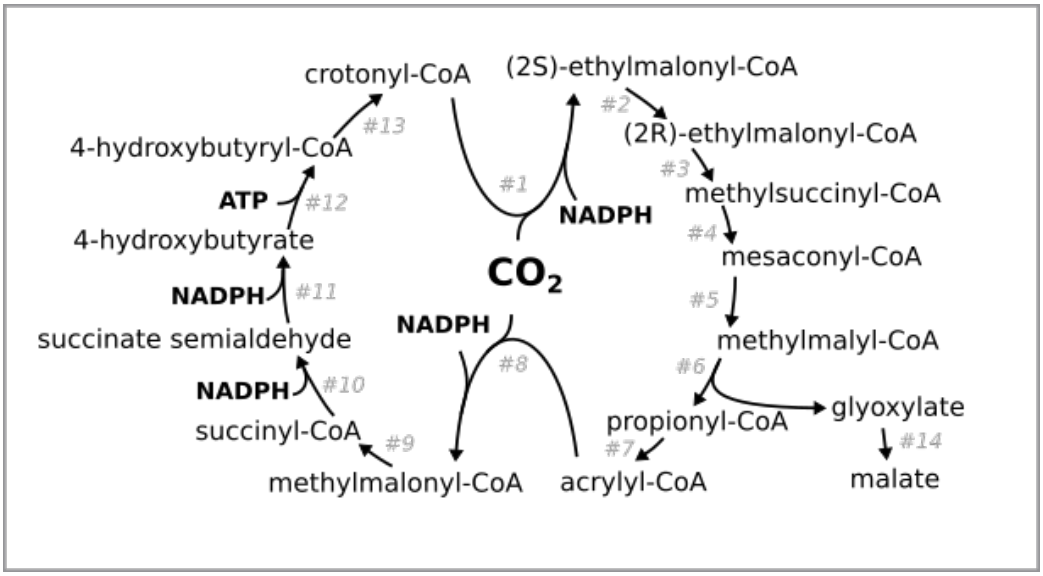

Figure 3.1: **Diagrammatic representation of the crotonyl-(CoA)/ethylmalonyl-CoA/hydroxybutyryl-CoA (CETCH) cycle.** Only cycle intermediates and important reactants are shown for clarity. Numbering of reactions corresponds to Table 3.1.

work, can reveal potential challenges in integrating artificial pathways into existing organisms. It may identify unexpected obstacles, while also suggesting optimal strategies for pathway implementation, such as the most effective subcellular locations for the pathway or individual enzymes. Furthermore, it can reveal additional changes that could be made to native metabolism to enhance the output from the artificial pathway, such as downregulating pathways that compete for the same substrates (Blazeck and Alper, 2010).

3.1.1 Aims

Accordingly, the aim of the work described in this chapter was to investigate whether artificial CO_2-fixing pathways, like the CETCH cycle, could be implemented to provide a novel avenue for nocturnal CO_2 refixation in plants. Using the "CO_2 uptake constrained & nocturnal PEPC limited" model created in Chapter

2, which is carbon-limited but does not use CAM cycling, I investigated how introducing the CETCH cycle would affect nocturnal carbon metabolism. The CETCH cycle was chosen because its metabolic reactions are well-defined, with precise stoichiometry available in the MetaCyc database (Caspi et al., 2018), and because of its superior energy efficiency compared to many other known CO_2-fixing cycles (Bar-Even et al., 2012b). Furthermore, the cycle's end product, malate, is already known to be suitable as a transient carbon storage compound in plants from CAM.

Using FBA, I added the reactions of the CETCH cycle into the dark phase of the carbon-limited diel plant model to examine, whether the cycle can be successfully integrated with existing plant metabolism, how the cycle affects overall carbon conversion efficiency and energy usage and what constraints might limit its effectiveness.

3.2 Methods

3.2.1 Model setup

The general diel plant model was set up as described in Chapter 2. To induce carbon-limitation, the upper bound of the daytime CO_2 uptake reaction was set to 6.643 µmol m^{-2} s^{-1}, as described in 2.3.5. CAM cycling was restricted by limiting the activities of the nocturnal PEPC reactions, as described in 2.3.6.3.

3.2.2 Obtaining reactions and metabolites of the CETCH cycle

Reactions representing the CETCH cycle as described by Schwander et al. (2016) were obtained from MetaCyc.org (Caspi et al., 2018) (entry: "crotonyl-CoA/ethylmalonyl-CoA/hydroxybutyryl-CoA cycle (engineered) (CETCH 5.4 cycle)". The reactions and their stoichiometries are listed in Table 3.1.

Table 3.1: **Reactions of the crotonyl-CoA/ethylmalonyl-CoA/ hydroxybutyryl-CoA (CETCH) cycle (version 5.4).**

#	Name	Full name	Substrates	Products
1	Ccr	crotonyl-CoA carboxylase/reductase	crotonyl-CoA + NADPH + CO_2	(2S)-ethylmalonyl-CoA + $NADP^+$
2	Epi	ethylmalonyl-CoA epimerase	(2S)-ethylmalonyl-CoA	(2R)-ethylmalonyl-CoA
3	Ecm	ethylmalonyl-CoA mutase	(2R)-ethylmalonyl-CoA	methylsyccinyl-CoA
4	Mco	methylsuccinyl-CoA oxidase	methylsuccinyl-CoA + O_2	mesaconyl-CoA + H_2O_2
5	Mch	mesaconyl-CoA hydratase	mesaconyl-CoA + H_2O	methylmalyl-CoA
6	Mcl	methylmalyl-CoA lyase	methylmalyl-CoA	glyoxylate + propionyl-CoA
7	Pco	propionyl-CoA oxidase	propionyl-CoA + O_2	acrylyl-CoA + H_2O_2
8	Ccr	crotonyl-CoA carboxylase/reductase	acrylyl-CoA + CO_2 + NADPH	methylmalonyl-CoA + $NADP^+$
9	Mcm	methylmalonyl-CoA mutase	methylmalonyl-CoA	succinyl-CoA
10	Scr	succinyl-CoA reductase	succinyl-CoA + NADPH + H^+	succinate semialdehyde + CoA + $NADP^+$
11	Ssr	succinate semialdehyde reductase	succinate semialdehyde + NADPH + H^+	4-hydroxybutyrate + $NADP^+$
12	Hbs	4-hydroxybutyrate-CoA ligase	4-hydroxybutyrate + ATP + CoA	4-hydroxybutyryl-CoA + ADP + P_i
13	Hbd	4-hydroxybutyryl-CoA dehydratase	4-hydroxybutyryl-CoA	crotonyl-CoA + H_2O
14	Mas	malate synthase	acetyl-CoA + glyoxylate	malate + CoA + H^+

Using the COBRApy package for Python (Ebrahim et al., 2013), a new model object was created containing only the reactions and metabolites of the CETCH cycle. Exchange reactions were added allowing input and output of all cofactors, substrates and products (NADPH, $NADP^+$, ATP, ADP, P_i, O_2, H_2O_2, H^+, CO_2, malate) (Fig. 3.2A). All reaction bounds of this test model were left at the default values (i.e. lower bound: –1000, upper bound: +1000), and the primary objective was set to maximising malate output.

3.2.3 Incorporating the CETCH cycle in the plant model

All CETCH cycle metabolites and reactions were added to every metabolic, subcellular compartment (cytosol, plastid, peroxisome and mitochondrion) of the diel plant model, in either only the dark phase or both the light and dark phase, and identifying suffixes were added accordingly ("_day" or "_night"). If the exact same metabolite or reaction was already present in the diel plant model compartment it was not copied.

Intracellular transport reactions were added to allow hypothetical bidirectional transfer of all CETCH cycle intermediates between the cytosol and each compartment. No energetic cost was assumed. Such transporters were not added for CETCH cycle metabolites that were also already present in the plant model. These were: H_2O, H^+, Coenzyme A (CoA), acetyl-CoA, glyoxylate, malate, ATP, ADP, phosphate, $NADP^+$, NADPH, succinate semialdehyde, succinyl-CoA, O_2, CO_2, H_2O_2, propionyl-CoA, acrylyl-CoA and crotonyl-CoA.

Protonation states were not implemented for CETCH cycle metabolites.

In the scenario where the CETCH cycle was added to both the light and dark phase of the plant model, transport reactions were added to allow transfer of CETCH cycle intermediates into and out of the vacuole and linker reactions were created

that represent vacuolar accumulation of the intermediate from day to night or *vice versa*.

3.2.4 Thermodynamic analysis

I used the Thermoflux package for Python, available at https://github.com/tednsmith/thermo_flux, to analyse the thermodynamic feasibility of CETCH cycle and plant-native reactions, particularly focusing on reaction directionality when using either NADPH or NADH as coenzymes, by exploring plausible ranges for change in Gibbs free energies of reactions across varying NADPH:$NADP^+$ and NADH:NAD^+ ratios.

The following assumptions were made: metabolite concentrations were allowed to vary between 0.01 and 20 mM, ionic strength was set to 0.25 M, temperature was kept at 298.15 K, and the pH was set to 7.0.

3.3 Results

3.3.1 Confirming the validity of metabolic reactions representing the CETCH cycle

To verify that the reactions obtained for the CETCH cycle from the MetaCyc enzymatic reactions database (Caspi et al., 2018) were correct in stoichiometry, I first tested whether the reactions would constitute the intended mass-balanced CETCH cycle in a test model. This test model contained only the metabolites and reactions for the CETCH cycle (version 5.4). Furthermore, I added exchange reactions to allow the provision of CO_2 as the substrate, the recycling of cofactors and the accumulation of the end product, malate. The model architecture is depicted in Figure 3.2A.

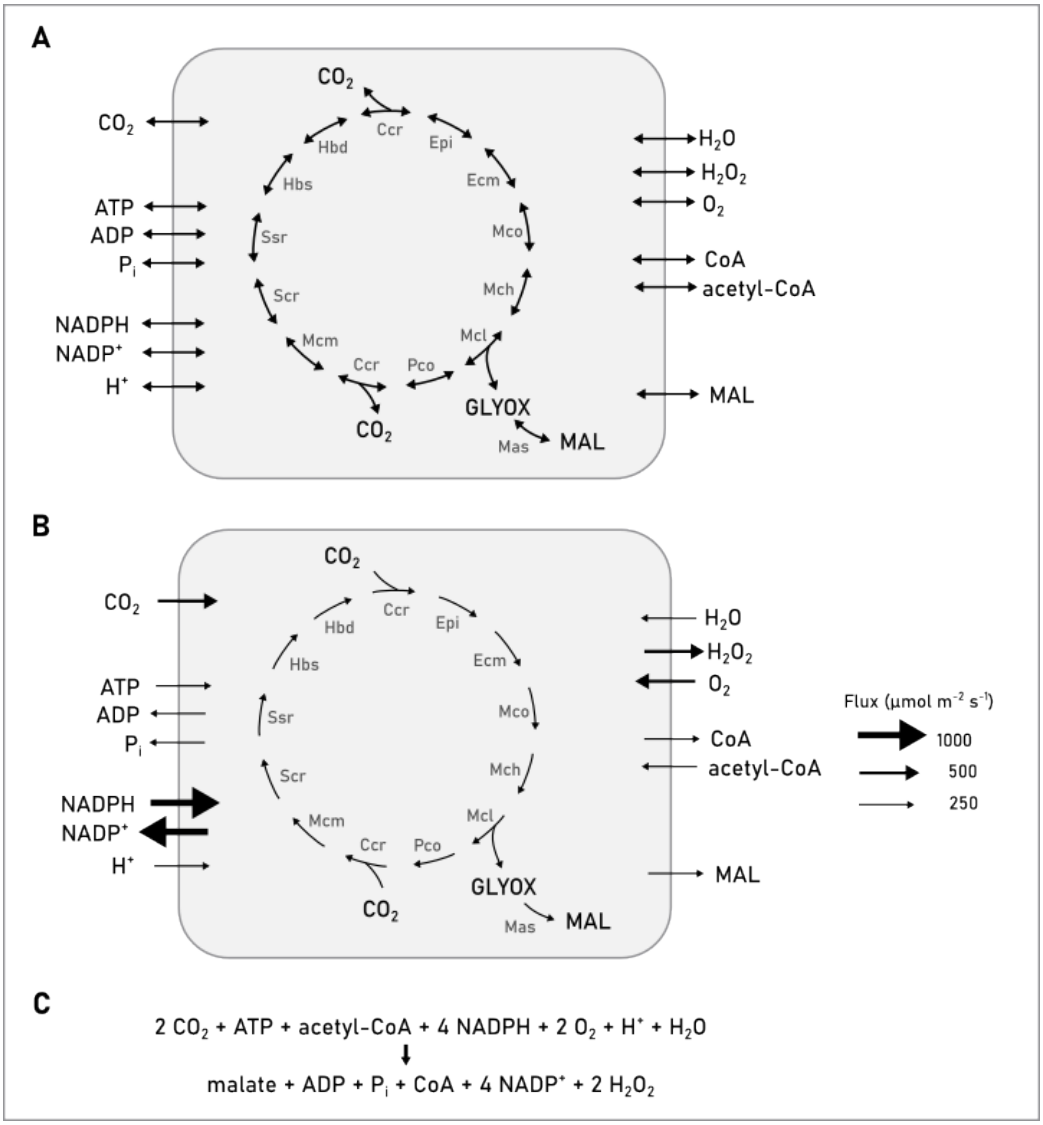

Figure 3.2: **Test metabolic model of the CETCH cycle.**
A) Model setup: The CETCH test model contained only the reactions of the CETCH cycle (version 5.4) and the exchange reactions to supply substrates and coenzymes and remove by-products and the end product, malate. B) Predicted fluxes after optimisation, maximising for malate output. C) Chemical equation of the complete CETCH cycle. Abbreviations: Ccr, crotonyl-CoA carboxylase/reductase; Epi, ethylmalonyl-CoA epimerase; Ecm, ethylmalonyl-CoA mutase; Mco, methylsuccinyl-CoA oxidase; Mch, mesaconyl-CoA hydratase; Mcl, methylmalyl-CoA lyase; Pco, propionyl-CoA oxidase; Mcm, methylmalonyl-CoA mutase; Scr, succinyl-CoA reductase; Ssr, succinate semialdehyde reductase; Hbs, 4-hydroxybutyrate-CoA ligase; Hbd, 4-hydroxybutyryl-CoA dehydratase; Mas, malate synthase

When optimising for maximum malate production (or maximum CO_2 consumption), the test model solution predicted flux through all CETCH cycle reactions in the expected direction (Fig. 3.2B). This confirmed that the stoichiometry was correctly balanced, as all metabolites were produced and consumed in the proper ratios to maintain a complete cycle. The chemical equation for the complete CETCH cycle is given in Figure 3.2C.

I then constrained the reactions of the CETCH cycle to only operate in this "forward" direction, according to their function in the CETCH cycle. This was to prevent the CETCH cycle reactions from taking on unexpected roles when added to the plant diel model, e.g. to produce rather than consume ATP. This "forward only" CETCH cycle was used in all subsequent modelling.

3.3.2 Integration of the CETCH cycle into plant carbon limited model - night-time only

The CETCH cycle was added to the plant diel model, initially only to the dark phase of the model, as I was interested in its potential to reassimilate nocturnally generated CO_2, not in its potential as an alternative to the CBB cycle for daytime CO_2 assimilation. The reactions of the cycle were added to all subcellular compartments of the model in case there were compartment-specific constraints that would make the cycle infeasible. For example, the cycle generates H_2O_2 and the only compartment in the plant model that contains an enzyme which can metabolise this H_2O_2 is the peroxisome which contains a catalase reaction. This is a limitation of the core model which does not contain a full accounting of antioxidant enzymes, rather than a biological reality. Hence, incorporating the CETCH cycle reactions in all compartments allows an initial test of the functionality of the cycle and its integration with endogenous nocturnal metabolism.

Likewise, transport reactions were added to allow all CETCH cycle intermediates to be moved between compartments. While this assumption of free transport is biologically unrealistic, it served as an initial test to examine the cycle's potential function without transport limitations. Such "free transport" reactions were not added if a CETCH cycle intermediate already existed as a metabolite in the plant model (see Methods), to prevent the model from exploiting new transporters to circumvent known transport reactions that have an associated cost.

I incorporated the CETCH cycle reactions into the diel plant models described in Chapter 2.

For an initial test, I used the "CO_2 uptake constrained" model, where carbon uptake was restricted but nocturnal PEPC activity remained unconstrained, resulting in CAM cycling (see 2.3.5). When I optimised this new "CO_2 uptake constrained + CETCH" model for maximum growth (biomass output), the CETCH cycle reactions remained unused, with the model continuing to use CAM cycling for all nocturnal CO_2 refixation.

Next, I tested the CETCH cycle in the baseline model ("CO_2 uptake constrained & nocturnal PEPC limited") (see 2.3.6.3). Upon re-optimisation, the CETCH cycle now carried metabolic flux. Evidently, the carbon-limited model was able to use the CETCH cycle for nocturnal CO_2 refixation but preferred using CAM cycling, if available.

A flux map representing the flux through the CETCH cycle reactions, and associated changes in the plant-native reactions, is given in Figure 3.3A. Only a single CETCH cycle reaction carried zero flux (in this and also in later implementations of the CETCH cycle), namely reaction #7, propionyl-CoA oxidase. Instead, the model chose to use the plant-native reaction catalysed by proprionyl-CoA dehydrogenase, which is present only in the peroxisome. This reaction similarly

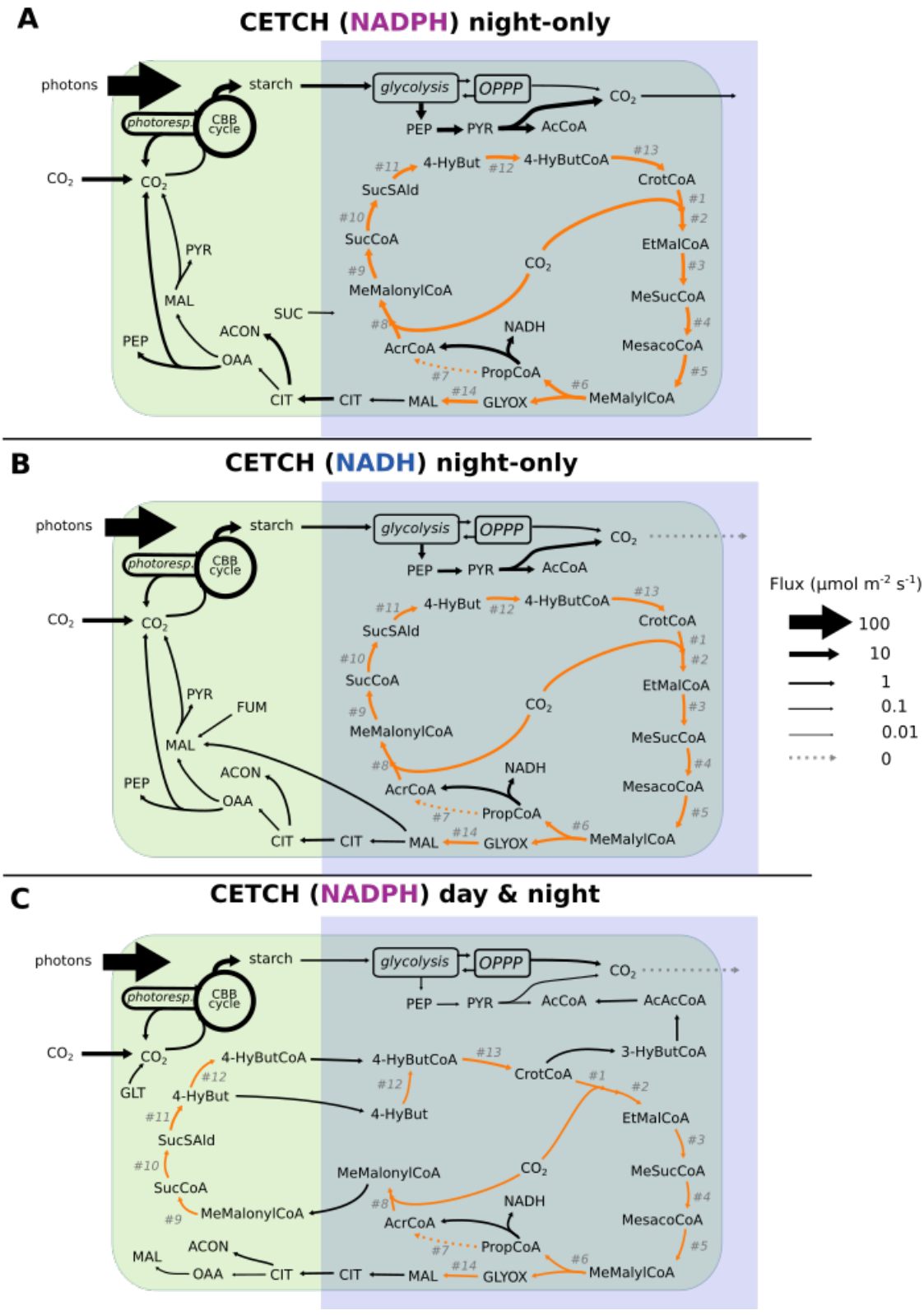
A
CETCH (NADPH) night-only
photons
starch
glycolysis
OPPP
CO2
photoresp.
CBB cycle
PEP
PYR
AcCoA
4-HyBut
4-HyButCoA
CrotCoA
SucSAld
SucCoA
EtMalCoA
MeMalonylCoA
MeSucCoA
MesacoCoA
MAL
SUC
ACON
NADH
AcrCoA
PropCoA
OAA
CIT
GLYOX
MeMalylCoA
B
CETCH (NADH) night-only
FUM
Flux (µmol m-2 s-1)
100
10
1
0.1
0.01
0
C
CETCH (NADPH) day & night
AcAcCoA
3-HyButCoA
GLT

Figure 3.3: **Major flux routes through the plant models with varying implementations of the CETCH cycle.**
Subcellular compartments are omitted for clarity. Arrow widths are proportional to the predicted flux. Reactions of the CETCH cycle are indicated in orange. Abbreviations: CIT, citrate; MAL, malate; GLYOX, glyoxylate; PYR, pyruvate; ACON, aconitate; SUC, succinate; PEP, phosphoenolyruvate; OAA, oxaloacetate; AcCOA, acetyl-CoA; GLT, glutamate; CBB cycle, Calvin-Benson-Bassham cycle; OPPP, oxidative pentose phosphate pathway; 4-HyBut, 4-hydroxybutyrate; 4-HyButCoA, 4-hydroxybutyryl-CoA; CrotCoA, crotonyl-CoA; EtMalCoA, ethylmalonyl-CoA; MeSucCoA, methylsuccinyl-CoA; MesacoCoA, mesaconyl-CoA; MeMalylCoA, methylmalyl-CoA; PropCoA, propionyl-CoA; AcrCoA, acrylyl-CoA; MeMalonylCoA, methylmalonyl-CoA; SucCoA, succinyl-CoA; SucSAld, succinate semialdehyde; 3-HyButCoA, 3-hydroxybutyryl-CoA

converts propionyl-CoA into acrylyl-CoA, but generates NADH rather than H_2O_2 in the process.

Overall, adding the CETCH cycle to the baseline model increased biomass output by 6.5% and the amount of nocturnal CO_2 that was refixed increased from 39.50% to 94.74% (Table 3.2). However, this increase in carbon conversion efficiency came with substantial metabolic costs: the total sum of fluxes increased by close to 2.5 times. The model now became light-limited, as it used 100% of available photons. In comparison, the baseline model used 61.17% of available photons.

Despite the CETCH cycle's reported ATP efficiency, the model required extensive starch production during the day, followed by its accumulation and breakdown at night to generate sufficient ATP to operate the nocturnal CETCH cycle. This increased starch breakdown released more nocturnal CO_2 than in the baseline model. To maintain growth, which requires carbon, the model used the CETCH cycle to refix this additional CO_2. While this achieved nearly complete nocturnal CO_2 refixation, it created an energetically costly cycle: more starch breakdown was needed to power the CETCH cycle, which in turn produced more CO_2 that

Table 3.2: **Key metrics for CETCH cycle modelling scenarios.**
Values in brackets represent the change compared to the baseline model.

	Carbon- & PEPC-limited baseline model	**+CETCH (NADPH) cycle at night**	**+CETCH (NADH) cycle at night**	**+CETCH (NADPH) cycle day and night**
Biomass output rate (µmol m^{-2} s^{-1})	0.0655	0.0698 (+6.57%)	0.0767 (+17.10%)	0.0767 (+17.10%)
Photon use	61.17%	100%	80.11%	67.40%
Daytime CO_2 uptake (µmol m^{-2} s^{-1})	6.643	6.643	6.643	6.643
Nocturnal CO_2 loss (µmol m^{-2} s^{-1})	0.970	0.597	0.0	0.0
Rubisco CO_2 assimilation flux (µmol m^{-2} s^{-1})	8.487	14.192	11.030	9.432
Nocturnal CO_2 refixation	39.50%	94.74%	100%	100%
Total carbon conversion efficiency	85.40%	91.01%	100%	100%
Total sum of fluxes (µmol m^{-2} s^{-1})	850.32	1809.90 (+112.1%)	1190.33 (+40%)	957.76 (+12.7%)

needed to be refixed. Although not entirely futile, since it supported increased growth, this cycle proved remarkably energy inefficient.

Given this unexpected inefficiency, I investigated the specific factors that made the CETCH cycle so energetically costly during the night phase. Looking at the nocturnal ATP and CO_2 budgets, I identified which reactions consumed extra ATP or produced more CO_2, compared to the baseline model (Fig. 3.4 and Fig. 3.5).

The ATP-dependent reactions of the CETCH cycle, 4-hydroxybutyrate-CoA ligase, # 12, contributed only marginally to the total ATP consumption.

NADH kinase, which was previously inactive in the baseline model, was now one of the biggest ATP-consumers at night. NADH kinase uses ATP to convert NADH into NADPH, which is required by four of the CETCH cycle reactions.

Another substantial ATP consumer at night was the cytosolic proton ATPase, which hydrolyses ATP to transport protons across the plasma membrane to the cell exterior. The CETCH cycle consumes one proton per complete cycle, and should therefore mitigate the need to export protons. These additional protons must therefore be generated by reactions of the plant metabolic network, as a wider consequence of running the CETCH cycle. The exact source remained unclear, as tracking proton production and consumption across the entire metabolic network is challenging due to the complex nature of proton-coupled reactions involving multiple compartments.

The massively increased ATP requirement in the model using the CETCH cycle at night necessitated increased nocturnal starch breakdown via glycolysis and the TCA cycle. The higher activity of pyruvate dehydrogenase, ICDH and 2OG dehydrogenase resulted in substantial CO_2 release. To maintain growth, this additional CO_2 needed to be refixed by the CETCH cycle, creating an energy-demanding cycle, ultimately limited by the availability of light to power daytime starch pro-

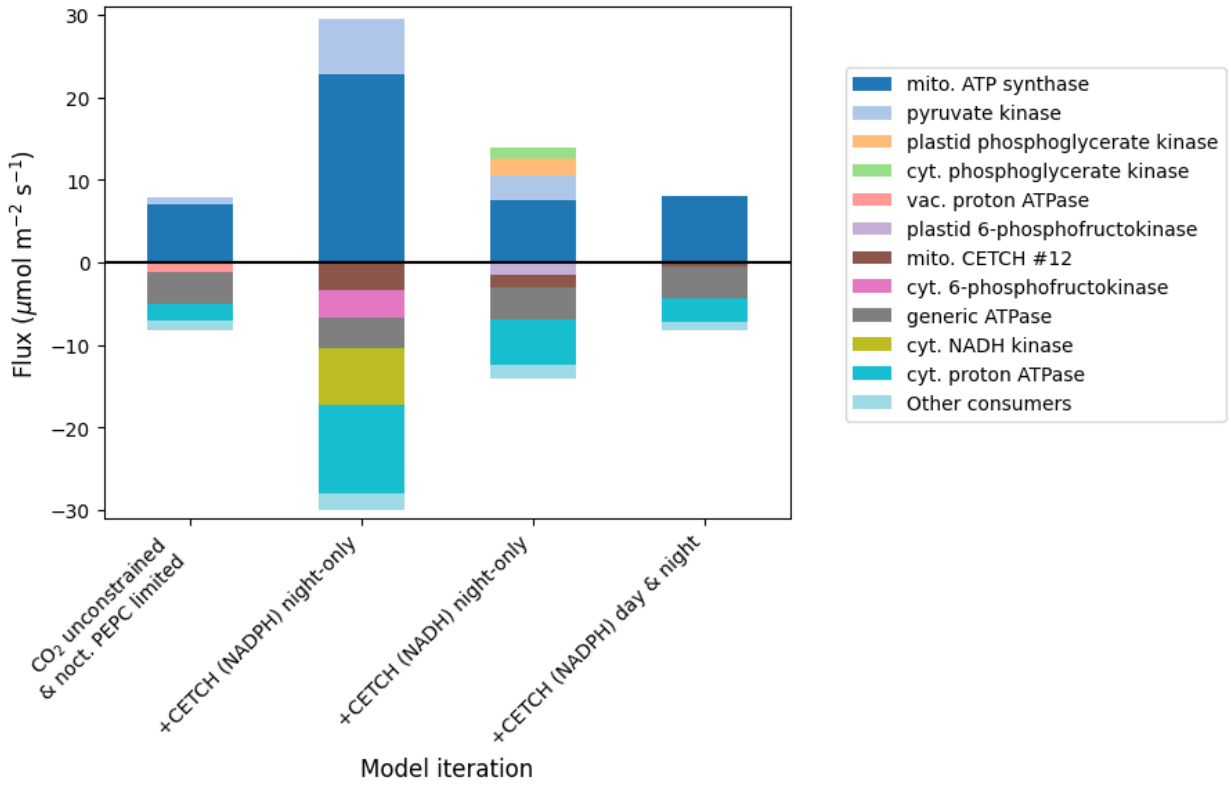

Figure 3.4: **Nocturnal ATP budgets across modelling scenarios.**
All reactions contributing to nocturnal ATP production or consumption across subcellular compartments were quantified, accounting for flux magnitude, direction, and stoichiometry. Positive values represent ATP-producing reactions, while negative values indicate ATP-consuming processes. Abbreviations: mito., mitochondrial; cyt., cytosolic; vac., vacuolar

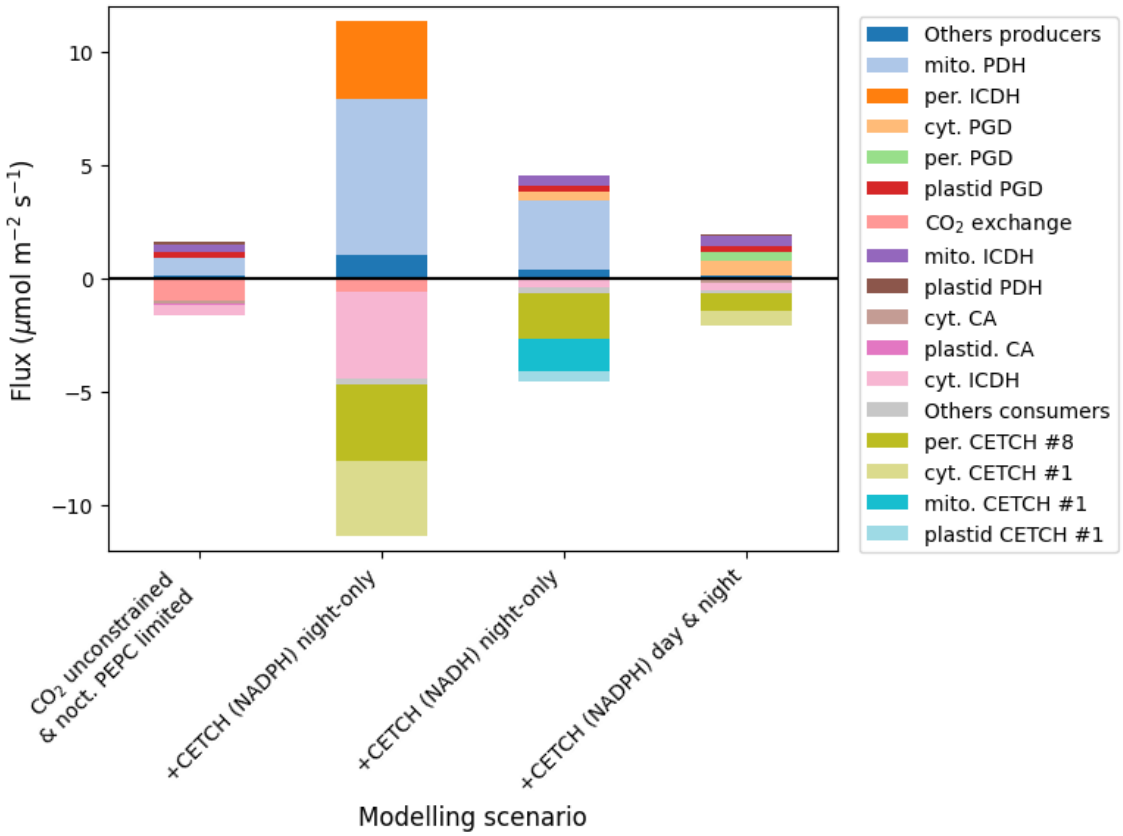

Figure 3.5: **Nocturnal CO_2 budgets across modelling scenarios.**
All reactions contributing to nocturnal CO_2 production or consumption across subcellular compartments were quantified, accounting for flux magnitude, direction, and stoichiometry. Positive values represent CO_2-producing reactions, while negative values indicate CO_2-consuming processes. Abbreviations: mito., mitochondrial; cyt., cytosolic; per., peroxisomal; PDH, pyruvate dehydrogenase; PGD, 6-phosphogluconate dehydrogenase; ICDH, isocitrate dehydrogenase; CA, carbonic anhydrase

duction.

3.3.2.1 Investigation of plant-native, nocturnal NADPH production capabilities

Much of the extra ATP requirement was due to NADH kinase activity. This seemed a very inefficient choice to generate NADPH, as both one molecule of NADH and a molecule of ATP are consumed in the process. I therefore looked at which other possible routes for NADPH generation the plant model has available at night, and explored why they are not utilised.

For this investigation, I first looked up all reactions of the plant metabolic network which contain NADPH, a total of 64 reactions (with some being replicates of identical reactions in multiple compartments). First, I filtered out all reactions that were specified to only occur in the NADPH-consuming direction, after which 18 reactions remained. Then, I removed Ferredoxin-$NADP^+$ reductase, since this reaction is linked to light-dependent reactions of photosynthesis and therefore cannot occur at night.

Of the 17 remaining reactions, one required ATP hydrolysis (NADH kinase, Fig. 3.6A), and ten involved the release of CO_2 (e.g. malic enzyme, Fig. 3.6B). The six remaining reactions were: non-phosphorylating glyceraldehyde 3-phosphate dehydrogenase (GAPDH), glucose-6-phosphate dehydrogenase (in three compartments), pyrroline-5-carboxylate dehydrogenase and methylenetetrahydrofolate dehydrogenase.

Closer examination of some of these remaining pathways showed, that even though they do not have a direct ATP or CO_2 cost, the model cannot use them for efficient NADPH production. For example, the non-phosphorylating GAPDH enzyme provides an alternative route in glycolysis to generate NADPH. However, as

depicted in Figure 3.6C, using the non-phosphorylating GAPDH enzyme means that the model misses out on the generation of one NADH molecule and one ATP molecule, via the phosphorylating GAPDH followed by phosphoglycerate kinase. In the case of glucose-6-phosphate dehydrogenase, the only available option to further metabolise the product of this reaction, 6-phosphogluconolactone, is to continue along the OPPP. This means the inevitable release of CO_2 from the downstream 6-phosphogluconate dehydrogenase reaction (Fig. 3.6D).

This suggests that the high energy cost of running the CETCH cycle at night stems to a large extent from the challenge of generating NADPH in the dark without also losing carbon as CO_2, consuming ATP or bypassing ATP-producing steps, rather than from the CETCH cycle's direct ATP requirements.

Lastly, I examined the reactions in the plant model, which are prohibited from operating in the NADPH-producing direction. For example, it appeared that the plastidic NADP-malate dehydrogenase (pMDH) could potentially provide an efficient NADPH-generating route if it could operate in reverse (NADPH + oxalate + H^+ –> $NADP^+$ + malate).

I therefore conducted a thermodynamic analysis, using the Thermoflux package (see Methods). Thermoflux uses eQuilibrator (Flamholz et al., 2012; Beber et al., 2021) to calculate feasible ranges for change in Gibbs free energy of reactions ($\Delta_r G$), given estimates of metabolite concentration ranges. From this, one can infer plausible reaction directionality under physiological conditions.

For the calculations, I specified typical plant cell conditions and physiologically relevant metabolite concentrations (0.01-20 mM for most metabolites). I then varied the ratios of NADPH:$NADP^+$ to see at what ratios NADPH production by pMDH may become feasible. The experimentally measured value for the ratio of NADPD:$NADP^+$ in plants was around 1 (Smith et al., 2021).

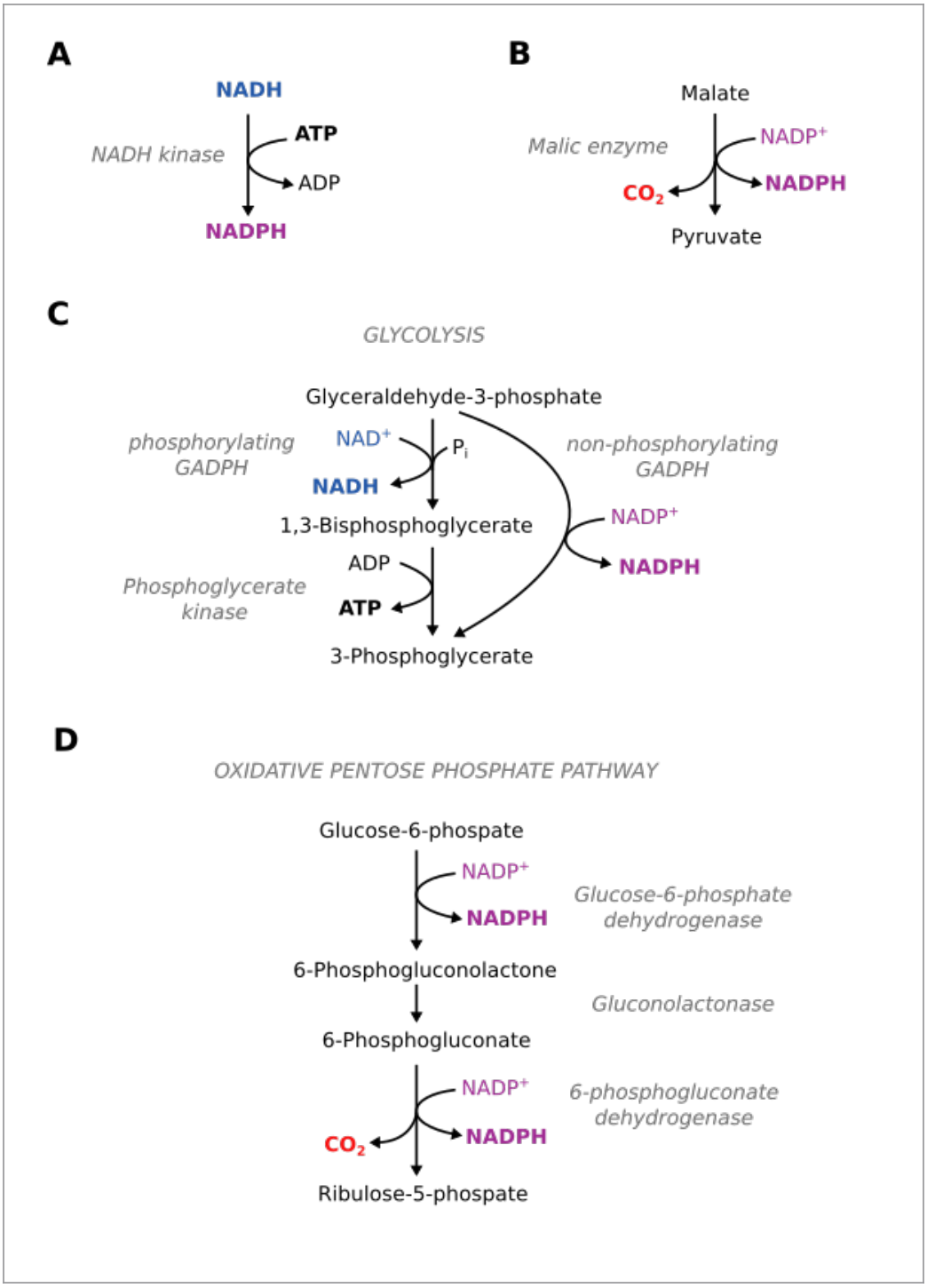

Figure 3.6: **Plant-native nocturnal NADPH generation routes.**
Depicted are four of the available routes for generating NADPH at night in the plant model. Abbreviations: GADPH, phosphorylating glyceraldehyde 3-phosphate dehydrogenase

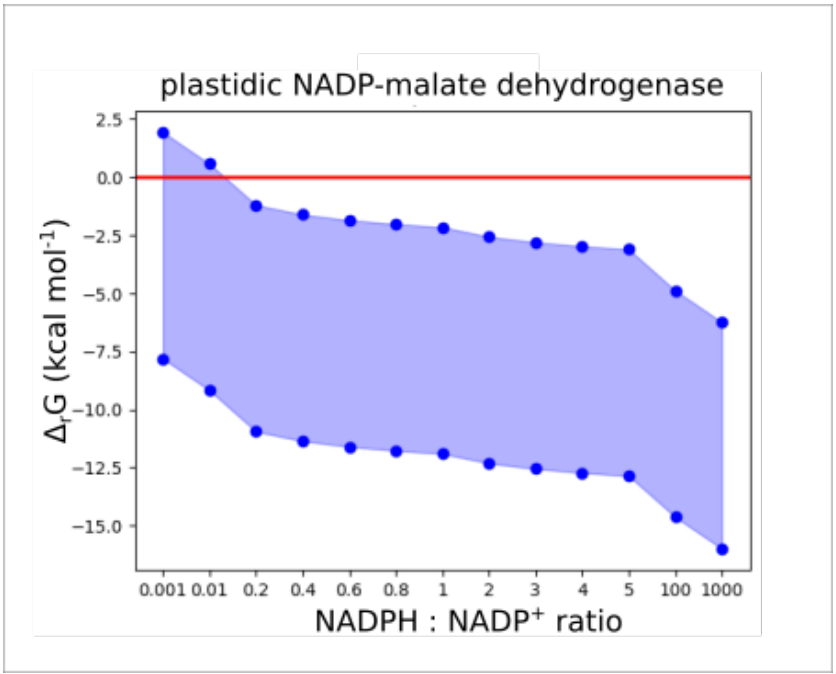

Figure 3.7: **Reaction directionality of plastidic NADP-malate dehydrogenase across varying NADPH:NADP⁺ ratios.**
Blue markers indicate the predicted minimum and maximum change in Gibbs free energy of the plastidic NADP-malate dehydrogenase at each NADPH:NADP⁺.

Thermoflux calculations showed that the pMDH reaction is irreversible in the NADPH-consuming direction at the physiologically relevant NADPH:NADP⁺ ratio of 1 (Fig. 3.7), as even the most extreme $\Delta_r G$ values remained negative at that point. Only extremely high NADP⁺ concentrations compared to NADPH, could potentially allow this reaction to act in reverse.

While this particular reaction was confirmed to best remain constrained in the NADPH-consuming direction only, future work could apply similar thermodynamic analysis to validate the directionality constraints of other NADPH-related reactions in the model.

3.3.3 Change of coenzyme use of CETCH cycle reactions from NADPH to NADH

I then went on to test whether NADPH generation at night was indeed the key factor limiting efficiency. Seeing how NADPH was produced from NADH by NADH kinase at night, I hypothesised that NADH would be more readily available to the model at night. I therefore modified the CETCH cycle reactions to use NADH instead of NADPH as a coenzyme (and likewise changed all $NADP^+$ to NAD^+).

This modified CETCH (NADH) cycle was added to all compartments during the dark phase. The results (Table 3.2, Fig. 3.3B) supported the hypothesis: the model achieved higher biomass growth rates, even higher than the CETCH (NADPH) cycle. The model also achieved 100% nocturnal CO_2 refixation, while producing less CO_2 overall at night than the CETCH (NADPH) cycle model (Fig. 3.5). The total metabolic flux increased only 1.3-fold compared to the baseline model.

Changing the coenzyme used by the nocturnal CETCH cycle from NADPH to NADH reduced the photon use substantially, from 100% to 80%, meaning that the model was no longer light-limited. In comparison, the baseline model exhibited photon use of 61%.

Overall, this result confirmed that a major limitation of using the CETCH (NADPH) cycle at night was the plant metabolic network's inability to efficiently generate NADPH at night. In contrast, NADH is readily generated by glycolysis and the TCA cycle, which are already active to generate the required ATP at night. Using NADH instead was therefore energetically more favourable, as additional ATP consumption and CO_2 release could be avoided.

However, despite its energetic advantages, there may be other obstacles to us-

ing NADH as a coenzyme at night. The feasibility of using different coenzymes depends not only on enzyme specificity but also on cellular coenzyme ratios. In plant cells, the NADPH:$NADP^+$ ratio is typically high, favouring NADPH-consuming reactions, like those in the original CETCH (NADPH) cycle. In contrast, NADH:NAD^+ ratios are much lower. Therefore, switching the CETCH cycle to use NADH could potentially reverse reaction directions. To assess this risk, I conducted a thermodynamic analysis using the Thermoflux package for the modified CETCH cycle reactions.

I calculated plausible $\Delta_r G$ ranges for each of the four CETCH cycle reaction, modified to use NADH instead of NADPH. I then tested how varying coenzyme ratios affected the reaction's directionality. For this, I varied the ratio of NADH:NAD^+ from 1:1000, which is the lowest value that had been measured experimentally in plants (see 3.4.3.4), to 1000:1.

All four reactions remained reversible across the specified range of NADH:NAD^+ ratios (see Fig 3.8). These results suggest that the CETCH cycle could, in principle, operate in the required direction using either coenzyme within physiologically relevant conditions.

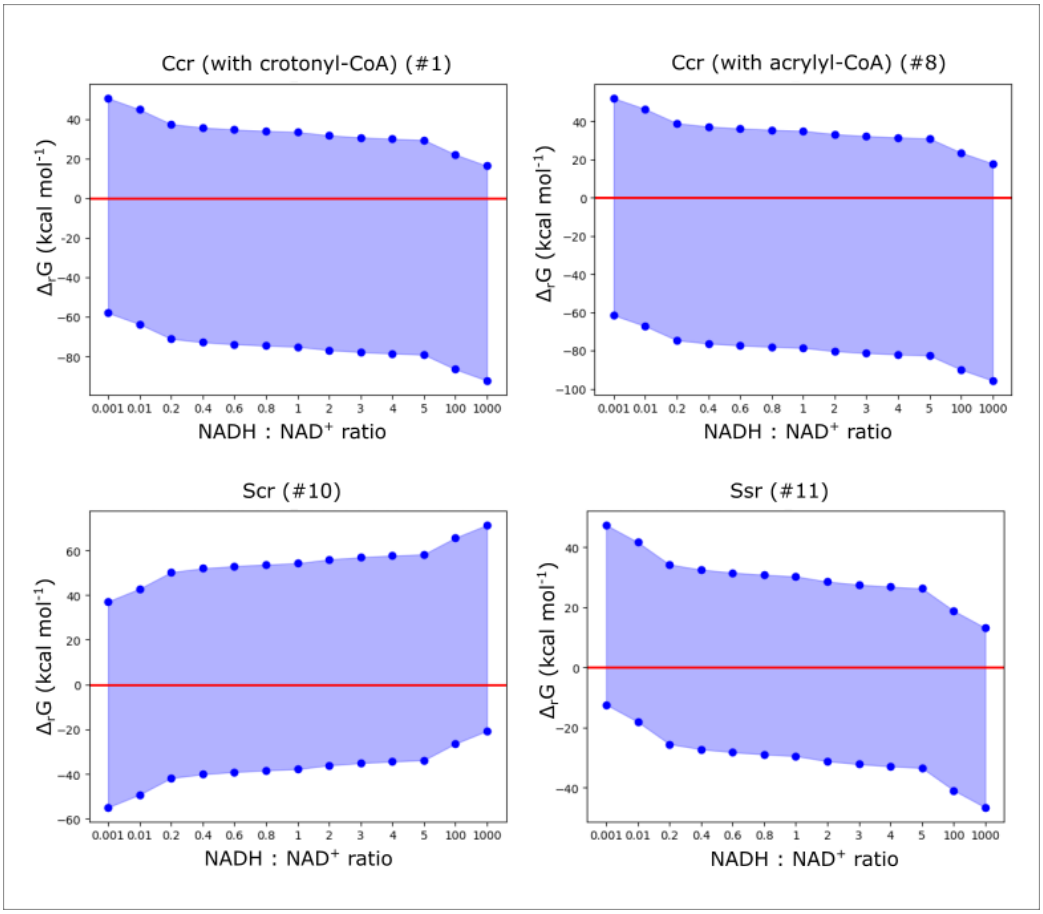

Figure 3.8: **Reaction directionality of NADH-dependent CETCH cycle reactions across varying NADH:NAD$^+$ ratios.**
Blue markers indicate the predicted minimum and maximum change in Gibbs free energy of the reaction at each NADH:NAD$^+$ ratio. Numbering of reactions corresponds to Table 3.1. Abbreviations: Ccr, crotonyl-CoA carboxylase/reductase; Scr, succinyl-CoA reductase; Ssr, succinic semialdehyde reductase.

3.3.4 Integration of the CETCH cycle into plant baseline carbon limited model - day and night

While NADPH production appeared to be limited to inefficient routes at night, during the day, NADPH is produced by the light-dependent reactions of photosynthesis. I therefore investigated whether allowing the CETCH cycle to operate partially during daytime could improve its efficiency by shifting the use of NADPH-dependent reactions to when this coenzyme can be generated by the light-dependent reactions, therefore avoiding additional nocturnal CO_2 release.

To test this, I added the CETCH (NADPH) cycle's reactions to both light and dark phases across all compartments. To focus specifically on nocturnal CO_2 refixation, I blocked the CETCH cycle's CO_2-consuming reactions during the light phase to prevent interference with Rubisco-based CO_2 fixation. I added transport reactions to allow CETCH cycle intermediates to move between compartments. Furthermore, I added transporters to enable vacuolar import and export and linker reactions to transfer these metabolites between the light and dark phase of the model. This enabled the model to generate CETCH cycle intermediates during the day for subsequent night-time use, and vice versa.

When allowed to operate across both day and night phases, the model indeed shifted some of the CETCH cycle reactions to the light phase. By doing this, the model achieved 100% nocturnal CO_2 refixation and increased biomass output compared to the baseline model by 17.1 %. Nevertheless, this day and night implementation of the CETCH (NADPH) cycle maintained relatively modest increases in total sum of fluxes compared to the baseline model. This was a major improvement compared to both previous implementations of the CETCH cycle (Table 3.2).

The CETCH cycle's temporal distribution showed interesting complexity (Fig. 3.3C). Reactions #9, #10 and #11 all took place during the day. Notably, two of these reactions consume NADPH. After reaction #11, the model split the metabolic flux: three-fifths of the produced 4-hydroxybutyrate proceeded through reaction #12 during the day and the product, 4-hydroxybutyryl-CoA, was stored in the vacuole for further processing at night. The other two-fifths of 4-hydroxybutyrate were directly accumulated in the vacuole until night-time, and reaction #12 then took place at night.

Reaction #12 consumes ATP. This arrangement therefore distributed the ATP demand of the CETCH cycle between day (60%) and night (40%). The reason for this was not apparent, as one would think that the model would benefit from shifting as much of the ATP consumption to the day as possible.

The remaining reactions of the CETCH cycle all occurred exclusively at night. This includes two more NADPH-consuming steps. But these were also the CO_2-consuming steps, which I had constrained to not occur during the day, and so they operated here to refix nocturnal CO_2 only.

Whereas in the previous setup, "CETCH (NADPH) night-only", in which all ATP and NADPH required to run the cycle needed to be generated at night, the model now shifted some of the costs to the daytime, when these coenzymes are more readily available via photosynthesis. Two NADPH-consuming reactions and about 60% of one ATP-dependent reactions of the CETCH cycle were now shifted to the daytime. Seeing that, compared to the baseline model, photon use and nocturnal ATP turnover increased only moderately (Fig. 3.4), this temporal segregation appeared to have reduced a metabolic burden imposed by running the CETCH cycle for nocturnal CO_2 fixation.

3.4 Discussion

3.4.1 Restricting native CO_2 refixation pathways enables evaluation of heterologous pathways

The analyses in this chapter demonstrate the value of the baseline model developed in Chapter 2 for evaluating potential metabolic engineering strategies for carbon refixation. When the CETCH cycle was added to a model that only was carbon-limited, but not constrained in its nocturnal PEPC activity, it remained inactive while CAM cycling persisted. This reveals that CAM cycling represents the most efficient solution for nocturnal CO_2 refixation in this specific model setup, both in terms of carbon conservation and total flux minimisation.

The nocturnal CETCH cycle became active only when carbon was limited and the activity of nocturnal PEPC activity was constrained to typical C3 plant levels. This highlights a potentially important principle for metabolic modelling studies in general: While a model's predicted fluxes under the condition of resource limitation might represent a feasible metabolic adaptation, perhaps even one known to occur in nature, restricting this response may be necessary to investigate alternative strategies that would otherwise remain hidden.

3.4.2 Limitations and future refinements of the model and heterologous pathway implementation

This modelling study provides an initial assessment of artificial CO_2-fixing pathways for nocturnal CO_2 refixation in a plant model, using the CETCH cycle as a test case. The primary aim was to evaluate whether the CETCH cycle could function and salvage nocturnal CO_2 in plants from a stoichiometric perspective.

This meant to investigate whether nocturnal plant metabolism could provide the pathway with enough of the necessary cofactors, process its by-products, and effectively make us of its end products to achieve higher levels of nocturnal carbon conservation, ultimately resulting in increased growth. Several simplifying assumptions were knowingly made to be able to address these fundamental questions. Future studies could incorporate additional modifications and constraints discussed below to improve the reliability of the modelling results by better reflecting real-world conditions.

3.4.2.1 Protonation states

While the core plant model accounts for different protonation states of native metabolites based on compartmental pH, this was not implemented for CETCH cycle intermediates. The Thermoflux package could also be used to determine appropriate protonation states for these molecules at different compartmental pH values. Including these protonation states could affect proton balance across compartments, potentially altering the activity of ATP-dependent proton pumps and thereby influencing the pathway's energy requirements.

3.4.2.2 Compartment localisation and transport

Another simplification in the current model is the unrestricted subcellular localisation of heterologous enzymes and transporters. In reality, targeting proteins to specific compartments can present significant challenges, and the enzyme activity may vary considerably depending on the compartmental environment (Yao et al., 2023).

Furthermore, the model assumes unrestricted transport and storage of CETCH cycle intermediates between compartments and in the vacuole. This simplification overlooks both physical constraints on metabolite movement and accumulation, as

well as the energetic costs of cross-membrane transport. A more realistic model would need to identify transporters that are specific for certain molecules of the CETCH cycle and incorporate them in the model with their exact transport mechanisms, such as ATP-dependent or proton gradient-facilitated transport. If suitable transporters can be found, the addition of these transport costs would likely reduce the pathway's efficiency.

One potential solution to these challenges could be the creation of a dedicated compartment for the CETCH cycle enzymes, similar to approaches being developed for other metabolic engineering applications. Several strategies exist for creating such artificial compartments, including liquid-liquid phase separation (Kang et al., 2024), protein-based encapsulation (like bacterial carboxysomes) (Fang et al., 2018), or modification of existing organelles such as the endoplasmic reticulum (Sandor et al., 2021). This approach could not only solve enzyme localisation and transport issues but could also concentrate pathway intermediates, thereby potentially improving pathway efficiency by reducing unwanted interactions with native metabolism. An additional benefit could be protection of introduced enzymes from proteolysis, thereby allowing accumulation of higher amounts of the enzymes (Lindström Battle and Sweetlove, 2025).

However, a significant challenge remains in delivering CO_2 to such a compartment. A promising solution could be derived from natural CO_2-concentrating mechanisms, particularly the pyrenoid systems found in algae. CO_2 is transported to Rubisco by first converting it to bicarbonate via CA. This bicarbonate is then actively transported into thylakoid membranes that penetrate the pyrenoid matrix, where it is locally converted back to CO_2 in close proximity to densely packed Rubisco enzymes (Mackinder, 2018). Current efforts to engineer pyrenoid-like structures in land plants for enhanced Rubisco-based CO_2 fixation (Atkinson et al., 2020) could be adapted to instead create microenvironments optimized for artifi-

cial CO_2-fixing pathways.

3.4.3 Metabolic modelling uncovers challenges in CETCH cycle implementation for nocturnal CO_2 refixation

3.4.3.1 NADPH production in previous CETCH cycle experiments

Integration of the CETCH cycle into the plant metabolic network revealed an unexpected challenge regarding the regeneration of NADPH at night. The limited availability of efficient NADPH-generating pathways during the dark phase emerged as a significant constraint. The few available options entailed CO_2 release or ATP consumption, both counteractive to the goal of nocturnal CO_2 refixation. This insight highlights the value of systems-level modelling. Only by examining the CETCH cycle within the broader metabolic context did it become apparent that not just ATP efficiency is important for a pathway's energetic costs, but also other required cofactors and the available routes for their regeneration.

The observed inefficiency of nocturnal NADPH production could be an issue because of unrealistically tight constraints set on allowed reaction directions in the plant core metabolic model. It is often not obvious why such directionality constraints were implemented. Future studies could use thermodynamic analysis, like the one presented here using Thermoflux, to validate the directionality constraints on NADPH-producing reactions. Reanalysis that is based on thermodynamic assessment could result in loosening of such constraints, if reactions are found to feasibly generate NADPH under physiologically relevant conditions in plant cells. For some reactions, the strict one-directionality may well be confirmed, as exemplified by the analysis done for pMDH, which would generate NADPH only at unrealistically low NADHP:$NADP^+$ ratios.

This observation of the issues brought by inefficient nocturnal NADPH production prompted me to examine how NADPH regeneration was achieved in previous experimental demonstrations of the CETCH cycle.

In the original *in vitro* demonstration of the CETCH cycle (Schwander et al., 2016), coenzyme recycling was achieved through auxiliary enzymes. While ATP was regenerated using polyphosphate kinase, NADPH recycling relied on formate dehydrogenase (FDH), which oxidises formate to CO_2 while reducing $NADP^+$ to NADPH. This means that for every turn of the CETCH cycle, which fixes two CO_2 molecules, regeneration of NADPH by FDH converted four formate molecules to four CO_2 molecules. Therefore, the complete stoichiometry of the *in vitro* system should state net release of two CO_2 molecules when formate dehydrogenase is used to regenerate NADPH.

It would therefore depend on the source of formate for microbial fermentation, whether there was an overall fixation of atmospheric CO_2. Formate can be produced from electrochemical conversion of CO_2 (Yishai et al., 2016), which would be in line with sustainability goals (as long as the required electricity was sourced from renewable, CO_2-neutral energy sources). However, in this form, the *in vitro* CETCH cycle would more accurately be labelled a formatotrophic cycle.

In subsequent experiments, researchers integrated the purified CETCH cycle enzymes with isolated plant thylakoid membranes (Miller et al., 2020). These membranes, which host photosynthetic light-dependent reactions, could generate ATP and NADPH when illuminated. Optimising the system, by including ferredoxins, enzyme modifications, and reactive oxygen species scavenging, enabled the CETCH cycle to function using only light energy for coenzyme regeneration. This eliminated the previous requirement for exogenous formate and its oxidation to CO_2, establishing a true CO_2-fixing system. Overall, this represents a similar ap-

proach to the one I modelled by allowing the CETCH cycle reactions to be used also during the day, and therefore to make use of NADPH generated via photosynthesis.

3.4.3.2 NADPH vs NADH as a coenzyme for enzymes of a nocturnal CETCH cycle

Metabolic modelling allowed me to test whether using NADH directly, rather than producing NADPH from NADH and ATP, would have a positive impact for nighttime CO_2 refixation. Indeed, the model showed that an NADH-dependent CETCH cycle would operate more efficiently at night, with photon use and total sum of fluxes much closer to the baseline model, suggesting less disruption to wider metabolism and better feasibility for implementation in plants.

However, this theoretical analysis rests on two critical assumptions: that the enzymes' cofactor preference could be altered, and that NADH use instead of NADPH would be thermodynamically feasible.

3.4.3.3 Changing coenzyme preference

There are numerous examples in the literature showing successful change of an enzyme's cofactor preference between NADPH and NADH (see Cui et al. (2015) for a list of 30 published studies), which in some cases was achieved with just a single amino acid substitution. Such engineering typically requires structural knowledge of the enzyme or related enzymes, though recent advances in computational methods are making it possible to identify functional domains from a protein's amino acid sequence alone, facilitating the identification of suitable amino acid targets for protein engineering (Cui et al., 2015).

One important potential caveat is that enzymes engineered to use NADH some-

times show inhibition by NADPH (Scrutton et al., 1990). This may be permissible for *in vitro* experiments, but certainly not for enzymes that are meant to operate within cells.

3.4.3.4 Thermodynamic feasibility of enzyme-catalysed reactions with different coenzyme ratios of reduced:oxidised forms

The directionality of biochemical reactions depends on the equilibrium constant of the reaction and the concentrations of reactants. This is relevant for NADH- and NADPH-dependent reactions presented in this work, as NADH:NAD^+ and NADPH:$NADP^+$ ratios differ significantly in plant cells. NADH exists primarily in its oxidised form (NAD^+), with NADH:NAD^+ ratios around 0.01 or even as low as 0.001 (Smith et al., 2021). In contrast, NADPH maintains higher reduced:oxidised ratios of approximately 1, reflecting its role as an electron donor in biosynthetic pathways rather than energy metabolism.

It was therefore of interest to determine whether these different coenzyme ratios would affect reaction directionality of the relevant CETCH cycle enzymes when simulating the switch from using NADPH to using NADH. I tested this using the Thermoflux package (an as of yet unpublished framework for incorporating thermodynamic analyses in FBA), varying values for the concentrations of the reduced and oxidised forms of the coenzyme to represent the ratios from 0.001 to 1000. Even across this extreme range, all reactions remained reversible regardless of which coenzyme was used, suggesting that either form could theoretically operate in the direction required for the CETCH cycle to fix CO_2 at night. However, it is important to realise that across this range of NADH:NAD^+ ratios, reaction direction would also depend on the concentrations of substrates and products. In the absence of experimental data on realistic concentrations ranges for specific metabolites, I allowed a wide range possible concentrations for the reactants and

products of the tested reactions (between 0.01 and 20 mM). In practice, achieving sufficiently high substrate levels while maintaining low product concentrations to drive the reaction forward at a realistic NADH:NAD^+ ratio, may be difficult, as this could require extensive engineering of adjacent metabolic pathways.

3.4.4 Modelling of the CETCH cycle informing alternative pathway design

In this work, I examined the potential benefit of the CETCH cycle for plant growth by enabling nocturnal CO_2 refixation, based on its reported ATP efficiency and successful *in vitro* implementation.

Previous studies have discussed the potential of implementing the CETCH cycle in plants (Bar-Even, 2018; Naseem et al., 2020; Osmanoglu et al., 2021), focusing on the CETCH operating during the day, to act as a complement or alternative to Rubisco-based daytime CO_2 assimilation. Nevertheless, several obstacles for *in vivo* implementation have been identified. The cycle's complexity - 14 enzymatic steps using enzymes from diverse organisms - would make its implementation and optimisation in plant cells particularly challenging (Bar-Even, 2018).

An additional concern raised by Strand and Walker (2023) relates to the ratio of ATP/NAD(P)H (0.66) of the CETCH cycle, which differs from Rubisco-based CO_2 fixation (1.5). Since the linear electron transport pathway of photosynthesis produces ATP and reducing equivalents in a specific ratio, this mismatch could cause metabolic disruptions. Although there is some capacity to adjust the ATP : NADPH ratio produced by photosynthesis by engagement of cyclic electron transport, a high flux CETCH cycle could exceed the capacity for adjustment leading to excess ATP which would need to be dissipated to avoid photosynthetic inhibition, or insufficient NADPH might leave cycle intermediates unprocessed. These

challenges would equally apply to nocturnal implementation of the CETCH cycle.

Moreover, my work demonstrates that the unmodified CETCH cycle, consuming NADPH, would not be effective for nocturnal CO_2 refixation. The theoretical solutions identified - switching to NADH use or redistributing NADPH-consuming reactions to daytime - would additionally require substantial enzyme engineering or careful control of temporal expression and metabolite accumulation.

The modelling framework presented here could be used to evaluate other, natural or artificial, CO_2-fixing pathways for the purpose of improving carbon-efficiency of nocturnal plant metabolism. Based on the critique of the CETCH cycle mentioned above and insights from this work, I propose that key selection criteria for other pathways should include: 1) a small number of reactions steps and therefore few genes to be expressed, 2) efficiency of ATP as well reducing equivalents use, particularly favouring NADH-dependent reactions over NADPH-dependent ones at night, 3) pathway end products that plants can readily accumulate and decarboxylate during the day, and potentially 4) pathway intermediates before the CO_2-fixation step that can be accumulated in plants, to enable the shift of metabolically costly reactions to the daytime. Moreover, to function in plants, enzymes of the pathway need to be insensitive to oxygen, which eliminates some of the natural, known CO_2-fixing pathways (Santos Correa et al., 2023).

3.4.5 Use modelling to identify completely new pathways

Another exciting potential application of this modelling framework could be to discover entirely novel pathways for nocturnal CO_2 refixation in plants. While most artificial CO_2-fixing pathways created so far have focused on their use *in vitro* and in microbes, this metabolic model could help to identify designs specifically suited for plant metabolism, for example, by exploiting the diel nature of

plant metabolism by shifting energy-intensive reactions to the daytime.

In order to achieve this, one could extract all known metabolic reactions from databases, such as Metacyc.org (Caspi et al., 2018). By making them available to the model, it could find its own ideal combination of reactions, in novel combinations, building pathways optimally suited to the given modelling objective.

A key challenge in approaching pathway discovery this way would be to integrate novel reactions into the existing metabolic model representing the organism of interest while predominantly preserving its core metabolic function. Simply adding all possible reactions to a plant metabolic model and optimising for biomass output would likely result in widespread metabolic restructuring, which no longer resembles the previous flux distribution. Instead, the goal is to identify minimal sets of novel reactions to integrate into the existing organism model, which could form a single beneficial pathway while maintaining the plant's native metabolic network largely intact.

Different approaches could be tested to achieve integration of only a small number of foreign reactions.

One strategy would be to add weights to all foreign reactions, essentially multiplying any flux they carry. By then also optimising for minimal sum of fluxes, the use of these foreign reactions will be penalised, unless they bring a substantial benefit towards the modelling objective. Similarly, one could apply penalties when native metabolic fluxes deviate from their original values, thereby favouring solutions that maintain a flux distribution close to the original plant model. However, this may lead to multiple, dispersed alterations rather than one pathway of consecutive reactions.

Alternatively, one may first try to build pathways for a particular purpose without yet considering their full integration into an organism's metabolism, as has been

done in previous publications (Schwander et al., 2016; Bar-Even et al., 2010; Trudeau et al., 2018). The process could be similar to what I described for the minimal model used to test the reactions obtained from MetaCyc for the CETCH cycle. Except in this case, instead of just featuring the reactions of the CETCH cycle, all known metabolic reactions would be allowed. For the goal of finding novel CO_2-fixing pathways or cycle from all these reactions, one would first allow CO_2 as an input metabolite. Consumption of CO_2 and the minimisation of total sum of fluxes, or minimisation of the sum of active reactions, would be set as the objective. Exchange reactions would be created for ATP, ADP, phosphate and the reduced and oxidised forms of reducing equivalents. Plant-native metabolites which are considered to be suited to accumulation may then be permitted as substrates and end products. After optimisation, I would expect the model to have selected a small number of reactions, starting from CO_2-fixation, eventually producing one of the permitted plant native metabolites. These pathways could then be inserted the model representing the organism of interest to test their impact, equivalent to how I tested the CETCH cycle in the plant metabolic model.

4 | Testing the hypothesis of enhanced carbon use efficiency in *Marchantia polymorpha* with constraint-based modelling and targeted experiments

4.1 Introduction

The bryophyte *Marchantia polymorpha* is a model for non-vascular plants, owing to the ease of propagation in the laboratory and its genetic tractability (Bowman et al., 2022). A series of advantageous properties, such as asexual propagation options, short generation times, a small genome with little genetic redundancy and a dominant haploid life stage, make Marchantia also a promising candidate for rapid prototyping of plant metabolic engineering strategies (Kohchi et al., 2021; Sauret-Güeto et al., 2020; Delmans et al., 2017). Tools have been developed for Agrobacterium-based transformation and high throughput imaging of early stage gemmae development (Annese et al., 2025).

Despite the growing interest and use of Marchantia in research, the only published work to create and use a metabolic model for the species was done by Cannell (2021). The Marchantia-specific model was created by modifying a model of core plant metabolism based on genomic information from Marchantia sequencing data (see 4.2). Analysis of the model integrated experimental data from Marchantia from the literature, for parameters such as biomass composition, growth rate and CO_2 assimilation rate, to further constrain the model in a species-specific manner.

As Marchantia is believed to be a C3 plant (Hanson et al., 2002; Shu et al., 2022),

Cannell also applied the method described in Shameer et al. (2019) (see Chapter 2, Method 1 - Constraining the model objective), to obtain realistic values for CO_2 uptake in a C3 leaf diel metabolic model, while discouraging CAM-like behaviour. However, with this constraint in place, the model was not able to achieve experimentally determined growth rates. When nocturnal refixation of CO_2 in the model was permitted, by constraining daytime CO_2 uptake rates directly, it was readily able to achieve the specified growth rates. These results were accompanied by predicted patterns of metabolism in the model that were reminiscent of CAM cycling. Included in the model setup was a constraint to only be able to lose CO_2 at night via the CO_2 exchange reaction. However, 100% of the respiratory CO_2 generated at night was fixed by PEPC, none was lost to the atmosphere. This refixed carbon, in the form of oxaloacetate was further converted to malate which was stored in the vacuole until daytime, for decarboxylation and reassimilation by Rubisco. While, given the constraints, there was no net fixation of CO_2 at night, refixing 100% of nocturnal respiratory CO_2, representing 100% carbon conversion efficiency, was enough to aid the model in increasing growth rates substantially.

This CAM cycling behaviour persisted when a sensitivity analysis of other model constraints was performed by Cannell. The parameters analysed included the composition of biomass, NGAM costs and Rubisco carboxylation: oxygenation ratio. The experimentally determined growth rates were only attainable if maintenance costs were substantially smaller than previously assumed. The conclusion drawn was that either Marchantia possesses some form of nocturnal carbon recycling, or that this plant has other key energetic differences such as extremely low NGAM costs. If Marchantia were to utilise nocturnal carbon recycling to improve its overall carbon conversion efficiency then it would merit further exploration in the context of this thesis.

C3-type metabolism is generally assumed for liverworts by default, because they

do not inhabit the arid environments which are usually associated with CAM, and they lack the anatomical complexity necessary for multi-cellular C4 metabolism. Nevertheless, time series data for metabolite concentrations or gas exchange is lacking for Marchantia and limited attention has been paid to Marchantia carbon metabolism (Hata et al., 2000). The anatomical simplicity of Marchantia tissue constitutes a barrier to efficient CO_2 uptake (Carriquí et al., 2019). The thallus only has fixed-open small air pores. In comparison, higher plants have leaves with specialized cell types, large air spaces and closable stomata. Furthermore, Marchantia has thick cell walls to prevent desiccation. All this severely limits the rate of diffusion of CO_2 into Marchantia cells and chloroplasts. As a consequence, CO_2 assimilation rates reported for Marchantia, and other bryophytes, are very low in comparison to vascular plants (Flexas and Carriquí, 2020).

In hornworts, close relatives of liverworts, such CO_2 limitation seems to have driven the evolution of CCMs multiple times independently (Villarreal and Renner, 2012). Similar to those found in some microalgae, their CCMs utilise non-membrane bound compartments, termed pyrenoids, to increase CO_2 concentrations around Rubisco.

Marchantia face the same limitations as hornworts regarding CO_2 uptake, and yet such CO_2-concentrating subcellular compartments have not been found in Marchantia or other liverworts. However, it is theoretically possible that they have evolved other, metabolic, strategies to increase their carbon use efficiency to cope with limited carbon availability.

4.1.1 Aims

This chapter addresses three interconnected aims. The first was to independently reconstruct and validate the previously described Marchantia metabolic model,

allowing careful examination of the underlying assumptions used in the model and the conclusions drawn.

The second aim was to collect experimental data on Marchantia growth rates, gas exchange and metabolite abundance under consistent conditions. The previously published model was constrained using data collected from multiple different sources in which plants were grown and measured under different conditions, including varying developmental age, light intensity, or photoperiod. By standardising growth conditions, I aimed to provide a more reliable set of empirical measurements. Furthermore, this analysis allowed me to look for evidence of nocturnal CO_2 refixation, particularly in the form of CAM cycling.

The third aim was to incorporate the newly collected experimental measurements as constraints into the reconstructed Marchantia metabolic model to test whether the original conclusions about nocturnal CO_2 refixation remained true.

4.2 Methods and Materials

4.2.1 Metabolic modelling

4.2.1.1 Model construction for Marchantia

A Marchantia-specific core plant metabolic version was created as described by Cannell (2021), by modifying the generic plant model from Shameer et al. (2019) ("PlantCoreMetabolism_v2_1_0.xml"). This meant removing reactions found not to be present in Marchantia (with MetaCyc identifiers RXN-1121, RXN-10773, MYO-INOSITOL-OXYGENASE-RXN, CONIFERIN-BETA-GLUCOSIDASE-RXN and 2.4.1.111-RXN) but adding 57 reactions and 56 metabolites for the synthesis of fatty acids. Additionally, the biomass output reaction was also modified as de-

scribed by Cannell , except for the removal of starch as a biomass component, to better reflect Marchantia biomass composition.

The setup of the diel model was predominantly the same as described in Chapter 2 (see General model setup). Constraint values and combinations (maximum CO_2 uptake rate, photon influx) were set according to experimental data cited in Cannell, or from new experimental data collected as part of this work, presented below. The maximisation of the flux through the Marchantia-specific biomass equation was set as the primary objective, the minimisation of the sum of fluxes as the secondary objective.

4.2.1.2 Calculation of % nocturnal CO_2 refixation

For details on calculating percentage of nocturnal CO_2 refixation, see 2.2.2.

4.2.1.3 Sensitivity analysis

200 quasi-random combinations of the chosen model parameters were created using the gmc module of the SciPy statistics package (Virtanen et al., 2020), using sobol sequences, and the model was updated and optimised anew with each quasi-random parameter combination.

4.2.2 Experiments

4.2.2.1 Plant growth conditions

For all experiments, gemmae of *Marchantia polymorpha* ssp. *ruderalis* accession, male Takaragaike-1 (Tak-1) and female Takaragaike-2 (Tak-2), were grown on 1.4% (w/v) agar with half strength Gamborg B5 medium (Gamborg et al., 1968), without sucrose or any other carbon source. Plates were sealed tightly with parafilm and micropore tape to prevent desiccation. The growth cabinets supplied

about 81 µmol m^{-2} s^{-1} of PPFD for 12 h, then lights were switched off for the remaining 12 h. Growth cabinets were set to a constant temperature of 22 °C.

4.2.2.2 Growth rate

Gemmae from Tak-1 and Tak-2 accessions were grown on agar and photographed every 2-3 d for 33 d using a ZEISS Stemi 508 microscope. Custom scripts for Fiji ImageJ (Schindelin et al., 2012) were created to automate image processing, including thallus-agar distinction, area measurement, and image stitching for larger specimens. Growth rates were calculated initially as an increase in thallus area per existing area over time (m^2 m^{-2} s^{-1}). This was converted to increase of biomass per area over time (µmol m^{-2} s^{-1}), assuming an area to mass relationship of 293 cm^2 per g dry weight (Voth, 1943). Data were collected from 27 individual plants per line.

4.2.2.3 Gas exchange

Gemmae of Tak-1 and Tak-2 were grown on agar for about 30 d. Multiple thalli of the same line were transferred to a new Petri dish. Photos were taken to then measure the combined area of all thalli. This Petri dish was then placed inside the Bryophyte Chamber (6800-24) attached to the LI-6800 device (LI-COR Biosciences, Lincoln, NE, USA), which was placed inside the growth cabinet. Due to the transparent film on top of the bryophyte chamber, the PPFD stayed as before, around 81 µmol m^{-2} s^{-1}.

For gas exchange measurements, the CO_2 concentration was set to be constant at 400 µmol mol^{-1} (approximately representing current atmospheric CO_2 concentrations (Lan et al., 2023), a flow rate of 400 µmol s^{-1}, and a temperature of 23 °C. The measurements started about 1 h before the onset of light in the growth cabinets and lasted for 1 h 30 min to 2 more h in the light. Measurements were

also collected for an empty chamber to control for baseline fluctuations of CO_2 concentrations in the device.

4.2.2.4 Metabolite accumulation

Gemmae of Tak-1 and Tak-2 lines were grown on agar for 50 d. Samples were collected every 4 h covering different time points over the course of one full day and night cycle of a 12 h/12 h photoperiod: 0 h, 4 h, 8 h, 12 h, 16 h, 20 h after the start of illumination. Where possible, individual, whole plants were collected and weighed, aiming for 100-300 mg of plant material. If a single plant had insufficient mass, multiple plants were pooled for one sample. Six replicates were collected per time point. It was found that Tak-1 plants were substantially smaller than Tak-2, making it impossible to collect enough plant material from individual plants. Therefore, experiments only proceeded with Tak-2.

Immediately after weighing, plants samples were frozen in liquid nitrogen. A steel ball was added, and plant material was homogenised using a Qiagen tissuelyser set to 30 times s^{-1} for 2 min. Metabolites were extracted from plant homogenates following a methanol-chloroform extraction protocol: "Extraction protocol for Metabolic Profiling of *A. thaliana* leaves for GC-MS" based on (Lisec et al., 2006). 60 µl ribitol were added as an internal standard. MSTFA was used for the derivatisation of the polar phase collected from plant samples and also for calibration solutions (for amino acids and organic acids) (see Table B.1).

Derivatised samples were then separated using gas chromatography and analysed by mass spectrometry. Samples from any of the time points were run in a randomised order along with derivatised samples of the calibration solutions. Compounds were identified and their peaks quantified using Agilent Masshunter Quantitative Analysis software (RRID:SCR_015040).

4.3 Results

4.3.1 Model reconstruction

The reactions and metabolites of the core plant metabolic model from Shameer et al. (2019) were modified as described by Cannell (2021), to better reflect enzymes determined to be present in Marchantia based on genomic analysis. This species-specific core model was then used to set up a diel plant model (as in Cheung et al. (2014)), to represent a photosynthetic cell of Marchantia with its distinct but connected metabolic behaviours in the light and in the dark. Constraints were applied to the model as described by Cannell, who used a combination of Marchantia-specific experimental data where possible or generic plants constraints from earlier plant metabolic modelling otherwise.

In the light phase of the model, I applied an upper bound constraint on the photon influx reaction of 174 μmol m^{-2} s^{-1} based on data reported by Carter and Romine (1969). The measured CO_2 assimilation rate in this same study was 1.16 μmol m^{-2} s^{-1}. I used two different methods to set this value as the maximum allowable daytime CO_2 uptake rate. These methods were both used in the Cannell study, and previously in Chapter 2. The model optimised with the first method, described in detail in 2.3.6.1, will be referred to as the "Objective constrained" model. In short, to apply this method, I kept the CO_2 uptake reaction unconstrained but changed the biomass output flux until the desired CO_2 uptake rate was achieved. The model optimised with the second method will be referred to as the "CO_2 uptake constrained" model. For this direct method, I specified the upper bound of the CO_2 uptake rate to not exceed the experimentally determined rate of 1.16 μmol m^{-2} s^{-1} and left the biomass output flux unconstrained.

4.3.2 Model behaviour

The "Objective constrained" model arrived at a CO_2 uptake rate of 1.16 μmol m^{-2} s^{-1} when the biomass output flux was constrained to 0.102 μmol m^{-2} s^{-1}. According to calculations done by Cannell, the expected growth rate for Marchantia was 0.238 μmol m^{-2} s^{-1}. The result achieved with this method, therefore fell short of the expected growth rate by about 63%.

The model behaviour was reminiscent of C3-like metabolism (Fig. 4.1A). CO_2 was generated at night at a rate of 0.89 μmol m^{-2} s^{-1} and most of this was lost to CO_2 exchange with the atmosphere, at a rate of 0.66 μmol m^{-2} s^{-1}. 25% of nocturnally generated CO_2 was refixed, mostly by the cytosolic PEPC. However, despite the use of PEPC for this purpose, malate did not accumulate at night. Instead, citrate accumulated at night at a rate of 0.009 μmol m^{-2} s^{-1}. During the day, citrate was consumed by aconitate dehydrogenase and participated in amino acid synthesis.

When using the second method, the "CO2 uptake constrained" model used the maximum allowable CO_2 uptake of 1.16 μmol m^{-2} s^{-1} and attained a growth rate of 0.248 μmol m^{-2} s^{-1}, thereby even exceeding the expected growth rate by 4.2%.

The metabolic behaviour shifted compared to the "Objective constrained" model and is shown in Figure 4.1B. 100% of nocturnally produced CO_2 was now refixed, predominantly by the cytosolic PEPC. This refixed carbon was converted to malate, which accumulated in the vacuole at night at a rate of 0.8751 μmol m^{-2} s^{-1} and was decarboxylated during the day.

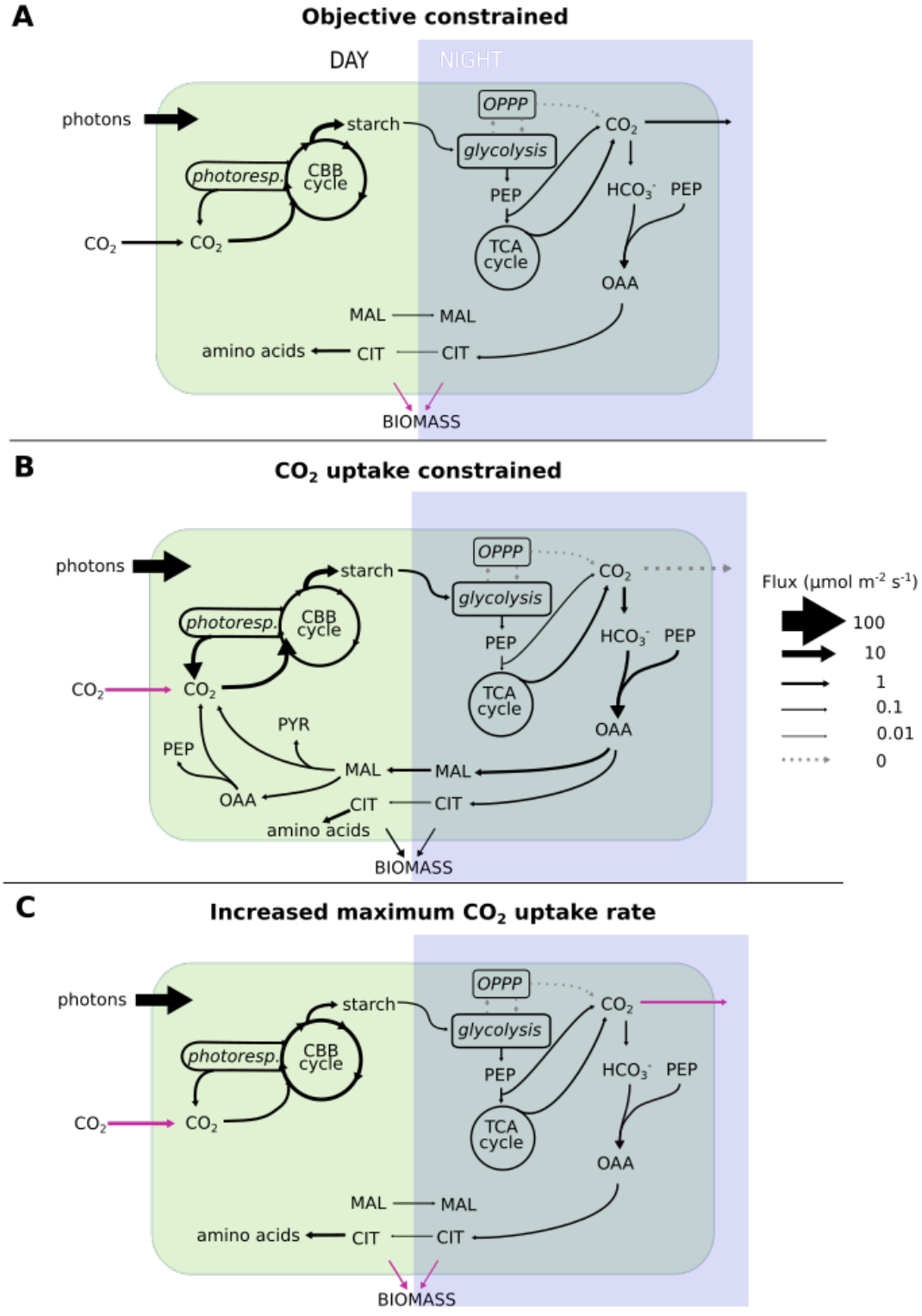
A
Objective constrained
DAY
NIGHT
photons
starch
OPPP
CO2
glycolysis
photoresp.
CBB cycle
PEP
HCO3-
PEP
CO2
CO2
TCA cycle
OAA
MAL
MAL
amino acids
CIT
CIT
BIOMASS
B
CO2 uptake constrained
photons
starch
OPPP
CO2
glycolysis
photoresp.
CBB cycle
PEP
HCO3-
PEP
CO2
CO2
TCA cycle
OAA
PYR
PEP
MAL
MAL
OAA
CIT
CIT
amino acids
BIOMASS
Flux (µmol m-2 s-1)
100
10
1
0.1
0.01
0
C
Increased maximum CO2 uptake rate
photons
starch
OPPP
CO2
glycolysis
photoresp.
CBB cycle
PEP
HCO3-
PEP
CO2
CO2
TCA cycle
OAA
MAL
MAL
amino acids
CIT
CIT
BIOMASS

Figure 4.1: **Major flux routes through the Marchantia models.**
Subcellular compartments are omitted for clarity. Arrow widths are proportional to the predicted flux. Reactions that were constrained to a maximum or minimum flux are marked in magenta. Abbreviations: CIT, citrate; PEP, phosphoenolpyruvate; OAA, oxaloacetate; MAL, malate; PYR, pyruvate; AcCoA, acetyl-CoA; CBB cycle, Calvin-Benson-Bassham cycle; photoresp., photorespiratory pathway; OPPP, oxidative pentose phosphate pathway; TCA cycle, tricarboxylic acid cycle

4.3.2.1 Comparison to previous modelling of Marchantia

Overall, these findings recapitulate the results presented by Cannell. Given the model parameters from the literature used to constrain CO_2 uptake, the Marchantia model was unable to attain the experimentally determined growth rate when C3-like behaviour was imposed. Less than half of the carbon gained via CO_2 assimilation during the day was converted into biomass, resulting in a carbon conversion efficiency of just 42%. One way to make the model achieve the expected growth rate, which was first explored by Cannell (2021) and repeated here, was to allow it to utilise nocturnal CO_2 refixation, by constraining the CO_2 uptake rate directly. This led to the carbon conversion efficiency increasing to 100%, achieved by the model by using CAM cycling.

To test whether some of the constraints that were imposed on the model were more influential on the modelling results than others, Cannell performed a sensitivity analysis. Particular focus was placed on constraints that were described in previous metabolic modelling of Arabidopsis (Cheung et al., 2013, Cheung et al., 2014, Shameer et al., 2019) and assumed, in the absence of species-specific experimental data, to hold true for Marchantia as well. Cannell analysed the following parameters: biomass composition, Rubisco carboxylase : oxygenase ratio, nitrate assimilation rate day : night ratio, biomass accumulation rate day : night ratio and NGAM costs. From varying these parameters in feasible ranges, it was

concluded that only substantially reduced NGAM costs, would allow the C3-like Marchantia model to attain experimental growth rates.

However, given the variability reported for CO_2 assimilation rates in Marchantia (from 0.79 μmol m^{-2} s^{-1} (Graham and Dixon, 2012) to 1.16 μmol m^{-2} s^{-1} (Carter and Romine, 1969)), I investigated how much higher the maximum allowable CO_2 uptake would have to be to permit growth of Marchantia using C3-like metabolism, and not CAM cycling. In this analysis, CAM cycling behaviour is approximated by the % nocturnal CO_2 refixation. A value of around 25% would be considered C3-like, as this was what was achieved in the "Objective constrained" model. Anything above that indicated increased nocturnal CO_2 refixation.

Specifically, to investigate this, I performed a sensitivity analysis, considering only the CO_2 uptake rate. To do this, I varied the maximum allowed flux through the CO_2 uptake rate between 1 and 2 μmol m^{-2} s^{-1}. Additionally, I varied the fixed flux through the biomass output reaction between 90% and 110% of the experimental growth rate of 0.238 μmol m^{-2} s^{-1}. Fixing the biomass output reaction's flux was necessary, as the model would otherwise always utilise CAM cycling to maximise biomass output.

Covering the space of all possible parameter combinations by systematically scanning through each parameter in turn would be computationally intensive. Therefore, the sensitivity analysis was performed by acquiring 200 samples of quasi-randomly distributed sets of the varied parameters (Rutjens et al., 2024). Each parameter combination was set as the new model constraints, and the model was re-optimised and the proportion of the expected growth rate, as well as the % nocturnal CO_2 refixation are reported. The results of this expanded sensitivity analysis are reported in Figure 4.2.

The lowest CO_2 uptake rate that allowed the model to reach the experimental

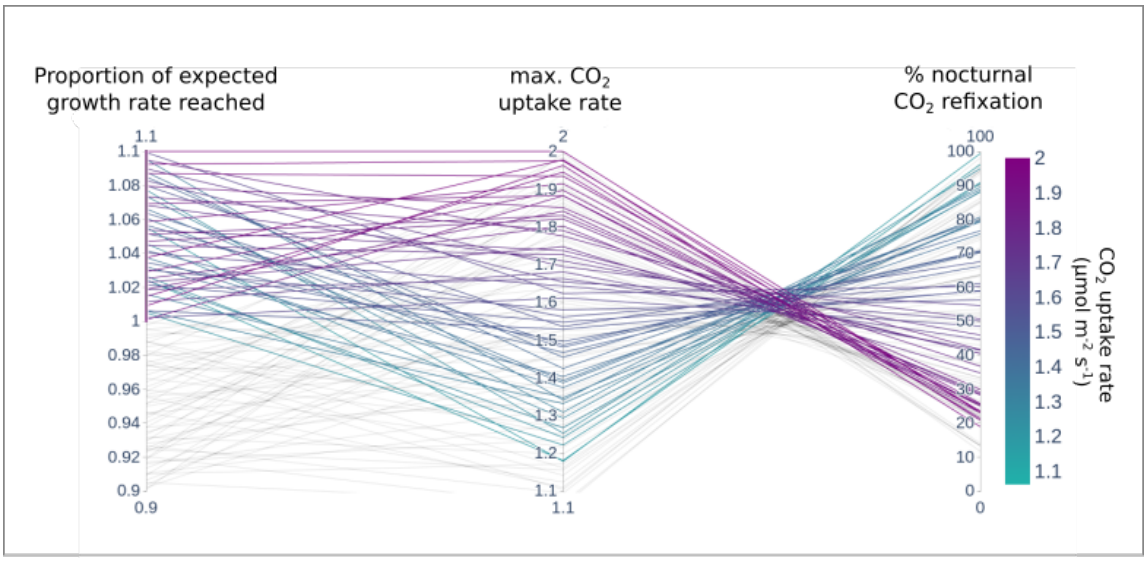

Figure 4.2: **Sensitivity analysis of Marchantia model to maximum allowed CO_2 uptake rates.**
Sensitivity analysis was performed using 200 iterations, varying maximum allowed CO_2 uptake rates and fixed flux through the biomass output reaction in the Marchantia model. Quasi-random distribution of parameter combinations were obtained using sobol sequences. All iterations that achieved or exceeded the experimental growth rate are coloured according to the CO_2 uptake rate flux, the rest are shown in grey.

growth rate was about 1.2 μmol m^{-2} s^{-1}, therefore just higher than the previously allowed maximum rate based on experimental data. This was however, linked to 100% nocturnal CO_2 refixation. As CO_2 uptake rates increased, this is correlated with decreasing nocturnal CO_2 refixation. Around a CO_2 uptake rate of 2 μmol m^{-2} s^{-1}, % nocturnal CO_2 refixation decreased to levels seen in the "Objective constrained", C3-like acting model. It appeared that if CO_2 assimilation rates in Marchantia were a bit higher than what was previously reported in the literature, the model would not choose to utilise CAM cycling to attain expected growth rates.

4.3.3 Obtaining new experimental data to constrain the Marchantia metabolic model

The aim of this section of work was to update and expand the Marchantia-specific experimental data available to parameterise the Marchantia diel plant metabolic model. In particular, having matching data for CO_2 assimilation rate and growth rate from the same batch of plants rather than taking these values from separate studies, will allow me to be more certain about the achievability of measured growth rates with measured CO_2 assimilation rates without needing to invoke CAM cycling. I also aimed to measure metabolites over the day-night cycle to examine whether there was any evidence of the cycles of carboxylic acid accumulation and depletion that could be indicative of CAM cycling.

Figure 4.3 illustrates the basic experimental setups to obtain data on growth rates, CO_2 assimilation and respiration rates and metabolite accumulation patterns.

The plant growth conditions were carefully selected to facilitate the use of the data in the model. I chose a 12 h/12 h light/dark photoperiod because having light and dark phases of equal length removes the need to scale the fluxes in each phase of

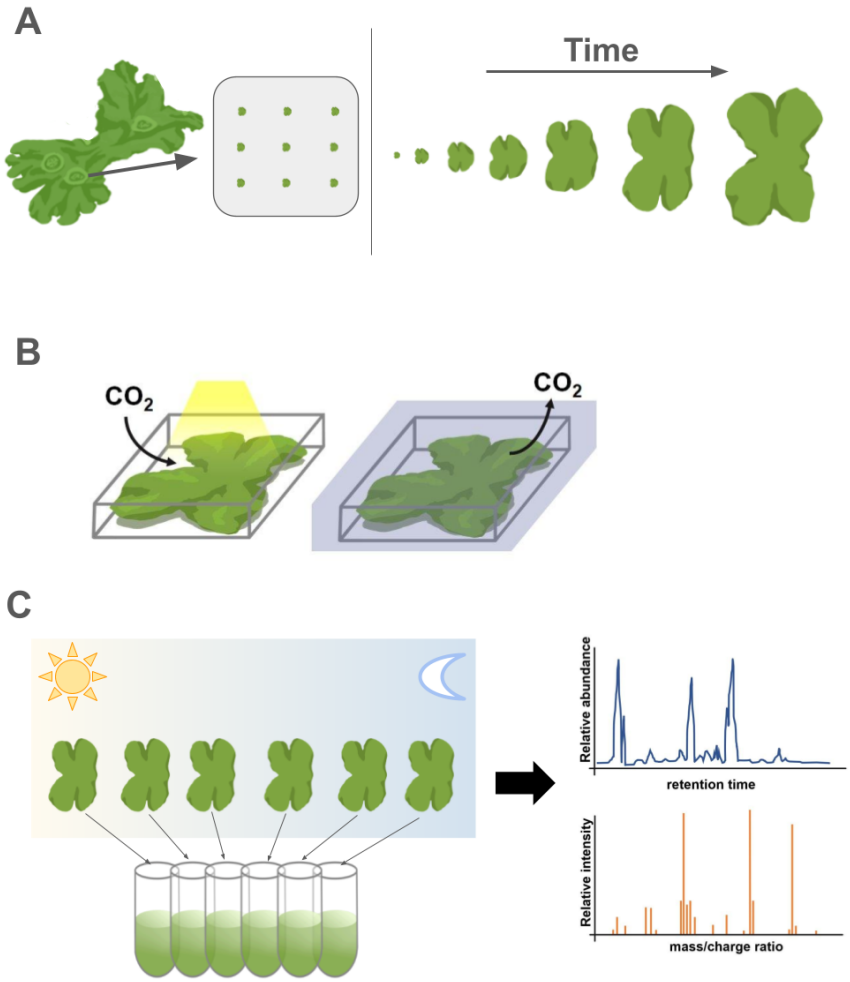

Figure 4.3: **Experimental approaches used to investigate growth, gas exchange, and metabolite accumulation in *M. polymorpha*.**
(A) Growth assay: gemmae were plated on agar medium without sucrose and photographed at regular intervals. Two-dimensional thallus area was quantified from the images and used to calculate growth rates. (B) Gas exchange measurements: mature thalli were placed in a chamber connected to an infra-red gas analyser to determine daytime CO_2 assimilation rates and night-time respiration rates. (C) Diel metabolite concentrations: thalli were harvested at multiple time points across the diel cycle, homogenised, and subjected to metabolite extraction, chemical derivatisation, and analysis by gas chromatography–mass spectrometry.

the metabolic model by their duration relative to one another. Furthermore, I ensured that the growth medium was free of sucrose, which would usually be added to the agar to promote the growth of Marchantia. Since in my experiments no carbon source is provided in the medium, CO_2 uptake is the sole carbon source and I could ignore any consideration of carbon gained via uptake from the medium, which would be a challenge to measure. Daytime CO_2 uptake can therefore be represented in the model as the only carbon-importing reaction.

4.3.3.1 Measuring growth rate

Growth rate is an important parameter in the model, as setting unrealistically high values could render the system infeasible, given the available resources and energy. Therefore, if growth rates obtained from the literature were inaccurate, the model might be forced into infeasibility or would only be able satisfy the constraints by invoking unrealistic mechanisms such as CAM cycling to conserve carbon.

The thalli of Marchantia grow relatively flat. I therefore used the increase in thallus area over time as a proxy for the growth rate of Marchantia. This allowed non-invasive measurements of the same individuals by taking multiple photographs over the course of about a month (Fig. 4.4).

Growth rates calculated from increase in thallus area for Tak-1 and Tak-2 are shown in Figure 4.5. I observed a similar trend in both lines, with growth rates initially declining sharply in the first week before increasing between 7 and 23 d after sowing, though with substantial plant-to-plant variability. After 24 d, this variability decreased, and growth rates declined gradually.

During the first 33 d after sowing, growth rates remained at least two times higher than the maximum growth rate that was achieved in previous modelling when

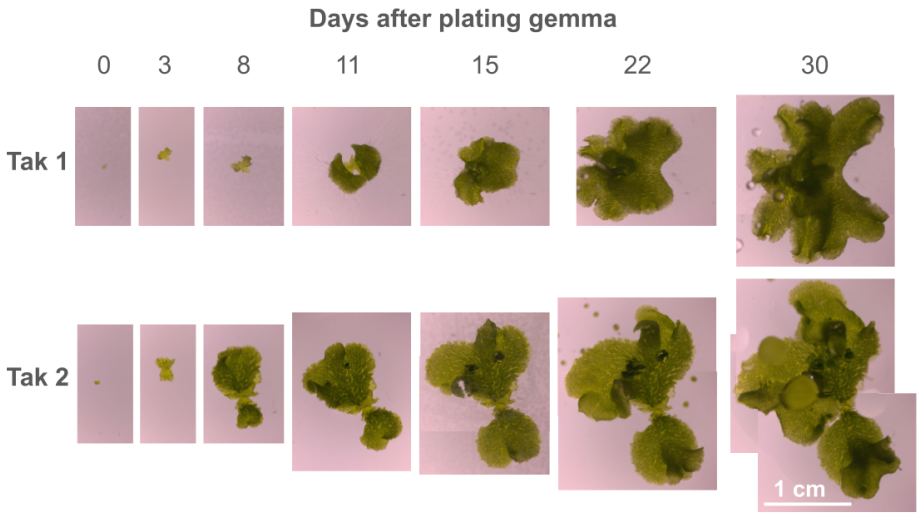

Figure 4.4: **Growth of *M. polymorpha* Tak-1 and Tak-2 thalli from gemmae.** Gemmae of *M. polymorpha* (Tak-1 and Tak-2) were plated on agar medium without sucrose and photographed at regular intervals up to 30 days after plating. Images illustrate progressive thallus expansion over time. The scale bar (1 cm) is identical for all images.

CO_2 refixation at night, and therefore CAM cycling, was prevented ("Objective constrained" model). Around 30 d, growth rates approached the maximum growth rates predicted when CO_2 refixation was permitted ("CO_2 uptake constrained").

4.3.3.2 Measuring gas exchange

Another important parameter in the model is the rate of CO_2 assimilation, as CO_2 is the only source of carbon and therefore directly limits the amount of biomass that can be produced. If the CO_2 uptake rate was set to an unrealistically low level, the model would be forced to conserve carbon.

Two different values for CO_2 assimilation rates in Marchantia had been reported: 1.16 µmol m^{-2} s^{-1} (Carter and Romine, 1969) and 0.794 µmol m^{-2} s^{-1} (Graham and Dixon, 2012) obtained at light intensities of 174 and 95 µmol m^{-2} s^{-1}, respectively.

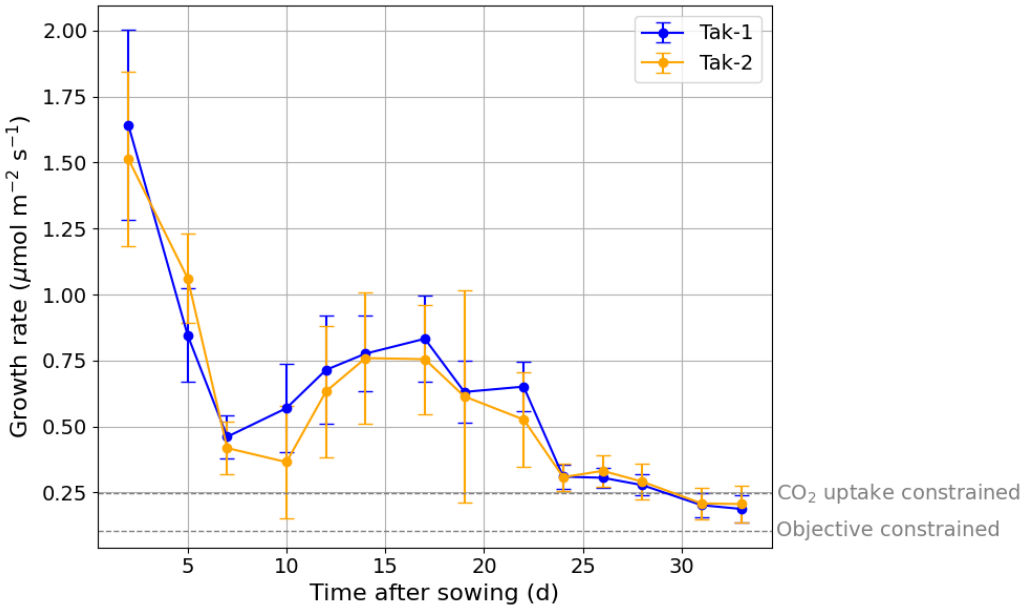

Figure 4.5: **Growth rates of wild-type *M. polymorpha* thalli over time.** Gemmae from Tak-1 and Tak-2 lines were grown on agar and imaged every few days and thallus areas were measured. Growth rates were calculated in terms of the rate of increase in biomass per thallus area from one time point to the next. Data from 27 individual plants was averaged per line. Maximum growth rates achieved in the metabolic model by when preventing or allowing the nocturnal re-fixation of CO_2 are indicated. Error bars represent standard deviation.

CO_2 assimilation rates are dependent on a variety of factors, including light intensity, atmospheric CO_2 concentration, temperature, and developmental age of the plant (Sage and Kubien, 2007). It was therefore essential to measure CO_2 assimilation rate for my specific growth conditions, to ensure the value specified in the model is not an over- or underestimation of CO_2 assimilation in Marchantia.

Furthermore, I aimed to obtain a value for CO_2 release at night. When CO_2 uptake rate was constrained directly the model predicted that there would be no CO_2 released at night since all respiratory CO_2 would be refixed (Fig. 4.1B). That was expected, as the model was set to maximise biomass output, and would therefore not readily lose any carbon. However, Marchantia do not have stomata which they could close to reduce gas exchange and we would expect to see at least some respiratory CO_2 to be lost at night.

To measure day- and night-time gas exchange in Marchantia, I placed multiple thalli of the same age and line in an infrared gas analyser before the start of the light period in the growth cabinet, to capture both the CO_2 respiration rate in the dark and the CO_2 assimilation rate in the light (Fig. 4.6).

The original intention was to measure at least three sets of experiments per line. However, this experiment was cut short due to technical difficulties (see Discussion) and only three sets of experiments, showing data for two separate experiments with Tak-1 thalli and one experiment with Tak-2 thalli, are reported here.

Between these three sets of separate experiments, the average highest measured CO_2 assimilation rate was 1.86 µmol m^{-2} s^{-1}, which is 1.6 and 2.3 times higher than the two values for CO_2 assimilation rates obtained from the literature, even though the light intensity was lower than in those studies (95 and 174 µmol m^{-2} s^{-1}, compared to 81 µmol m^{-2} s^{-1} here). However, CO_2 assimilation rates gradually decreased in all three experiments after initial light exposure.

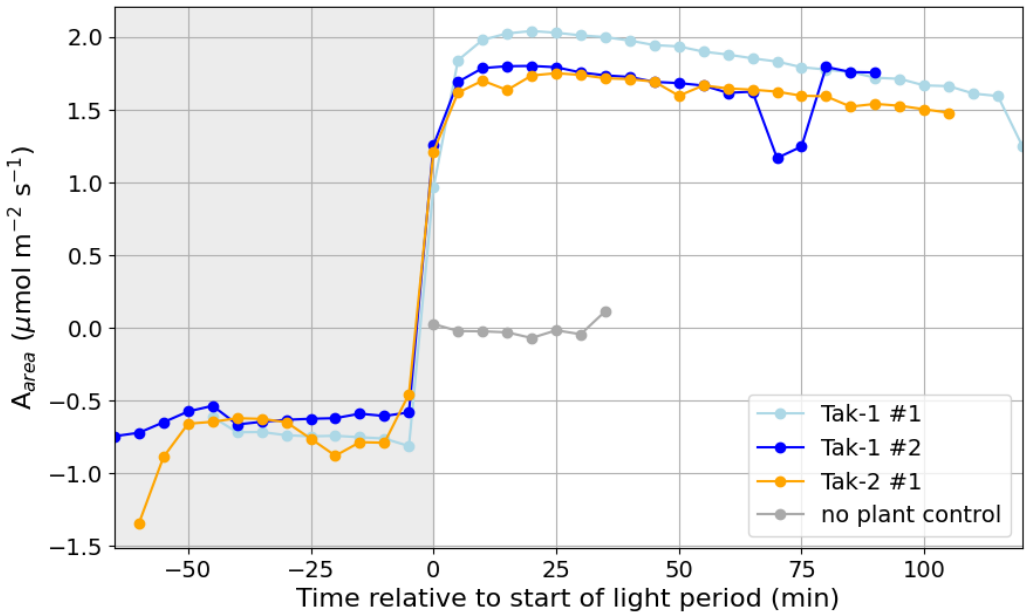

Figure 4.6: **CO_2 assimilation rates of *M. polymorpha* wild-type thalli.** In three separate experiments, multiple plants of the same line, Tak-1 or Tak-2, were placed inside the LICOR small plant chamber and CO_2 assimilation rates were measured at a CO_2 concentration of 400 µmol mol^{-1}. The shaded area indicates the dark period. A_{area} is the CO_2 assimilation rate normalised by total area of thalli.

Though CO_2 assimilation rates start out higher than the values obtained from the literature, if they continue to decline in the light the average daily CO_2 assimilation rate might approach or fall below the values previously set in the model. It was also seen that CO_2 is released at night, at an average rate of 0.7 μmol m^{-2} s^{-1}, meaning that not all, if any, respiratory CO_2 was recycled.

4.3.3.3 Measuring metabolite accumulation

Diel measurements of metabolites of Marchantia thallus

The "CO_2 uptake constrained" Marchantia model predicted an increase in carbon conversion efficiency by refixing respiratory CO_2 at night in the form of malate, which would accumulate until the daytime, followed by decarboxylation and ultimately fixation of the released CO_2 by Rubisco.

I investigated whether there is experimental evidence for accumulation of malate, or another compound that could serve as a transient carbon store, by extracting metabolites from Marchantia thallus tissue at different times of the day and night, and measuring their abundance using gas chromatography mass spectrometry (GC-MS). Figures 4.7 and 4.8 show the measured diurnal patterns of concentrations for selected organic acid and amino acids, respectively, in the Tak-2 line of Marchantia.

The average abundance of malate stayed approximately constant with no evidence of a strong diel pattern of change. Other dicarboxylic acids, fumarate and succinate, were present at lower levels than malate and also did not show a clear diel pattern (Fig. 4.7). The tricarboxylic acid citrate, however, showed a clear diel signature, steadily accumulating at night at a rate of approx. 0.09 μmol gFW^{-1} h^{-1} and then being consumed again during the day. Diel changes in amino acid concentrations were observed for glycine, which accumulated during the day, and

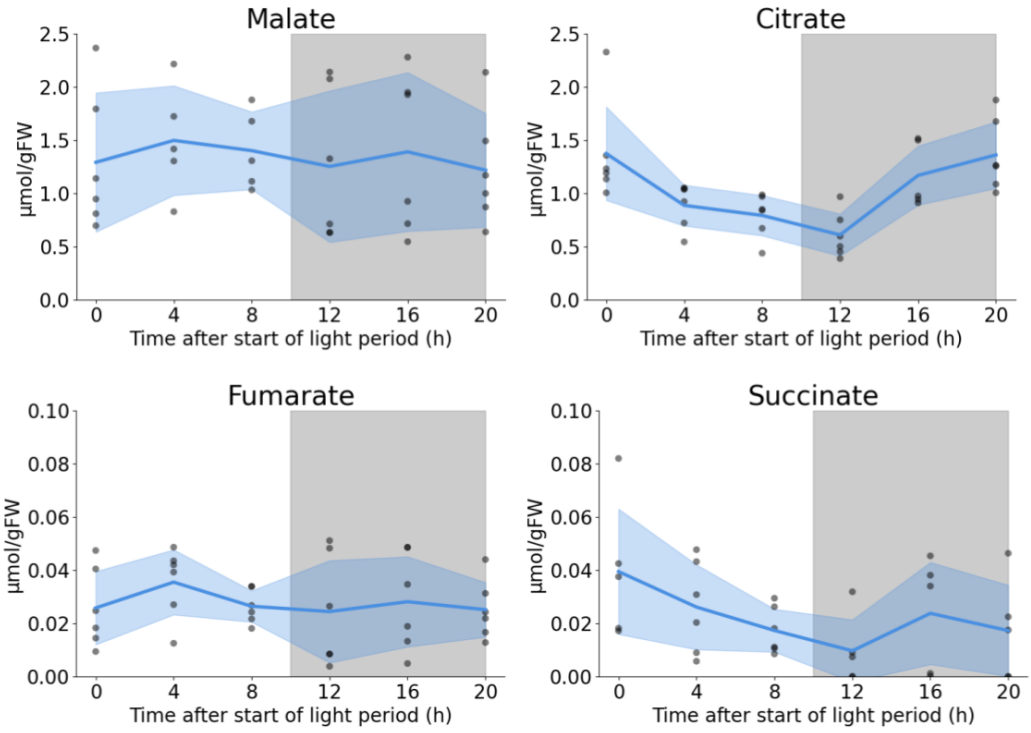

Figure 4.7: **Diel patterns of organic acid abundance in wild-type Tak-2 *M. polymorpha*.**
Blue line represents the mean, blue-shaded area indicates one standard deviation from the mean. Number of plants per time point = 6. The grey-shaded area indicates the dark period. Note that scales differ by one order of magnitude between top and bottom row.

serine, aspartate and glutamate, which accumulated at night (Fig. 4.8).

Comparison of citrate accumulation

Based on the absence of malate accumulation at night, it is apparent that the model's prediction of classical CAM cycling was incorrect. However, it is known that some plants classified as CAM use citrate accumulation for this purpose (Igamberdiev and Eprintsev, 2016). Nocturnal citrate accumulation can, however, also be observed in C3 plants where it serves to provide carbon skeletons for daytime nitrate assimilation following its release from the vacuolar store (Gauthier

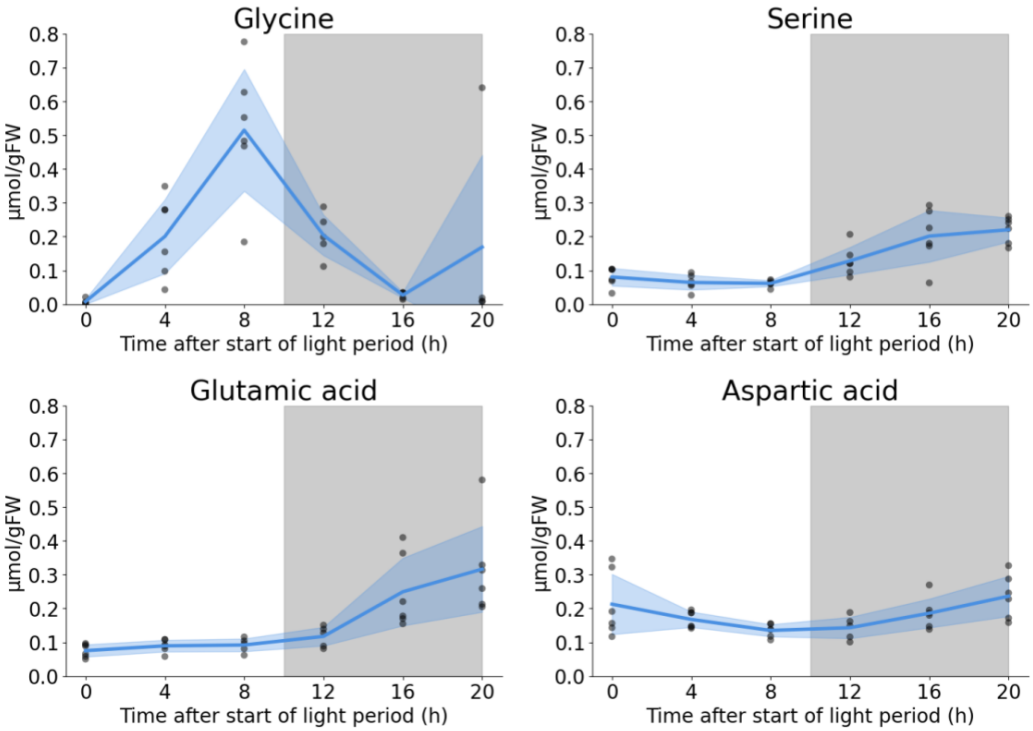

Figure 4.8: **Diel patterns of amino acid abundance in wild-type Tak-2 *M. polymorpha*.**
Blue line represents the mean, blue-shaded area indicates one standard deviation from the mean. Number of plants per time point = 6. The grey-shaded area indicates the dark period.

et al., 2010). The observed rate of nocturnal citrate accumulation in Marchantia therefore needs to be compared to those in C3 and CAM plants to discern whether it could serve an additional role to refix respiratory CO_2 in Marchantia via an alternative form of CAM cycling.

Comparing the accumulation rates between Marchantia and other plants requires normalisation to the plant's carbon assimilation rates, as accumulation rates would be expected to be higher in a plant that assimilates more carbon overall and grows faster.

I obtained data on nocturnal carboxylic acid accumulation rates for C3, CAM cycling and full CAM plants from (Frei et al., 2018; Wang et al., 2020b; Borland, 1996; Chen et al., 2002; Scheible et al., 2000; Ceusters et al., 2019; Sulpice et al., 2014; Flis et al., 2019; Dodd et al., 2003). This included not just malate but also citrate and isocitrate, and the reported amounts were added up, before normalising by the reported CO_2 assimilation rate. The results are shown in Figure 4.9. The amount of citrate accumulation observed in Marchantia was within the range seen in C3 plants and much lower than the total carboxylic acid accumulation seen in known CAM cycling plants.

4.3.4 Changes to model setup based on new experimental data

Based on the new experimental data collected from Marchantia grown under standardised conditions, I updated several parameters in the Marchantia-specific plant metabolic model.

From the experimental gas exchange measurements, I applied two key constraints. First, the mean CO_2 assimilation rate in light of 1.86 µmol m^{-2} s^{-1} was set as the CO_2 uptake rate to be reached in the "Objective constrained" model, or the upper bound of the CO_2 uptake reaction in the "CO2 uptake constrained" model.

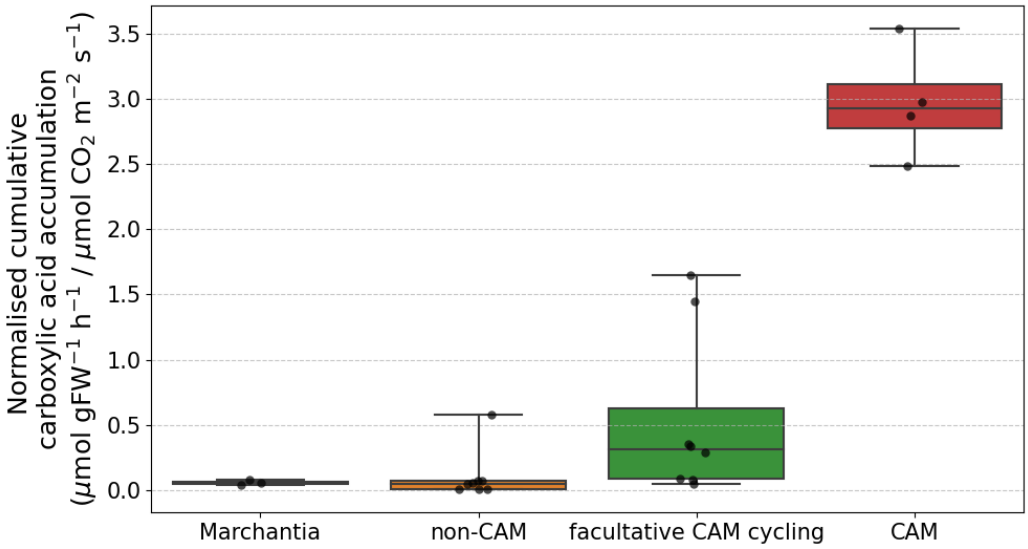

Figure 4.9: **Comparison of nocturnal carboxylic acid accumulation across plant metabolic types.**
Reported rates of nocturnal malate, citrate or isocitrate accumulation were added up and normalised by dividing by the plant species' reported CO_2 assimilation rates. Bars represent the range of reported values. See text for references.

Secondly, the bounds of the CO_2 exchange reaction in the dark were set to 0.7 μmol m^{-2} s^{-1}, forcing the model to release CO_2 at night.

On top of that, I restricted nocturnal accumulation of organic acids according to the experimental data from GC-MS analysis. Since there were no clear accumulation patterns for malate, fumarate or succinate, I prevented the nocturnal accumulation of these metabolites in the model. The only organic acid allowed to accumulate at night was citrate, though I calculated a maximally permissible nocturnal citrate accumulation rate from the GC-MS data described above. To do this, I took the difference between the highest abundance of citrate at night and its lowest abundance during the day (taking into account the standard deviation of the data) to obtain the greatest possible difference, and divided it by the time between the measurements. According to these calculations, the upper bound for nocturnal citrate accumulation should be set to 0.0166 μmol m^{-2} s^{-1}, which is about 28% lower than the predicted rate of citrate accumulation in the previous "Objective constrained" Marchantia modelling iteration (0.0231 μmol m^{-2} s^{-1}).

4.3.5 Model behaviour with constraints based on new experimental data

The results obtained with both methods for optimisation, by constraining the objective or the CO_2 uptake rate, yielded identical results and the model behaviour is shown in Figure 4.1C. The model achieved a growth rate of 0.248 μmol m^{-2} s^{-1}, exceeding the experimental growth rate by 4.2%. CO_2 was taken up at the maximum allowed rate of 1.86 μmol m^{-2} s^{-1}. 24.5% of nocturnally produced CO_2 was refixed, and CO_2 was released at night at the minimum set rate of 0.7 μmol m^{-2} s^{-1}. Citrate accumulated up to the maximum allowed rate of 0.0166 μmol m^{-2} s^{-1}. Overall, this resulted in a carbon conversion efficiency of 62.4%.

Evidently, by increasing the daytime CO_2 uptake rate according to my experimental measurements, the updated Marchantia model, despite being forced to lose some of this CO_2 again at night, had enough carbon available to create sufficient biomass without a substantial increase in nocturnal CO_2 refixation.

Based on these findings, I conclude that the model, when constrained with experimentally determined parameters, no longer requires substantial refixation of nocturnally generated CO_2 to achieve the observed growth rate. The observed accumulation of citrate does not appear to function as an alternative form of CAM cycling, as it does not substantially contribute to salvaging nocturnal respiratory CO_2. The updated Marchantia model indeed reached experimental growth rate while maintaining metabolic behaviour in line with C3 metabolism.

4.4 Discussion

4.4.1 Limitations of experiments

4.4.1.1 Growth rate experiments

As explained above, I used the increase in Marchantia thallus area as a proxy for growth, as this non-invasive approach allowed me to monitor multiple individual plants throughout the experiment by simply photographing them as they grew on agar. However, this measurement has several limitations that should be acknowledged.

This two-dimensional area measurement cannot capture increases in thallus thickness, rhizoid development, or gemma cup formation. Additionally, the method becomes less reliable as thalli mature and begin to curl at their edges. In my experiments, such curling started even earlier for thalli of the Tak-1 line than for

Tak-2. These limitations may explain some of the observed fluctuations and variability in growth rate patterns. It is possible that photographs failed to accurately capture growth of the whole plant at certain developmental stages, and that the true increase in biomass over time would follow a different trajectory.

After approximately 33 d, edge curling became pronounced enough that I deemed thallus area measurements to be unreliable indicators of growth. However, to obtain sufficient plant material for the GC-MS experiments, plants were grown for about 50 d, creating a discrepancy in developmental age between experiments. By 50 d of age, when thalli were harvested for metabolite extraction, growth rates may have decreased further, or metabolite profiles might have differed from those at 30 d. Ideally, all experiments would use thalli of identical age.

Alternative methods for cultivating Marchantia could potentially provide more accurate, non-invasive measurements of plant mass that account for total growth including rhizoids, gemma cups and gemmae, as well as variation in thallus thickness. A particular challenge with agar-based cultivation is that substrate mass varies considerably with water content. Future studies might explore growing Marchantia hydroponically or by growing thalli without direct contact the growth medium. For example, Marchantia propagation protocols suggest cultivation of Marchantia spores on a fine nylon mesh positioned on top the agar allowing for non-destructive removal. This setup allows water and nutrient transfer from the agar while preventing rhizoid attachment, which could allow separation of plants from the agar for weighing.

4.4.1.2 Gas exchange experiments

For the gas exchange experiments, my setup was designed to monitor one sample of plants throughout their typical day-night cycle. This approach led me to set

up the experiment before the start of the light period in the growth chambers. My intention was to first measure respiration rates in the darkness, then continue measurements through the entire 12 h light period to capture CO_2 assimilation rates across a complete day. This method limited me to surveying only one set of plants per day, requiring new plant samples each day to obtain replicates.

I did not complete the full number of intended replicates (at least three per line) as I observed that the current setup was causing plant samples to dry out within just one h of light exposure. The data showed that CO_2 assimilation rates declined rapidly after light onset, which I attributed to this desiccation. The gas flow rate set in the gas analyser device (400 µmol s^{-1}) was likely causing the plants and agar to dry out. I was reluctant to reduce the flow rate for fear of inadequate gas mixing within the chamber, which could lead to fluctuating, unreliable readings. Notably, the manufacturer's guidelines for the bryophyte chamber suggested a much higher flow rate of 700 µmol s^{-1}, though these recommendations may be intended for very short-term measurements only.

To obtain more accurate CO_2 assimilation rates for Marchantia under my specified growth conditions, the experimental approach should be modified. Rather than monitoring a single sample for an entire day, multiple samples should be prepared and measured for brief periods, just long enough for gas exchange readings to stabilise. Taking multiple measurements from different samples throughout the day would provide more representative data. This approach aligns with recommendations by Busch et al. (2024), who note that CO_2 assimilation rates can fluctuate diurnally. This recommendation specifically referred to capturing the phenomenon of midday depression, in which plants close their stomata during the hotter hours of the day. Marchantia lack stomata to do this, but it would nevertheless be valuable to determine whether CO_2 assimilation rates in Marchantia vary throughout the day. Such measurements would enable calculation of more

accurate average CO_2 uptake rates for the metabolic model.

4.4.1.3 Metabolite accumulation experiments

For the metabolite accumulation experiments, I used older plants than in other experiments to obtain sufficient plant material for analysis. The recommended amount of tissue and the entire metabolite extraction and derivatisation protocol were originally designed for vascular plants (Lisec et al., 2006). There is considerable scope for optimising these procedures specifically for Marchantia, to ensure that chemical compounds of interest are extracted and derivatised properly.

4.4.2 The revised metabolic model does not support the need for nocturnal CO_2 refixation in Marchantia

Both the modelling results reported by Cannell (2021) and my first modelling iteration, which repeated an almost identical model setup to the previous study, reached the same important conclusion: A metabolic model of Marchantia that is limited to C3-like metabolism and maximum allowed CO_2 uptake rates, below 1.2 µmol m^{-2} s^{-1}, would fall short of the expected growth rate.

However, my second modelling iteration, reported in this chapter, using newly acquired experimental data from standardised growth conditions challenges this conclusion. The higher net CO_2 uptake rates that I measured eliminated the need for the model to use nocturnal CO_2 refixation to reach the measured growth rates and could even accommodate the imposed nocturnal losses of CO_2.

Given the various limitations of the experimental methods described above, I am cautious about drawing definitive conclusions from the updated Marchantia model presented here. The evidence suggests that with the higher CO_2 assimilation rates observed in the gas exchange experiments, Marchantia could likely support the

observed growth and respiration rates without employing carbon conservation mechanisms such as CAM cycling. This was, however, only true when applying the CO_2 assimilation rates measured immediately after the start of light exposure, and obtaining a measurement of average daytime CO_2 assimilation rates, in a way that avoids dessication of samples, would be preferable.

Nevertheless, the patterns of carboxylic acid accumulation measured by GC-MS do not suggest that carboxylic acids are stored at quantities expected for CAM cycling. However, there was marked nocturnal accumulation of a few amino acids, namely serine, glutamate and aspartate at night. Nocturnal accumulation of amino acids was not previously allowed in the model, based on experimental data obtained from tobacco leaves (Scheible et al., 2000). Future metabolic modelling of Marchantia should reconsider this constraint and investigate potential roles for nocturnal amino acid accumulation.

As noted in the introduction, many hornworts, which are close relatives of liverworts like Marchantia, possess pyrenoids (Villarreal and Renner, 2012). These structures are known to function to increase local CO_2 concentrations around Rubisco and can therefore be considered an adaptation to low CO_2 availability. A valuable extension of this work would be to compare growth rates, CO_2 assimilation rates and respiration rates between Marchantia and hornwort species, including those with and without pyrenoids. Such comparisons within the bryophyte clade could provide insights into whether the presumed C3 metabolism of Marchantia and hornwort species without pyrenoids, is reflected in lower growth rates compared to species with enhanced carbon conversion efficiency facilitated by a pyrenoid-based CCM.

5 | General Discussion

5.1 Summary of main findings

In Chapter 2, I investigated the effects of carbon limitation on a metabolic model of a growing leaf with the aim of finding endogenous metabolic mechanisms to improve carbon use efficiency by recapturing respiratory CO_2 at night. The main finding was that the model adopted CAM cycling metabolism. This metabolic adaptation has been observed in previous modelling studies focused on CAM (Tay et al., 2021). My work supports the hypothesis that CAM cycling could be an adaptation to cope not just with water stress, but also limited availability of carbon.

A novel aspect of my research was investigating whether the plant model could employ mechanisms other than CAM cycling to refix nocturnal CO_2. My analysis revealed that no other efficient mechanism was available within the current model structure. While ICDH could be used to fix CO_2 at night, it could only refix about a quarter of all nocturnal respiratory carbon. This limitation likely stemmed from difficulties in obtaining its substrate in a carbon-efficient manner or converting the carboxylation product of ICDH into a suitable transient carbon storage compound. Previous modelling studies suggest that allowing amino acid accumulation at night would allow ICDH to support an alternative pathway available to the plant metabolic network to refix nocturnal CO_2 (Töpfer et al., 2020).

In Chapter 3, I used the carbon constrained metabolic model (in which CAM cycling was prevented) to investigate whether synthetic CO_2-fixing pathways could enhance nocturnal CO_2 refixation and improve growth. I focused on the CETCH cycle, an ATP-efficient pathway that produces glyoxylate or malate, which I assumed should integrate well with native plant metabolism. I found that while the

CETCH cycle could indeed refix almost all nocturnally produced CO_2, it operated with surprising inefficiency. Introduction of the cycle into the model dramatically increased nocturnal energy production to power the cycle, which itself released CO_2, resulting in minimal net carbon fixation per cycle turn. This high energy demand caused the model to become light-limited, as substantial daytime starch production was needed to generate sufficient energy for nocturnal CETCH cycle operation. This outcome was unexpected since I had specifically chosen the CETCH cycle for its ATP efficiency. Further analysis revealed that the model's primary challenge was providing sufficient NADPH at night in a carbon-efficient way to run the cycle. This was, in principle, solvable by switching the coenzyme requirement of the CETCH cycle from NADPH to NADH, or by shifting shifting some NADPH-consuming reactions of the cycle to the daytime, when NADPH is more readily available from photosynthetic light reactions. While neither modifying coenzyme requirements nor distributing cycle operations across day and night phases would be practical or even possible to implement, this analysis provides valuable insights for future synthetic pathway designs in plants. Specifically, it highlights that both ATP and coenzyme requirements are important considerations, and that the design of pathways specifically for plants should account for the diel nature of plant metabolism.

Finally, in Chapter 4 I re-examined claims made in a previous metabolic modelling study of *M. polymorpha* which concluded that Marchantia would need some form of nocturnal CO_2 refixation to achieve experimentally determined growth rates, suggesting CAM cycling might be active (Cannell, 2021). While I was able to recapitulate this modelling result, my analysis revealed that the model could reach the experimentally determined growth rates if the CO_2 uptake rate was only slightly higher than the previously allowed maximum limit.

To further investigate this, I measured key parameters for Marchantia under stan-

dardised growth conditions specifically suited for implementation in the metabolic model. Measurements of the abundance of carboxylic acids and amino acids over day-night cycles did not support the existence of CAM cycling in Marchantia. A final model iteration with updated parameters based on these measurements and my measurements of CO_2 assimilation and growth rates confirmed that the Marchantia model could function without nocturnal CO_2 refixation to reach experimental growth rates, suggesting that, despite low rates of photosynthesis, there appear to be no significant carbon-use efficiency adaptations in this organism. Overall, while this study provides evidence countering the previous conclusion that Marchantia requires nocturnal CO_2 refixation, it would benefit from repeated experiments with improved methodologies to obtain more accurate parameters for model constraints.

5.2 Prospects for nocturnal CO_2 refixation to increase carbon conversion efficiency

The metabolic modelling framework applied in this work suggests that substantial improvements in plant growth could be achieved through nocturnal refixation of respiratory CO_2. This theoretical benefit was consistently demonstrated across multiple modelling scenarios.

In Chapter 2, the CAM cycling model demonstrated a 20% increase in predicted growth compared to a C3-like ("objective constrained") model with the same rate of daytime CO_2 uptake. This growth enhancement persisted across the range of CO_2 assimilation rates measured in *Arabidopsis* and even beyond. In Chapter 3, implementing either the NADH-dependent CETCH cycle operating at night, or the NADPH-dependent CETCH cycle distributed across both day and night phases

enabled 100% nocturnal CO_2 refixation, leading to a 17% increase in growth rate relative to the carbon-limited baseline model. Similarly, in Chapter 4, under low CO_2 uptake conditions, CAM cycling in the *Marchantia* model predicted growth increases exceeding 140%.

5.2.1 Limitations of modelling predictions

There are several, yet to be addressed, caveats in the modelling work done so far, which may reduce the growth benefits which can realistically be expected from nocturnal CO_2 refixation.

5.2.1.1 Missing thermodynamic constraints and enzyme costs of nocturnal CO_2 pathways

These outcomes represent idealised scenarios where nocturnal CO_2 refixation, daytime decarboxylation, and reassimilation all operate with perfect efficiency. In reality, metabolic pathways face thermodynamic constraints, enzyme kinetic limitations, and transport barriers that reduce efficiency (Noor et al., 2014; Bar-Even et al., 2012a). While the current model accounts for some metabolic costs associated with processes like CAM cycling (such as the energy required to acidify the vacuole and import carboxylic acids), several important factors remain unrepresented.

The synthesis of transporters and enzymes required to catalyse CO_2 refixation pathways demands energy and cellular resources. These costs are currently only indirectly represented by the increased total sum of fluxes. Although the model is set to minimise these costs through pFBA, they are not explicitly constrained according to physical or biochemical limits.

Future iterations of this modelling approach should relate the predicted flux of

each reaction to the catalytic rate of the associated enzyme and account for the costs of synthesising enzymes in sufficient quantities. Such enzyme-constrained models, similar to those developed for microbial systems (Sánchez et al., 2017), would provide more realistic assessments of metabolic engineering strategies for plants.

5.2.1.2 Distinguishing between CO_2 uptake rates and CO_2 assimilation rates

It is important to note that to implement carbon limitation in the model, I consistently constrained the CO_2 exchange reaction during the day to match experimentally measured CO_2 assimilation rates. This served as a simple measure to constrain the total amount of carbon that could enter the system. However, the biophysical process of CO_2 uptake from the atmosphere into cytosol (represented by the CO_2 uptake reaction) and further into the chloroplast and the biochemical process of CO_2 assimilation by the CBB cycle are distinct processes, and subject to different barriers and limitations.

Setting an upper bound on the CO_2 uptake reaction would represent the conductance of the tissue, which determines the rate at which CO_2 can move from the atmosphere to the site of carboxylation. This pathway involves multiple diffusional resistances: CO_2 must cross the cell wall and the plasma membrane, diffuse in the cytosol, and finally traverse the chloroplast and thylakoid membranes to reach Rubisco (Evans et al., 2009).

The maximum rate of CO_2 assimilation, on the other hand, is constrained by a series of biochemical limitations. First, chloroplast CO_2 concentration, which directly affects the carboxylation efficiency of Rubisco. Additionally, the regeneration capacity of RuBP can become limiting, particularly under high light or

elevated CO_2 conditions, as it depends on adequate electron transport rates and the activities of numerous CBB cycle enzymes (Sharkey et al., 2007). Lastly, limitations can arise from insufficient capacity to utilise the products of the CBB cycle, commonly referred to as triose phosphate utilisation limitation (McClain and Sharkey, 2019).

In my models, I have so far left CO_2 assimilation rates unconstrained, essentially assuming they are limited only by the total carbon that could be gained via gas exchange. Rubisco and the rest of the CBB cycle were unrestricted in processing the additional CO_2 which was released during the day by decarboxylation of the transient carbon storage compound from nocturnal CO_2 refixation, as well as any CO_2 released by daytime respiration and photorespiration. For a more accurate picture, future experiments and application of experimental data should seek to incorporate information about the maximum achievable rates of physical CO_2 uptake, affected by the conductance of the tissue to CO_2 diffusion into the chloroplasts, as well as maximum rates of biochemical CO_2 assimilation by the CBB.

5.2.1.3 Unrealistically short photoperiod

I should also acknowledge that the current 12 h/12 h photoperiod model likely overstates the benefits of nocturnal CO_2 refixation compared to realistic growing conditions. This was chosen primarily for ease of application of experimental data from plants grown in growth cabinets with adjustable light settings. Crops in the field typically experience longer light than dark periods, especially in non-equatorial agricultural settings. Under these conditions, less carbon would be lost and subsequently salvaged at night. Future modelling should incorporate more realistic light regimes to better assess the potential benefits in agricultural contexts.

5.2.2 Potential CO_2-concentrating effects

One potential benefit of nocturnal CO_2 refixation strategies not explored in this modelling work is a possible CO_2-concentrating effect around Rubisco. If respiratory CO_2 refixed at night is released during the day via decarboxylation processes, this could create localised elevated CO_2 concentrations around Rubisco, potentially decreasing photorespiration rates. In the current models, I maintained a constant Rubisco carboxylation ratio of 3:1, which does not capture this potential effect. Shameer et al. (2018) suggested that CAM productivity may be underestimated in metabolic models because the CO_2-concentrating effect of full CAM is neglected. Their modelling of increased Rubisco carboxylation ratios suggested that CAM could achieve productivity comparable to C3 metabolism when this effect is considered.

It is important to note, however, that while full CAM plants have closed stomata during daylight, which traps released CO_2, the nocturnal CO_2 refixation mechanisms proposed here would still require open daytime stomata for primary atmospheric CO_2 assimilation. Therefore, nocturnal CO_2 refixation pathways may not achieve the same degree of CO_2-concentrating effect as full CAM.

This highlights another design consideration for future nocturnal CO_2 refixation pathways: the decarboxylation of transient carbon storage compounds should ideally be engineered to occur within the chloroplast in close proximity to Rubisco, where it could have a beneficial effect on Rubisco carboxylation activity.

5.3 Concluding remarks

This work has explored nocturnal CO_2 refixation as a novel and potentially valuable strategy to reduce respiratory losses of carbon in plants and thereby increase

plant productivity. While the magnitude of growth benefits achievable in real-world applications depends on numerous factors not yet fully captured in the modelling approach used here, this research provides a theoretical foundation. The stoichiometric analyses presented demonstrate that, from a metabolic network perspective, nocturnal CO_2 refixation pathways could potentially offset the incurred costs by salvaging previously assimilated carbon from being lost and thereby offer meaningful improvements in carbon use efficiency.

References

Adler, L., Díaz-Ramos, A., Mao, Y., Pukacz, K. R., Fei, C., and McCormick, A. J. (2022). New horizons for building pyrenoid-based CO2-concentrating mechanisms in plants to improve yields. *Plant Physiology*, 190(3):1609–1627.

Ainsworth, E. A. and Long, S. P. (2005). What have we learned from 15 years of free-air CO2 enrichment (FACE)? A meta-analytic review of the responses of photosynthesis, canopy properties and plant production to rising CO2. *New Phytologist*, 165(2):351–372.

Amthor, J. (1989). Respiration and Crop Productivity | SpringerLink.

Amthor, J. S. (2000). The McCree–de Wit–Penning de Vries–Thornley Respiration Paradigms: 30 Years Later. *Annals of Botany*, 86(1):1–20.

Amthor, J. S., Bar-Even, A., Hanson, A. D., Millar, A. H., Stitt, M., Sweetlove, L. J., and Tyerman, S. D. (2019). Engineering Strategies to Boost Crop Productivity by Cutting Respiratory Carbon Loss. *The Plant Cell*, 31(2).

Andersson, I. and Backlund, A. (2008). Structure and function of Rubisco. *Plant Physiology and Biochemistry*, 46(3):275–291.

Annese, D., Romani, F., Grandellis, C., Ives, L., Frangedakis, E., Buson, F. X., Molloy, J. C., and Haseloff, J. (2025). Semi-automated workflow for high-throughput *Agrobacterium* -mediated plant transformation. *The Plant Journal*, 122(1):e70118.

Arnold, A. and Nikoloski, Z. (2014). Bottom-up Metabolic Reconstruction of Arabidopsis and Its Application to Determining the Metabolic Costs of Enzyme Production. *Plant Physiology*, 165(3).

Atkinson, N., Mao, Y., Chan, K. X., and McCormick, A. J. (2020). Condensation of Rubisco into a proto-pyrenoid in higher plant chloroplasts. *Nature Communications*, 11(1).

Bar-Even, A. (2018). Daring metabolic designs for enhanced plant carbon fixation. *Plant Science*, 273:71–83.

Bar-Even, A., Flamholz, A., Noor, E., and Milo, R. (2012a). Thermodynamic constraints shape the structure of carbon fixation pathways. *Biochimica et Biophysica Acta (BBA) - Bioenergetics*, 1817(9):1646–1659.

Bar-Even, A., Noor, E., Flamholz, A., and Milo, R. (2013). Design and analysis of metabolic pathways supporting formatotrophic growth for electricity-dependent cultivation of microbes. *Biochimica et Biophysica Acta (BBA) - Bioenergetics*, 1827(8-9):1039–1047.

Bar-Even, A., Noor, E., Lewis, N. E., and Milo, R. (2010). Design and analysis of synthetic carbon fixation pathways. *Proceedings of the National Academy of Sciences*, 107(19).

Bar-Even, A., Noor, E., and Milo, R. (2012b). A survey of carbon fixation pathways through a quantitative lens. *Journal of Experimental Botany*, 63(6):2325–2342.

Bar-Even, A., Noor, E., Savir, Y., Liebermeister, W., Davidi, D., Tawfik, D. S., and Milo, R. (2011). The Moderately Efficient Enzyme: Evolutionary and Physicochemical Trends Shaping Enzyme Parameters. *Biochemistry*, 50(21):4402–4410.

Bathellier, C., Tcherkez, G., Lorimer, G. H., and Farquhar, G. D. (2018). Rubisco is not really so bad. *Plant, Cell & Environment*, 41(4):705–716.

Beber, M. E., Gollub, M. G., Mozaffari, D., Shebek, K. M., Flamholz, A. I., Milo,

R., and Noor, E. (2021). eQuilibrator 3.0: a database solution for thermodynamic constant estimation. *Nucleic Acids Research*.

Betti, M., Bauwe, H., Busch, F. A., Fernie, A. R., Keech, O., Levey, M., Ort, D. R., Parry, M. A. J., Sage, R., Timm, S., Walker, B., and Weber, A. P. M. (2016). Manipulating photorespiration to increase plant productivity: recent advances and perspectives for crop improvement. *Journal of Experimental Botany*, 67(10):2977–2988.

Bierbaumer, S., Nattermann, M., Schulz, L., Zschoche, R., Erb, T. J., Winkler, C. K., Tinzl, M., and Glueck, S. M. (2023). Enzymatic Conversion of CO2: From Natural to Artificial Utilization. *Chemical Reviews*, 123(9):5702–5754.

Blazeck, J. and Alper, H. (2010). Systems metabolic engineering: Genome-scale models and beyond. *Biotechnology Journal*, 5(7):647–659.

Borland, A. M. (1996). A model for the partitioning of photosynthetically fixed carbon during the C3-CAM transition in Sedum telephium. *New Phytologist*, 134(3):433–444.

Borland, A. M., Hartwell, J., Weston, D. J., Schlauch, K. A., Tschaplinski, T. J., Tuskan, G. A., Yang, X., and Cushman, J. C. (2014). Engineering crassulacean acid metabolism to improve water-use efficiency. *Trends in Plant Science*, 19(5):327–338.

Bowman, J. L., Arteaga-Vazquez, M., Berger, F., Briginshaw, L. N., Carella, P., Aguilar-Cruz, A., Davies, K. M., Dierschke, T., Dolan, L., Dorantes-Acosta, A. E., Fisher, T. J., Flores-Sandoval, E., Futagami, K., Ishizaki, K., Jibran, R., Kanazawa, T., Kato, H., Kohchi, T., Levins, J., Lin, S.-S., Nakagami, H., Nishihama, R., Romani, F., Schornack, S., Tanizawa, Y., Tsuzuki, M., Ueda, T., Watanabe, Y., Yamato, K. T., and Zachgo, S. (2022). The renaissance and

enlightenment of Marchantia as a model system. *The Plant Cell*, 34(10):3512–3542.

Burgos, A., Miranda, E., Vilaprinyo, E., Meza-Canales, I. D., and Alves, R. (2022). CAM Models: Lessons and Implications for CAM Evolution. *Frontiers in Plant Science*, 13:893095.

Busch, F. A., Ainsworth, E. A., Amtmann, A., Cavanagh, A. P., Driever, S. M., Ferguson, J. N., Kromdijk, J., Lawson, T., Leakey, A. D. B., Matthews, J. S. A., Meacham-Hensold, K., Vath, R. L., Vialet-Chabrand, S., Walker, B. J., and Papanatsiou, M. (2024). A guide to photosynthetic gas exchange measurements: Fundamental principles, best practice and potential pitfalls. *Plant, Cell & Environment*, 47(9):3344–3364.

Busch, F. A., Sage, T. L., Cousins, A. B., and Sage, R. F. (2013). C3 plants enhance rates of photosynthesis by reassimilating photorespired and respired CO2. *Plant, Cell & Environment*, 36(1):200–212.

Cannell, M. and Thornley, J. (2000). Modelling the Components of Plant Respiration: Some Guiding Principles. *Annals of Botany*, 85(1):45–54.

Cannell, N. (2021). *Investigation of Early-Diverging Land Plant Metabolism*. PhD Thesis, University of Oxford.

Carmo-Silva, E., Scales, J. C., Madgwick, P. J., and Parry, M. A. J. (2015). Optimizing R ubisco and its regulation for greater resource use efficiency. *Plant, Cell & Environment*, 38(9):1817–1832.

Carriquí, M., Roig-Oliver, M., Brodribb, T. J., Coopman, R., Gill, W., Mark, K., Niinemets, U., Perera-Castro, A. V., Ribas-Carbó, M., Sack, L., Tosens, T., Waite, M., and Flexas, J. (2019). Anatomical constraints to nonstomatal

diffusion conductance and photosynthesis in lycophytes and bryophytes. *New Phytologist*, 222(3):1256–1270.

Carter, J. L. and Romine, K. G. (1969). The Effects of Long and Short Photoperiods on the Rate of Growth and Gemmae Cup Production in Marchantia polymorpha L. *Transactions of the Kansas Academy of Science (1903-)*, 72(1):98–107.

Caspi, R., Billington, R., Fulcher, C. A., Keseler, I. M., Kothari, A., Krummenacker, M., Latendresse, M., Midford, P. E., Ong, Q., Ong, W. K., Paley, S., Subhraveti, P., and Karp, P. D. (2018). The MetaCyc database of metabolic pathways and enzymes. *Nucleic Acids Research*, 46(Database issue):D633–D639.

Catherall, E., Musial, S., Atkinson, N., Walker, C. E., Mackinder, L. C. M., and McCormick, A. J. (2025). From algae to plants: understanding pyrenoid-based CO2-concentrating mechanisms. *Trends in Biochemical Sciences*, 50(1):33–45.

Ceusters, N., Frans, M., Van den Ende, W., and Ceusters, J. (2019). Maltose Processing and Not -Amylase Activity Curtails Hydrolytic Starch Degradation in the CAM Orchid Phalaenopsis. *Frontiers in Plant Science*, 10:1386.

Chatterjee, A., Abeydeera, N. D., Bale, S., Pai, P.-J., Dorrestein, P. C., Russell, D. H., Ealick, S. E., and Begley, T. P. (2011). Saccharomyces cerevisiae THI4p is a suicide thiamine thiazole synthase. *Nature*, 478(7370):542–546.

Chen, L., Lin, Q., and Nose, A. (2002). A comparative study on diurnal changes in metabolite levels in the leaves of three crassulacean acid metabolism (CAM) species, Ananas comosus, Kalanchoë daigremontiana and K. pinnata. *Journal of Experimental Botany*, 53(367):341–350.

Chen, T., Hojka, M., Davey, P., Sun, Y., Dykes, G. F., Zhou, F., Lawson, T., Nixon,

P. J., Lin, Y., and Liu, L.-N. (2023). Engineering -carboxysomes into plant chloroplasts to support autotrophic photosynthesis. *Nature Communications*, 14(1):2118.

Cheung, C. M., Poolman, M. G., Fell, D. A., Ratcliffe, R. G., and Sweetlove, L. J. (2014). A Diel Flux Balance Model Captures Interactions between Light and Dark Metabolism during Day-Night Cycles in C $_3$ and Crassulacean Acid Metabolism Leaves. *Plant Physiology*, 165(2):917–929.

Cui, D., Zhang, L., Jiang, S., Yao, Z., Gao, B., Lin, J., Yuan, Y. A., and Wei, D. (2015). A computational strategy for altering an enzyme in its cofactor preference to NAD(H) and/or NADP(H). *The FEBS Journal*, 282(12):2339–2351.

Cushman, J. C. (2001). Crassulacean Acid Metabolism. A Plastic Photosynthetic Adaptation to Arid Environments. *Plant Physiology*, 127(4).

Delmans, M., Pollak, B., and Haseloff, J. (2017). MarpoDB: An Open Registry for Marchantia Polymorpha Genetic Parts. *Plant and Cell Physiology*, 58(1):e5–e5.

Diffenbaugh, N. S., Singh, D., Mankin, J. S., Horton, D. E., Swain, D. L., Touma, D., Charland, A., Liu, Y., Haugen, M., Tsiang, M., and Rajaratnam, B. (2017). Quantifying the influence of global warming on unprecedented extreme climate events. *Proceedings of the National Academy of Sciences*, 114(19):4881–4886.

Dodd, A. N., Griffiths, H., Taybi, T., Cushman, J. C., and Borland, A. M. (2003). Integrating diel starch metabolism with the circadian and environmental regulation of Crassulacean acid metabolism in Mesembryanthemum crystallinum. *Planta*, 216(5):789–797.

Donahue, R. A., Poulson, M. E., and Edwards, G. E. (1997). A method for measuring whole plant photosynthesis in Arabidopsis thaliana. page 7.

Ebrahim, A., Lerman, J. A., Palsson, B. O., and Hyduke, D. R. (2013). COBRApy: COnstraints-Based Reconstruction and Analysis for Python. *BMC Systems Biology*, 7:74.

Ehleringer, J. R., Cerling, T. E., and Helliker, B. R. (1997). C 4 photosynthesis, atmospheric CO 2 , and climate. *Oecologia*, 112(3):285–299.

Ehleringer, J. R., Sage, R. F., Flanagan, L. B., and Pearcy, R. W. (1991). Climate change and the evolution of C4 photosynthesis. *Trends in Ecology & Evolution*, 6(3):95–99.

Ellis, R. J. (2010). Tackling unintelligent design. *Nature*, 463(7278):164–165.

Erb, T. J., Jones, P. R., and Bar-Even, A. (2017). Synthetic metabolism: metabolic engineering meets enzyme design. *Current Opinion in Chemical Biology*, 37:56–62.

Erb, T. J. and Zarzycki, J. (2016). Biochemical and synthetic biology approaches to improve photosynthetic CO2-fixation. *Current Opinion in Chemical Biology*, 34:72–79.

Erb, T. J. and Zarzycki, J. (2018). A short history of RubisCO: the rise and fall (?) of Nature's predominant CO2 fixing enzyme. *Current Opinion in Biotechnology*, 49:100–107.

Ermakova, M., Danila, F. R., Furbank, R. T., and Von Caemmerer, S. (2020). On the road to C_4 rice: advances and perspectives. *The Plant Journal*, 101(4):940–950.

Evans, J. R. (1989). Photosynthesis and nitrogen relationships in leaves of C3 plants. *Oecologia*, 78(1):9–19.

Evans, J. R., Kaldenhoff, R., Genty, B., and Terashima, I. (2009). Resistances

along the CO2 diffusion pathway inside leaves. *Journal of Experimental Botany*, 60(8):2235–2248.

Fang, Y., Huang, F., Faulkner, M., Jiang, Q., Dykes, G. F., Yang, M., and Liu, L.-N. (2018). Engineering and Modulating Functional Cyanobacterial CO2-Fixing Organelles. *Frontiers in Plant Science*, 9:739.

Farquhar, G. D., Von Caemmerer, S., and Berry, J. A. (1980). A biochemical model of photosynthetic CO2 assimilation in leaves of C3 species. *Planta*, 149(1):78–90.

Fei, C., Wilson, A. T., Mangan, N. M., Wingreen, N. S., and Jonikas, M. C. (2022). Modelling the pyrenoid-based CO2-concentrating mechanism provides insights into its operating principles and a roadmap for its engineering into crops. *Nature Plants*, 8(5):583–595.

Fernie, A. R., Carrari, F., and Sweetlove, L. J. (2004). Respiratory metabolism: glycolysis, the TCA cycle and mitochondrial electron transport. *Current Opinion in Plant Biology*, 7(3):254–261.

Flamholz, A., Noor, E., Bar-Even, A., and Milo, R. (2012). eQuilibrator—the biochemical thermodynamics calculator. *Nucleic Acids Research*, 40(D1):D770–D775.

Flexas, J., Barbour, M. M., Brendel, O., Cabrera, H. M., Carriquí, M., Díaz-Espejo, A., Douthe, C., Dreyer, E., Ferrio, J. P., Gago, J., Gallé, A., Galmés, J., Kodama, N., Medrano, H., Niinemets, , Peguero-Pina, J. J., Pou, A., Ribas-Carbó, M., Tomás, M., Tosens, T., and Warren, C. R. (2012). Mesophyll diffusion conductance to CO2: An unappreciated central player in photosynthesis. *Plant Science*, 193-194:70–84.

Flexas, J., Bota, J., Galmés, J., Medrano, H., and Ribas-Carbó, M. (2006). Keep-

ing a positive carbon balance under adverse conditions: responses of photosynthesis and respiration to water stress. *Physiologia Plantarum*, 127(3):343–352.

Flexas, J. and Carriquí, M. (2020). Photosynthesis and photosynthetic efficiencies along the terrestrial plant's phylogeny: lessons for improving crop photosynthesis. *The Plant Journal*, 101(4):964–978.

Flis, A., Mengin, V., Ivakov, A. A., Mugford, S. T., Hubberten, H.-M., Encke, B., Krohn, N., Höhne, M., Feil, R., Hoefgen, R., Lunn, J. E., Millar, A. J., Smith, A. M., Sulpice, R., and Stitt, M. (2019). Multiple circadian clock outputs regulate diel turnover of carbon and nitrogen reserves. *Plant, Cell & Environment*, 42(2):549–573.

Frei, B., Eisenach, C., Martinoia, E., Hussein, S., Chen, X.-Z., Arrivault, S., and Neuhaus, H. E. (2018). Purification and functional characterization of the vacuolar malate transporter tDT from *Arabidopsis*. *Journal of Biological Chemistry*, 293(11):4180–4190.

Furbank, R. T. (2011). Evolution of the C4 photosynthetic mechanism: are there really three C4 acid decarboxylation types? *Journal of Experimental Botany*, 62(9):3103–3108.

Gamborg, O., Miller, R., and Ojima, K. (1968). Nutrient requirements of suspension cultures of soybean root cells. *Experimental Cell Research*, 50(1):151–158.

Gauthier, P. P. G., Bligny, R., Gout, E., Mahé, A., Nogués, S., Hodges, M., and Tcherkez, G. G. B. (2010). In folio isotopic tracing demonstrates that nitrogen assimilation into glutamate is mostly independent from current CO2 assimilation in illuminated leaves of Brassica napus. *New Phytologist*, 185(4):988–999.

Grafahrend-Belau, E., Schreiber, F., Koschützki, D., and Junker, B. H. (2009).

Flux Balance Analysis of Barley Seeds: A Computational Approach to Study Systemic Properties of Central Metabolism. *Plant Physiology*, 149(1).

Graham, T. and Dixon, M. A. (2012). Liverwort Control: An Ancillary Role for Ozone-based Irrigation Water Treatment Systems? *HortScience*, 47(3).

Gupta, S. K., Ku, M. S. B., Lin, J.-H., Zhang, D., and Edwards, G. E. (1994). Light/dark modulation of phosphoenolpyruvate carboxylase in C3 and C4 species. *Photosynthesis Research*, 42(2):133–143.

Hanson, D., Andrews, T. J., and Badger, M. R. (2002). Variability of the pyrenoid-based CO2 concentrating mechanism in hornworts (Anthocerotophyta). *Functional Plant Biology*, 29(3):407–416.

Hata, J.-i., Hua, Q., Yang, C., Shimizu, K., and Taya, M. (2000). Characterization of energy conversion based on metabolic flux analysis in mixotrophic liverwort cells, *Marchantia polymorpha*. *Biochemical Engineering Journal*, 6(1):65–74.

Hatch, M. D. (1987). C4 photosynthesis: a unique elend of modified biochemistry, anatomy and ultrastructure. *Biochimica et Biophysica Acta (BBA) - Reviews on Bioenergetics*, 895(2):81–106.

Heyduk, K., McKain, M. R., Lalani, F., and Leebens-Mack, J. (2016). Evolution of a CAM anatomy predates the origins of Crassulacean acid metabolism in the Agavoideae (Asparagaceae). *Molecular Phylogenetics and Evolution*, 105:102–113.

Hibberd, J. M., Sheehy, J. E., and Langdale, J. A. (2008). Using C4 photosynthesis to increase the yield of rice—rationale and feasibility. *Current Opinion in Plant Biology*, 11(2):228–231.

Holzhütter, H.-G. (2004). The principle of flux minimization and its application

to estimate stationary fluxes in metabolic networks. *European Journal of Biochemistry*, 271(14):2905–2922.

Igamberdiev, A. U. and Eprintsev, A. T. (2016). Organic Acids: The Pools of Fixed Carbon Involved in Redox Regulation and Energy Balance in Higher Plants. *Frontiers in Plant Science*, 7:1042.

Ivanov, A. G., Rosso, D., Savitch, L. V., Stachula, P., Rosembert, M., Oquist, G., Hurry, V., and Hüner, N. P. A. (2012). Implications of alternative electron sinks in increased resistance of PSII and PSI photochemistry to high light stress in cold-acclimated Arabidopsis thaliana. *Photosynthesis Research*, 113(1):191–206.

Jordan, D. B. and Ogren, W. L. (1984). The CO2/O2 specificity of ribulose 1,5-bisphosphate carboxylase/oxygenase. *Planta*, 161(4):308–313.

Joshi, J., Amthor, J. S., McCarty, D. R., Messina, C. D., Wilson, M. A., Millar, A. H., and Hanson, A. D. (2023). Why cutting respiratory CO2 loss from crops is possible, practicable, and prudential. *Modern Agriculture*, 1(1):16–26.

Joshi, J., Beaudoin, G. A., Patterson, J. A., García-García, J. D., Belisle, C. E., Chang, L.-Y., Li, L., Duncan, O., Millar, A. H., and Hanson, A. D. (2020). Bioinformatic and experimental evidence for suicidal and catalytic plant THI4s. *Biochemical Journal*, 477(11):2055–2069.

Kang, W., Ma, X., Liu, C., Wang, S., Zhou, Y., Xue, C., Xu, Y., and Li, B. (2024). Liquid-liquid phase separation (LLPS) in synthetic biosystems. *Materials Science and Engineering: R: Reports*, 157:100762.

Kangasjärvi, S., Neukermans, J., Li, S., Aro, E.-M., and Noctor, G. (2012). Photosynthesis, photorespiration, and light signalling in defence responses. *Journal of Experimental Botany*, 63(4):1619–1636.

Kebeish, R., Niessen, M., Oksaksin, M., Blume, C., and Peterhaensel, C. (2012). Constitutive and dark-induced expression of *Solanum tuberosum* phosphoenolpyruvate carboxylase enhances stomatal opening and photosynthetic performance of *Arabidopsis thaliana*. *Biotechnology and Bioengineering*, 109(2):536–544.

Kebeish, R., Niessen, M., Thiruveedhi, K., Bari, R., Hirsch, H.-J., Rosenkranz, R., Stäbler, N., Schönfeld, B., Kreuzaler, F., and Peterhänsel, C. (2007). Chloroplastic photorespiratory bypass increases photosynthesis and biomass production in Arabidopsis thaliana. *Nature Biotechnology*, 25(5):593–599.

Keeley, J. E. (1998). CAM photosynthesis in submerged aquatic plants. *The Botanical Review*, 64(2):121–175.

Keeley, J. E. and Busch, G. (1984). Carbon Assimilation Characteristics of the Aquatic CAM Plant, Isoetes howellii 1. *Plant Physiology*, 76(2):525–530.

Kimball, B. A. (2016). Crop responses to elevated CO2 and interactions with H2O, N, and temperature. *Current Opinion in Plant Biology*, 31:36–43.

Kohchi, T., Yamato, K. T., Ishizaki, K., Yamaoka, S., and Nishihama, R. (2021). Development and Molecular Genetics of Marchantia polymorpha. *Annual Review of Plant Biology*, 72(1):677–702.

Küken, A. and Nikoloski, Z. (2019). Computational Approaches to Design and Test Plant Synthetic Metabolic Pathways1[OPEN]. *Plant Physiology*, 179(3):894–906.

Lake, J. A. (2004). Gas exchange: new challenges with Arabidopsis. *New Phytologist*, 162(1):1–3.

Lan, X., Tans, P., Thoning, K., and NOAA Global Monitoring Laboratory (2023).

Trends in globally-averaged CO2 determined from NOAA Global Monitoring Laboratory measurements.

Leakey, A. D. B., Ainsworth, E. A., Bernacchi, C. J., Rogers, A., Long, S. P., and Ort, D. R. (2009). Elevated CO2 effects on plant carbon, nitrogen, and water relations: six important lessons from FACE. *Journal of Experimental Botany*, 60(10):2859–2876.

Lim, S. D., Lee, S., Choi, W.-G., Yim, W. C., and Cushman, J. C. (2019). Laying the Foundation for Crassulacean Acid Metabolism (CAM) Biodesign: Expression of the C4 Metabolism Cycle Genes of CAM in Arabidopsis. *Frontiers in Plant Science*, 10.

Lin, H., Arrivault, S., Coe, R. A., Karki, S., Covshoff, S., Bagunu, E., Lunn, J. E., Stitt, M., Furbank, R. T., Hibberd, J. M., and Quick, W. P. (2020). A Partial C4 Photosynthetic Biochemical Pathway in Rice. *Frontiers in Plant Science*, 11.

Lindström Battle, A. L. and Sweetlove, L. J. (2025). Bryophytes as metabolic engineering platforms. *Current Opinion in Plant Biology*, 85:102702.

Lisec, J., Schauer, N., Kopka, J., Willmitzer, L., and Fernie, A. R. (2006). Gas chromatography mass spectrometry–based metabolite profiling in plants | Nature Protocols. *Nature Protocols*, 1:387–396.

Liu, D., Hu, R., Zhang, J., Guo, H.-B., Cheng, H., Li, L., Borland, A. M., Qin, H., Chen, J.-G., Muchero, W., Tuskan, G. A., and Yang, X. (2021). Overexpression of an Agave Phosphoenolpyruvate Carboxylase Improves Plant Growth and Stress Tolerance. *Cells*, 10(3).

Long, S. P. (1991). Modification of the response of photosynthetic productivity to rising temperature by atmospheric CO_2 concentrations: Has its importance been underestimated? *Plant, Cell & Environment*, 14(8):729–739.

Long, S. P., Ainsworth, E. A., Leakey, A. D. B., Nösberger, J., and Ort, D. R. (2006). Food for Thought: Lower-Than-Expected Crop Yield Stimulation with Rising CO2 Concentrations. *Science*, 312(5782).

Luo, S., Diehl, C., He, H., Bae, Y., Klose, M., Claus, P., Cortina, N. S., Fernandez, C. A., Schulz-Mirbach, H., McLean, R., Ramírez Rojas, A. A., Schindler, D., Paczia, N., and Erb, T. J. (2023). Construction and modular implementation of the THETA cycle for synthetic CO2 fixation. *Nature Catalysis*, 6(12).

Lüttge, U. (2002). CO2-concentrating: consequences in crassulacean acid metabolism. *Journal of Experimental Botany*, 53(378):2131–2142.

Lüttge, U., Smith, J., Marigo, G., and Osmond, C. (1981). Energetics of malate accumulation in the vacuoles of *Kalanchoë tubiflora* cells. *FEBS Letters*, 126(1):81–84.

Mackinder, L. C. M. (2018). The Chlamydomonas CO2-concentrating mechanism and its potential for engineering photosynthesis in plants. *New Phytologist*, 217(1):54–61.

McClain, A. M. and Sharkey, T. D. (2019). Triose phosphate utilization and beyond: from photosynthesis to end product synthesis. *Journal of Experimental Botany*, 70(6):1755–1766.

McLean, R., Schwander, T., Diehl, C., Cortina, N. S., Paczia, N., Zarzycki, J., and Erb, T. J. (2023). Exploring alternative pathways for the in vitro establishment of the HOPAC cycle for synthetic CO_2 fixation. *Science Advances*, 9(24):eadh4299.

Miller, T. E., Beneyton, T., Schwander, T., Diehl, C., Girault, M., McLean, R., Chotel, T., Claus, P., Cortina, N. S., Baret, J.-C., and Erb, T. J. (2020). Light-

powered CO_2 fixation in a chloroplast mimic with natural and synthetic parts. *Science*, 368(6491):649–654.

Miskovic, L., Tokic, M., Fengos, G., and Hatzimanikatis, V. (2015). Rites of passage: requirements and standards for building kinetic models of metabolic phenotypes. *Current Opinion in Biotechnology*, 36:146–153.

Muhaidat, R., Sage, R. F., and Dengler, N. G. (2007). Diversity of Kranz anatomy and biochemistry in C_4 eudicots. *American Journal of Botany*, 94(3):362–381.

Naseem, M., Osmanoglu, , and Dandekar, T. (2020). Synthetic Rewiring of Plant CO2 Sequestration Galvanizes Plant Biomass Production. *Trends in Biotechnology*, 38(4):354–359.

Nelson, E. A. and Sage, R. F. (2007). Functional constraints of CAM leaf anatomy: tight cell packing is associated with increased CAM function across a gradient of CAM expression. *Journal of Experimental Botany*, 59(7):1841–1850.

Nikoloski, Z., Perez-Storey, R., and Sweetlove, L. J. (2015). Inference and Prediction of Metabolic Network Fluxes. *Plant Physiology*, 169(3).

Nimmo, H. G. (2000). The regulation of phosphoenolpyruvate carboxylase in CAM plants. *Trends in Plant Science*, 5(2):75–80.

Noor, E., Bar-Even, A., Flamholz, A., Reznik, E., Liebermeister, W., and Milo, R. (2014). Pathway Thermodynamics Highlights Kinetic Obstacles in Central Metabolism. *PLOS Computational Biology*, 10(2):e1003483.

O'Leary, B., Park, J., and Plaxton, W. C. (2011). The remarkable diversity of plant PEPC (phosphoenolpyruvate carboxylase): recent insights into the physiological functions and post-translational controls of non-photosynthetic PEPCs. *Biochemical Journal*, 436(1):15–34.

O'Leary, B. M., Asao, S., Millar, A. H., and Atkin, O. K. (2019). Core principles which explain variation in respiration across biological scales. *New Phytologist*, 222(2):670–686.

Orth, J. D., Thiele, I., and Palsson, B. (2010). What is flux balance analysis? *Nature biotechnology*, 28(3):245–248.

Osmanoglu, , Khaled AlSeiari, M., AlKhoori, H. A., Shams, S., Bencurova, E., Dandekar, T., and Naseem, M. (2021). Topological Analysis of the Carbon-Concentrating CETCH Cycle and a Photorespiratory Bypass Reveals Boosted CO2-Sequestration by Plants. *Frontiers in Bioengineering and Biotechnology*, 9.

O'Brien, E. J., Monk, J. M., and Palsson, B. O. (2015). Using Genome-Scale Models to Predict Biological Capabilities. *Cell*, 161(5):971–987.

O'Leary, B. M., Lee, C. P., Atkin, O. K., Cheng, R., Brown, T. B., and Millar, A. H. (2017). Variation in Leaf Respiration Rates at Night Correlates with Carbohydrate and Amino Acid Supply1[OPEN]. *Plant Physiology*, 174(4):2261–2273.

Plaxton, W. C. and Podestá, F. E. (2006). The Functional Organization and Control of Plant Respiration. *Critical Reviews in Plant Sciences*, 25(2):159–198.

Portis, A. R. and Jr. (2003). Rubisco activase – Rubisco's catalytic chaperone. *Photosynthesis Research*, 75(1):11–27.

Poulson, M. E., Edwards, G. E., and Browse, J. (2002). Photosynthesis is limited at high leaf to air vapor pressure deficit in a mutant of Arabidopsis thaliana that lacks trienoic fatty acids. *Photosynthesis Research*, 72(1):55–63.

Rae, B. D., Long, B. M., Badger, M. R., and Price, G. D. (2013). Functions, Compositions, and Evolution of the Two Types of Carboxysomes: Polyhedral

Microcompartments That Facilitate CO_2 Fixation in Cyanobacteria and Some Proteobacteria. *Microbiology and Molecular Biology Reviews*, 77(3):357–379.

Raines, C. A. (2011). Increasing Photosynthetic Carbon Assimilation in C3 Plants to Improve Crop Yield: Current and Future Strategies. *Plant Physiology*, 155(1):36–42.

Robison, T. A., Oh, Z. G., Lafferty, D., Xu, X., Villarreal, J. C. A., Gunn, L. H., and Li, F.-W. (2025). Hornworts reveal a spatial model for pyrenoid-based CO2-concentrating mechanisms in land plants. *Nature Plants*, 11(1):63–73.

Rosa-Téllez, S., Alcántara-Enguídanos, A., Martínez-Seidel, F., Casatejada-Anchel, R., Saeheng, S., Bailes, C. L., Erban, A., Barbosa-Medeiros, D., Alepúz, P., Matus, J. T., Kopka, J., Muñoz-Bertomeu, J., Krueger, S., Roje, S., Fernie, A. R., and Ros, R. (2024). The serine-glycine-one-carbon metabolic network orchestrates changes in nitrogen and sulfur metabolism and shapes plant development. *The Plant Cell*, 36(2):404–426.

Rutjens, R. J. L., Evers, J. B., Band, L. R., Jones, M. D., and Owen, M. R. (2024). Are we focusing on the right parameters? Insights from Global Sensitivity Analysis of a Functional-Structural Plant Model. *in silico Plants*, 6(2):diae011.

Saadat, N. P., van Aalst, M., Brand, A., Ebenhöh, O., Tissier, A., and Matuszyńska, A. B. (2023). Shifts in carbon partitioning by photosynthetic activity increase terpenoid synthesis in glandular trichomes. *The Plant Journal*, n/a(n/a).

Sage, R. F. (2002). Variation in the kcat of Rubisco in C3 and C4 plants and some implications for photosynthetic performance at high and low temperature. *Journal of Experimental Botany*, 53(369):609–620.

Sage, R. F. and Kubien, D. S. (2007). The temperature response of C_3 and C_4 photosynthesis. *Plant, Cell & Environment*, 30(9):1086–1106.

Sage, R. F., Sage, T. L., and Kocacinar, F. (2012). Photorespiration and the Evolution of C_4 Photosynthesis. *Annual Review of Plant Biology*, 63(1):19–47.

Sandor, A., Fricker, M. D., Kriechbaumer, V., and Sweetlove, L. J. (2021). IntEResting structures: formation and applications of organized smooth endoplasmic reticulum in plant cells. *Plant Physiology*, 185(3):550–561.

Santos Correa, S., Schultz, J., Lauersen, K. J., and Soares Rosado, A. (2023). Natural carbon fixation and advances in synthetic engineering for redesigning and creating new fixation pathways. *Journal of Advanced Research*, 47:75–92.

Satanowski, A., Marchal, D. G., Perret, A., Petit, J.-L., Bouzon, M., Döring, V., Dubois, I., He, H., Smith, E. N., Pellouin, V., Petri, H. M., Rainaldi, V., Nattermann, M., Burgener, S., Paczia, N., Zarzycki, J., Heinemann, M., Bar-Even, A., and Erb, T. J. (2025). Design and implementation of aerobic and ambient CO2-reduction as an entry-point for enhanced carbon fixation. *Nature Communications*, 16(1):3134.

Sauret-Güeto, S., Frangedakis, E., Silvestri, L., Rebmann, M., Tomaselli, M., Markel, K., Delmans, M., West, A., Patron, N. J., and Haseloff, J. (2020). Systematic Tools for Reprogramming Plant Gene Expression in a Simple Model, *Marchantia polymorpha*. *ACS Synthetic Biology*, 9(4):864–882.

Savir, Y., Noor, E., Milo, R., and Tlusty, T. (2010). Cross-species analysis traces adaptation of Rubisco toward optimality in a low-dimensional landscape. *Proceedings of the National Academy of Sciences*, 107(8):3475–3480.

Scheffen, M., Marchal, D. G., Beneyton, T., Schuller, S. K., Klose, M., Diehl, C., Lehmann, J., Pfister, P., Carrillo, M., He, H., Aslan, S., Cortina, N. S., Claus,

P., Bollschweiler, D., Baret, J.-C., Schuller, J. M., Zarzycki, J., Bar-Even, A., and Erb, T. J. (2021). A new-to-nature carboxylation module to improve natural and synthetic CO 2 fixation. *Nature Catalysis*, pages 1–11.

Scheible, W.-R., Krapp, A., and Stitt, M. (2000). Reciprocal diurnal changes of phosphoenolpyruvate carboxylase expression and cytosolic pyruvate kinase, citrate synthase and NADP-isocitrate dehydrogenase expression regulate organic acid metabolism during nitrate assimilation in tobacco leaves. *Plant, Cell & Environment*, 23(11):1155–1167.

Schindelin, J., Arganda-Carreras, I., Frise, E., Kaynig, V., Longair, M., Pietzsch, T., Preibisch, S., Rueden, C., Saalfeld, S., Schmid, B., Tinevez, J.-Y., White, D. J., Hartenstein, V., Eliceiri, K., Tomancak, P., and Cardona, A. (2012). Fiji: an open-source platform for biological-image analysis. *Nature Methods*, 9(7).

Schluter, U. (2003). Photosynthetic performance of an Arabidopsis mutant with elevated stomatal density (sdd1-1) under different light regimes. *Journal of Experimental Botany*, 54(383):867–874.

Schuler, M. L., Mantegazza, O., and Weber, A. P. (2016). Engineering C_4 photosynthesis into C_3 chassis in the synthetic biology age. *The Plant Journal*, 87(1):51–65.

Schwander, T., Schada von Borzyskowski, L., Burgener, S., Cortina, N. S., and Erb, T. J. (2016). A synthetic pathway for the fixation of carbon dioxide in vitro. *Science*, 354(6314):900–904.

Schwender, J., Shachar-Hill, Y., and Ohlrogge, J. B. (2006). Mitochondrial Metabolism in Developing Embryos of Brassica napus. *Journal of Biological Chemistry*, 281(45):34040–34047.

Scrutton, N. S., Berry, A., and Perham, R. N. (1990). Redesign of the coenzyme

specificity of a dehydrogenase by protein engineering. *Nature*, 343(6253):38–43.

Shameer, S., Baghalian, K., Cheung, C. Y. M., Ratcliffe, R. G., and Sweetlove, L. J. (2018). Computational analysis of the productivity potential of CAM. *Nature Plants*, 4(3).

Shameer, S., Ratcliffe, R. G., and Sweetlove, L. J. (2019). Leaf Energy Balance Requires Mitochondrial Respiration and Export of Chloroplast NADPH in the Light. *Plant Physiology*, 180(4):1947.

Shameer, S., Wang, Y., Bota, P., Ratcliffe, R. G., Long, S. P., and Sweetlove, L. J. (2022). A hybrid kinetic and constraint-based model of leaf metabolism allows predictions of metabolic fluxes in different environments. *The Plant Journal*, 109(1):295–313.

Sharkey, T. D., Bernacchi, C. J., Farquhar, G. D., and Singsaas, E. L. (2007). Fitting photosynthetic carbon dioxide response curves for C_3 leaves. *Plant, Cell & Environment*, 30(9):1035–1040.

Shen, B. R., Wang, L. M., Lin, X. L., Yao, Z., Xu, H. W., Zhu, C. H., Teng, H. Y., Cui, L. L., Liu, E. E., Zhang, J. J., He, Z. H., and Peng, X. X. (2019). Engineering a New Chloroplastic Photorespiratory Bypass to Increase Photosynthetic Efficiency and Productivity in Rice. *Molecular Plant*, 12(2):199–214.

Shen, C., Dupont, C. L., and Hopkinson, B. M. (2017). The diversity of CO2-concentrating mechanisms in marine diatoms as inferred from their genetic content. *Journal of Experimental Botany*, 68(14):3937–3948.

Shu, J.-P., Yan, Y.-H., and Wang, R.-J. (2022). Convergent molecular evolution of phosphoenolpyruvate carboxylase gene family in C4 and crassulacean acid metabolism plants. *PeerJ*, 10:e12828.

Silvera, K., Neubig, K. M., Whitten, W. M., Williams, N. H., Winter, K., and Cushman, J. C. (2010). Evolution along the crassulacean acid metabolism continuum. *Functional Plant Biology*, 37(11):995.

Smith, E. and Griffiths, H. (1996). A pyrenoid-based carbon-concentrating mechanism is present in terrestrial bryophytes of the class Anthocerotae. *Planta*, 200(2).

Smith, E. N., Schwarzländer, M., Ratcliffe, R. G., and Kruger, N. J. (2021). Shining a light on NAD- and NADP-based metabolism in plants. *Trends in Plant Science*.

Smith, E. N., Van Aalst, M., Weber, A. P. M., Ebenhöh, O., and Heinemann, M. (2025). Alternatives to photorespiration: A system-level analysis reveals mechanisms of enhanced plant productivity. *Science Advances*, 11(13):eadt9287.

Smith, J. A. (1987). Vacuolar Accumulation of Organic Acids and their Anions in CAM Plants. In Marin, B., editor, *Plant Vacuoles*, pages 79–87. Springer US, Boston, MA.

Smith, K., Strand, D. D., and Walker, B. J. (2024). Evaluating the contribution of plant metabolic pathways in the light to the ATP:NADPH demand using a meta-analysis of isotopically non-stationary metabolic flux analyses. *Photosynthesis Research*, 161(3):177–189.

South, P. F., Cavanagh, A. P., Liu, H. W., and Ort, D. R. (2019). Synthetic glycolate metabolism pathways stimulate crop growth and productivity in the field. *Science*, 363(6422):eaat9077.

Stitt, M., Lunn, J., and Usadel, B. (2010). Arabidopsis and primary photosynthetic metabolism – more than the icing on the cake. *The Plant Journal*, 61(6):1067–1091.

Strand, D. D. and Walker, B. J. (2023). Energetic considerations for engineering novel biochemistries in photosynthetic organisms. *Frontiers in Plant Science*, 14:1116812.

Sulpice, R., Flis, A., Ivakov, A. A., Apelt, F., Krohn, N., Encke, B., Abel, C., Feil, R., Lunn, J. E., and Stitt, M. (2014). Arabidopsis Coordinates the Diurnal Regulation of Carbon Allocation and Growth across a Wide Range of Photoperiods. *Molecular Plant*, 7(1):137–155.

Sun, J., Okita, T. W., and Edwards, G. E. (1999). Modification of Carbon Partitioning, Photosynthetic Capacity, and O2 Sensitivity in Arabidopsis Plants with Low ADP-Glucose Pyrophosphorylase Activity. *Plant Physiology*, 119(1).

Sweetlove, L. J., Beard, K. F. M., Nunes-Nesi, A., Fernie, A. R., and Ratcliffe, R. G. (2010). Not just a circle: flux modes in the plant TCA cycle. *Trends in Plant Science*, 15(8):462–470.

Sweetlove, L. J. and Ratcliffe, R. G. (2011). Flux-Balance Modeling of Plant Metabolism. *Frontiers in Plant Science*, 2.

Sweetlove, L. J., Williams, T. C. R., Cheung, C. Y. M., and Ratcliffe, R. G. (2013). Modelling metabolic CO2 evolution – a fresh perspective on respiration. *Plant, Cell & Environment*, 36(9):1631–1640.

Sánchez, B. J., Zhang, C., Nilsson, A., Lahtvee, P., Kerkhoven, E. J., and Nielsen, J. (2017). Improving the phenotype predictions of a yeast genome-scale metabolic model by incorporating enzymatic constraints. *Molecular Systems Biology*, 13(8):935.

Tay, I. Y. Y., Odang, K. B., and Cheung, C. Y. M. (2021). Metabolic Modeling of the C3-CAM Continuum Revealed the Establishment of a Starch/Sugar-Malate Cycle in CAM Evolution. *Frontiers in Plant Science*, 11.

Tcherkez, G., Gauthier, P., Buckley, T. N., Busch, F. A., Barbour, M. M., Bruhn, D., Heskel, M. A., Gong, X. Y., Crous, K. Y., Griffin, K., Way, D., Turnbull, M., Adams, M. A., Atkin, O. K., Farquhar, G. D., and Cornic, G. (2017). Leaf day respiration: low CO2 flux but high significance for metabolism and carbon balance. *New Phytologist*, 216(4):986–1001.

Tcherkez, G. G. B., Farquhar, G. D., and Andrews, T. J. (2006). Despite slow catalysis and confused substrate specificity, all ribulose bisphosphate carboxylases may be nearly perfectly optimized. *Proceedings of the National Academy of Sciences*, 103(19).

Ting, I. P. (1985). Crassulacean Acid Metabolism. page 28.

Tocquin, P. and Périlleux, C. (2004). Design of a versatile device for measuring whole plant gas exchanges in *Arabidopsis thaliana*. *New Phytologist*, 162(1):223–229.

Trudeau, D. L., Edlich-Muth, C., Zarzycki, J., Scheffen, M., Goldsmith, M., Khersonsky, O., Avizemer, Z., Fleishman, S. J., Cotton, C. A. R., Erb, T. J., Tawfik, D. S., and Bar-Even, A. (2018). Design and in vitro realization of carbon-conserving photorespiration. *Proceedings of the National Academy of Sciences*.

Töpfer, N., Braam, T., Shameer, S., Ratcliffe, R. G., and Sweetlove, L. J. (2020). Alternative CAM Modes Provide Environment-Specific Water-Saving Benefits in a Leaf Metabolic Model. *The Plant Cell*.

Villarreal, J. C. and Renner, S. S. (2012). Hornwort pyrenoids, carbon-concentrating structures, evolved and were lost at least five times during the last 100 million years. *Proceedings of the National Academy of Sciences*, 109(46).

Virtanen, P., Gommers, R., Oliphant, T. E., Haberland, M., Reddy, T., Cournapeau, D., Burovski, E., Peterson, P., Weckesser, W., Bright, J., van der Walt,

S. J., Brett, M., Wilson, J., Millman, K. J., Mayorov, N., Nelson, A. R. J., Jones, E., Kern, R., Larson, E., Carey, C. J., Polat, , Feng, Y., Moore, E. W., VanderPlas, J., Laxalde, D., Perktold, J., Cimrman, R., Henriksen, I., Quintero, E. A., Harris, C. R., Archibald, A. M., Ribeiro, A. H., Pedregosa, F., and van Mulbregt, P. (2020). SciPy 1.0: fundamental algorithms for scientific computing in Python. *Nature Methods*, 17(3):261–272.

Von Caemmerer, S. and Furbank, R. T. (2003). [No title found]. *Photosynthesis Research*, 77(2/3):191–207.

Voth, P. D. (1943). Effects of Nutrient-Solution Concentration on the Growth of Marchantia polymorpha. *Botanical Gazette*, 104(4):591–601.

Walker, B. J., VanLoocke, A., Bernacchi, C. J., and Ort, D. R. (2016). The Costs of Photorespiration to Food Production Now and in the Future. *Annual Review of Plant Biology*, 67:107–129.

Wang, L.-M., Shen, B.-R., Li, B.-D., Zhang, C.-L., Lin, M., Tong, P.-P., Cui, L.-L., Zhang, Z.-S., and Peng, X.-X. (2020a). A Synthetic Photorespiratory Shortcut Enhances Photosynthesis to Boost Biomass and Grain Yield in Rice. *Molecular Plant*, 13(12):1802–1815.

Wang, Y., Song, Q., Jaiswal, D., P. De Souza, A., Long, S. P., and Zhu, X.-G. (2017). Development of a Three-Dimensional Ray-Tracing Model of Sugarcane Canopy Photosynthesis and Its Application in Assessing Impacts of Varied Row Spacing. *BioEnergy Research*, 10(3):626–634.

Wang, Y., Wang, L., Micallef, B. J., Tetlow, I. J., Mullen, R. T., Feil, R., Lunn, J. E., and Emes, M. J. (2020b). AKIN1, a subunit of SnRK1, regulates organic acid metabolism and acts as a global modulator of genes involved in carbon,

lipid, and nitrogen metabolism. *Journal of Experimental Botany*, 71(3):1010–1028.

Whitney, S. M., Houtz, R. L., and Alonso, H. (2011). Advancing Our Understanding and Capacity to Engineer Nature's CO2-Sequestering Enzyme, Rubisco. *Plant Physiology*, 155(1):27–35.

Winter, K. and Holtum, J. A. M. (2014). Facultative crassulacean acid metabolism (CAM) plants: powerful tools for unravelling the functional elements of CAM photosynthesis. *Journal of Experimental Botany*, 65(13):3425–3441.

Yang, X., Cushman, J. C., Borland, A. M., Edwards, E. J., Wullschleger, S. D., Tuskan, G. A., Owen, N. A., Griffiths, H., Smith, J. A. C., De Paoli, H. C., Weston, D. J., Cottingham, R., Hartwell, J., Davis, S. C., Silvera, K., Ming, R., Schlauch, K., Abraham, P., Stewart, J. R., Guo, H.-B., Albion, R., Ha, J., Lim, S. D., Wone, B. W. M., Yim, W. C., Garcia, T., Mayer, J. A., Petereit, J., Nair, S. S., Casey, E., Hettich, R. L., Ceusters, J., Ranjan, P., Palla, K. J., Yin, H., Reyes-García, C., Andrade, J. L., Freschi, L., Beltrán, J. D., Dever, L. V., Boxall, S. F., Waller, J., Davies, J., Bupphada, P., Kadu, N., Winter, K., Sage, R. F., Aguilar, C. N., Schmutz, J., Jenkins, J., and Holtum, J. A. M. (2015). A roadmap for research on crassulacean acid metabolism (CAM) to enhance sustainable food and bioenergy production in a hotter, drier world. *The New Phytologist*, 207(3):491–504.

Yao, L., Wu, X., Jiang, X., Shan, M., Zhang, Z., Li, Y., Yang, A., Li, Y., and Yang, C. (2023). Subcellular compartmentalization in the biosynthesis and engineering of plant natural products. *Biotechnology Advances*, 69:108258.

Yin, X. and Struik, P. C. (2018). The energy budget in C4 photosynthesis: insights from a cell-type-specific electron transport model. *New Phytologist*, 218(3):986–998.

Yishai, O., Lindner, S. N., Gonzalez De La Cruz, J., Tenenboim, H., and Bar-Even, A. (2016). The formate bio-economy. *Current Opinion in Chemical Biology*, 35:1–9.

Yuan, G., Hassan, M. M., Liu, D., Lim, S. D., Yim, W. C., Cushman, J. C., Markel, K., Shih, P. M., Lu, H., Weston, D. J., Chen, J.-G., Tschaplinski, T. J., Tuskan, G. A., and Yang, X. (2020). Biosystems Design to Accelerate C3-to-CAM Progression.

Zhu, X.-G., Long, S. P., and Ort, D. R. (2008). What is the maximum efficiency with which photosynthesis can convert solar energy into biomass? *Current Opinion in Biotechnology*, 19(2):153–159.

A | Code

The code to generate data is available at https://github.com/corihart/Hartinger_PhD_thesis_code.

B | Data

B.1 GC-MS calibration mixes

Table B.1: **Standard solutions prepared for GCMS quantification.**

Amino acid mix 1	**Amino acid mix 2**	**Organic acid mix**
Alanine	Isoleucine	Citrate
Glycine	Leucine	Succinate
Cysteine	Methionine	Malate
Serine	Proline	Putrescine
Threonine	Valine	Fumarate
Aspartic acid	Arginine	Pyruvate
Glutamic acid	Histidine	Lactate
Phenylalanine	Lysine	Glycolate
Tryptophan	Asparagine	Quinate
Tyrosine	Glutamine	Gamma-aminobutyric acid (GABA)